Characterizing Inhibition of Recombinant Sialyltransferases

by

Jeremy Jerasi

A thesis submitted in partial fulfillment of the requirements for the degree of

Master of Science

Department of Chemistry

University of Alberta

Abstract

Sialic acid is a monosaccharide found at the non-reducing end of cell surface glycans. Among the many important roles in mammals, sialic acid commonly serves as a ligand for glycan binding proteins, such as in host self-recognition (Siglecs), response to infection (Selectins), and in viral infection (Hemagglutinins). Sialic acid plays important roles in health and disease, as evidenced by upregulation of Neu5Ac in cancers, as well as in viral and bacterial attachment. The enzymes that catalyze the transfer of sialic acid to glycans are called sialyltransferases, and are localized in the *trans*-Golgi. In humans, twenty sialyltransferases are present and show expression across tissues. As such, the biological roles of sialic acid expression on the cell surface are difficult to probe, and vary between tissues. Chemical tools that modulate cell surface sialic acid have the potential to elucidate these roles, and offer therapeutic potential in pathologies characterized by dysregulated sialic acid expression. In the context of sialic acid, such a strategy involves the direct inhibition of sialyltransferases. While many small molecules have been studied for their ability to inhibit sialyltransferases *in vitro*, few have the ability to do so in cells.

CMP-3F_{ax}-Neu5Ac is reported as one of the only sialyltransferase inhibitors capable of decreasing cell surface sialic acid in cells. Two mechanisms-of-action have been proposed: direct inhibition of sialyltransferases and feedback inhibition of sialic acid biosynthesis. More studies are needed to identify which is the dominant mechanism. Studying CMP-3F_{ax}-Neu5Ac inhibition of sialyltransferases in controlled enzymatic reactions, outside of the context of a living system, allows for testing of only the first mechanism-of-action. To do this, recombinant sialyltransferases are needed, as well as robust inhibition assays that can detect rates of reaction.

Here, a recombinant cloning strategy was developed and implemented to generate soluble human sialyltransferases in a mammalian expression system. These constructs consist of the catalytic region of a given sialyltransferase fused to an IgG Fc domain, also containing two purification tags (His_6 and Strep II Tag). The catalytic activities of purified constructs were

assessed using a quantitative enzymatic assay and found to exhibit similar properties to recombinant sialyltransferases generated previously in the literature. To investigate inhibition, a fluorescence polarization(FP)-based assay was developed. While optimizing the assay, reaction conditions which influenced the observed inhibitor potencies were characterized, finding that reaction buffer pH, buffer composition, and acceptor glycoprotein concentrations significantly altered the IC_{50} values generated in the FP-based assay. Using the optimized conditions, the inhibitory potency of CMP-3F_{ax}-Neu5Ac and CMP-7F-Neu5Ac were determined towards human ST6Gal1 and ST3Gal1. The IC_{50} values measured for CMP-3F_{ax}-Neu5Ac were approximately 15-30 μM towards both sialyltransferases, corroborating the literature evidence of the direct mode of inhibition. Then, IC_{50} values were measured for CMP-7F-Neu5Ac, with potencies of approximately 15-50 μM. This is the first demonstration of CMP-7F-Neu5Ac acting as a competitive sialyltransferase inhibitor, which will lay the groundwork for future studies of this compound in cells. Finally, the polysialyltransferase ST8Sia2 was assessed using the FP-based inhibition assay, finding that autopolysialylation activity could be detected and inhibited with nucleotide inhibitor CTP. The tools generated in this Thesis will pave the way for the identification of biologically relevant inhibitors which selectively inhibit sialyltransferases and may offer great therapeutic potential.

Acknowledgements

During the pursuit of my master's degree at the University of Alberta, I have learned countless lessons and developed as a scientist and an individual. This would not be possible without the support from my supervisor, Professor Matthew S. Macauley, who welcomed me into the lab, guided me with patience, and provided boundless wisdom and insight. There have been many challenges throughout my degree, and I am thankful for your guidance which helped lead me to where I am today.

I would like to thank all members of the Macauley Lab, for their support in teaching me techniques and providing support. Thank you for taking the time to impart your knowledge and skills to me, and for your listening ear and advice in the best and worst of times. I would also like to those close to me who supported me during the pursuit of my degree, including Himanshi Dhawan, Evan Lessard, Alex Kilborn, Ray Ishida, Anders Palmgren, Oleg Krushelnytskyy, Nikita Yevtukh, Sam Habtu, Sam Farberman, Marko Szmihelsky, and Aaron Tronsgard. Thank you for being great friends, I am grateful for the time we spent and the memories we made, which have supported me through the pursuit of this degree.

Last but certainly not least I would like to thank my parents, Tanya Cann and Yair Jerasi, my stepfather Ronald Cann, my grandmother Anna Vishnevsky, and my sister Natalie Jerasi. Thank you for your love and unconditional support throughout my life and especially the past few years. I am forever grateful for all that you have done for me, and I hope that I will be able to support you similarly in the years to come.

Table of Contents

List of Tables

List of Figures

List of Abbreviations

ASF	Asialofetuin
ATP	Adenosine triphosphate
CAZy	Carbohydrate active enzyme database
CDP	Cytidine diphosphate
CHO	Chinese Hamster Ovary
CMAS	CMP *N*-Acetylneuraminic acid synthetase
CMP	Cytidine monophosphate
CTP	Cytidine triphosphate
DMEM	Dulbecco's modified eagle medium
DNA	Deoxyribonucleic acid
DTT	Dithiothreitol
EDTA	(Ethane-1,2-diyldinitrilo)tetraacetic acid
ELISA	Enzyme-Linked Immunosorbent Assay
ESI-TOF	Electrospray ionization time-of-flight
FBS	Fetal bovine serum
FITC	Fluorescein isothiocyanate
FP	Fluorescence polarization
FRT	Flippase recognition target
GalNAc	*N*-Acetyl galactosamine
GFP	Green fluorescent protein
GlcNAc	*N*-Acetyl glucosamine
GNE	UDP-GlcNAc 2-epimerase
HABA	2-(4-hydroxyphenylazo)benzoic acid
HEK293	Human embryonic kidney 293
HPLC	High performance liquid chromatography
HPTLC	High performance thin layer chromatography
HRP	Horseradish peroxidase
IgG	Immunoglobulin γ
Fc	Fragment crystallizable region
IL2	Interleukin-2

IC_{50}	Half maximal inhibitory concentration
k_{cat}	Turnover number
kDa	Kilodalton
K_i	Inhibition constant
K_M	Michaelis constant
LacNAc	*N*-acetyl lactosamine
LB	Luria-Bertani (Media)
LNnT	Lacto-*N*-neotetraose
MES	2-(*N*-morpholino)ethanesulfonic acid
MOPS	3-morpholinopropane-1-sulfonic acid
mP	Milli polarization
NCAM	Neural cell adhesion molecule
NmCSS	*N. meningitidis* CMP-sialic acid synthetase
NTP	Nucleotide triphosphate
PAIN	Pan-assay interference compound
PBS	Phosphate buffered saline
PCR	Polymerase chain reaction
PmST1	*P. multocida* α2-3 sialyltransferase
RCF	Relative centrifugal force
RLU	Relative light units
SDS	Sodium dodecyl sulfate
SOC	Super optimal broth with catabolite repression
TAE	Tris acetate EDTA
TEV	Tobacco etch virus
V_{max}	Maximum velocity of reaction rate

Chapter 1

Introduction

1.1: Sialic-acid Containing Glycans

Cells interact with their environment through interactions between cell surface receptors and ligands, both in solution and present on the surface of other cells. Given the abundance of carbohydrates on the cell surface, called glycans, many of these cell surface receptors are glycan binding proteins. However, glycan ligands are diverse and heterogenous, complicating the study of their expression on the cell surface. Unlike proteins, glycans are not directly encoded by the genetic code, but rather by spatiotemporal controls of glycosyltransferases and their donor sugars. Three of the many glycoconjugates forms are: N-linked glycoproteins, O-linked glycoproteins, and glycolipids. Both N- and O-linked glycans are present on proteins, on asparagine and serine/threonine residues respectively[1]. Glycolipids, as their name suggests, are glycans covalently linked to lipids, which embed into the cell membrane. Different cell types, even within similar lineages, can differentially express glycosyltransferases[2]. Modulation of the glycosyltransferases which produce cell surface glycan ligands allows for concomitant modulation of the receptors which bind to glycan ligands.

One monosaccharide of interest in the context of human immunology is sialic acid (*N*-acetylneuraminic acid; Neu5Ac) **(Figure 1.1A)**. Neu5Ac is a 9-carbon alpha keto acid sugar and a member of the large family of nonulosonic acids[3]. Neu5Ac on the cell surface is linked to underlying glycans in three distinct linkages: α2-3 linkages, α2-6 linkages, and α2-8 linkages[1] **(Figure 1.1B)**. In all linkage types, carbon 2 (C2) of Neu5Ac is involved in a glycosidic linkage to the underlying carbohydrate residue. In the case of α2-3 and α2-6 linkages, the underlying residue is galactose (Gal) or *N*-acetyl galactosamine (GalNAc), with some exceptions for *N*-acetyl glucosamine (GlcNAc) residues substituting for GalNAc[4]. In the case of α2-8 linkages, the

underlying residue is Neu5Ac. This α2-8 linkage can be further extended with additional Neu5Ac residues to form polysialic acid, also called PolySia[5]. Neu5Ac in humans acts as a capping sugar, meaning that the addition of Neu5Ac to an elongated glycan polymer is typically the final step in its biosynthesis. Cell surface glycans can also possess multiple branches, or antennae, allowing for multiple Neu5Ac residues to be conjugated to a single glycan structure[1]. As the most distal monomer from the reducing end of the glycan, Neu5Ac is present at the interface of many cell-surface interactions. This is evidenced in Neu5Ac's role in viral attachment[6], bacterial infection[7], and immune cell signalling via. glycan binding proteins such as Selectins[8] and Siglecs[9].

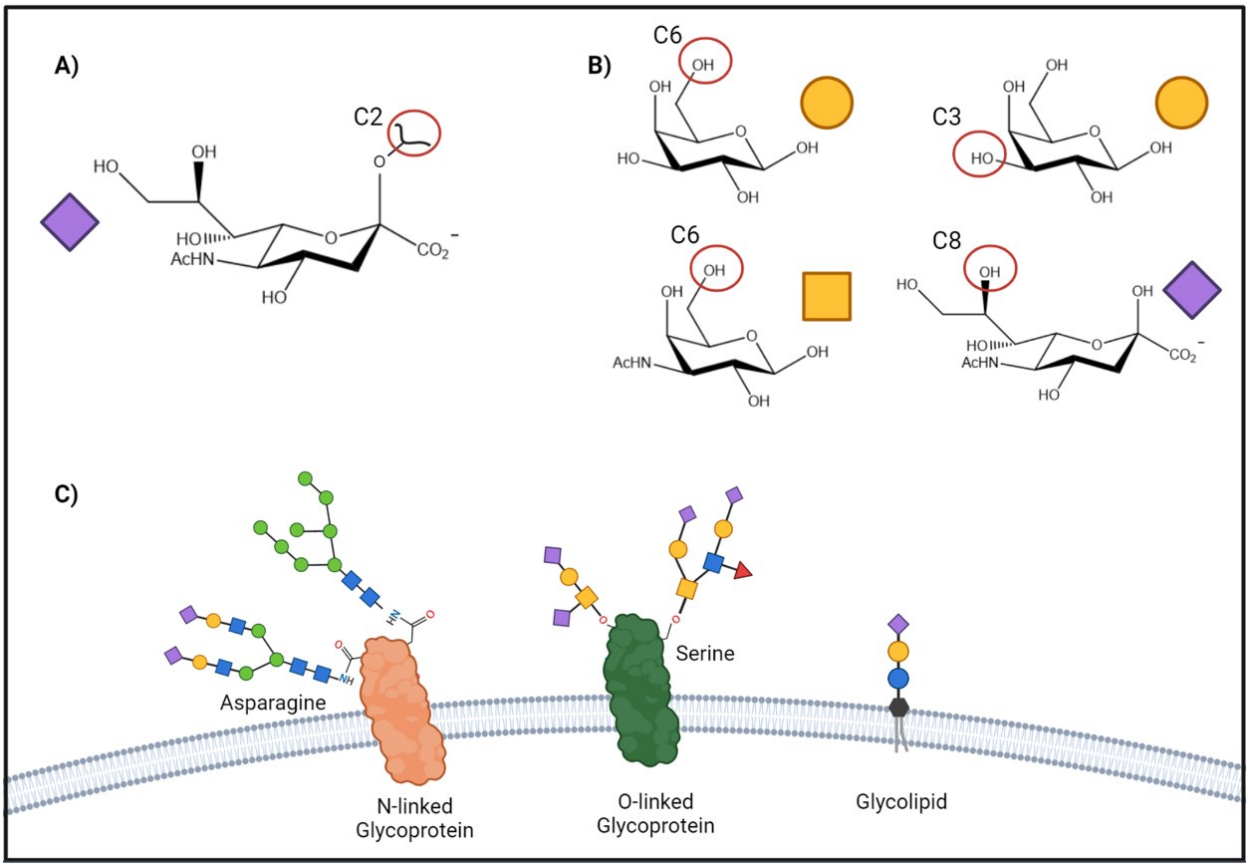

Figure 1.1: Canonical Sialic Acid Presentations in Mammals. A) Structure of nonulosonic acid Neu5Ac with red circle indicating C2. **B)** Underlying glycan residues used as acceptors for Neu5Ac transfer with SNFG symbol. Carbons involved in glycosidic linkages are circled in red. **C)** Three presentation of glycans on biological macromolecules that commonly contain terminal Neu5Ac residues.

A crucial step in the installation of Neu5Ac onto glycans is the formation of cytidine monophosphate Neu5Ac (CMP-Neu5Ac), which serves as the Leloir donor for a family of enzymes called sialyltransferases. Biosynthesis of CMP-Neu5Ac occurs in the cell nucleus by an enzyme called CMP sialic acid synthetase (CMAS) that uses CTP[1]. The charged donor sugar CMP-Neu5Ac acts as a substrate for sialyltransferases, the glycosyltransferase enzymes that catalyze the formation of sialylated glycans.

1.2: Sialyltransferases and GT29 Subfamilies

Sialyltransferases catalyze the transfer of CMP-Neu5Ac to various glycan acceptors in the *trans*-Golgi pathway with an S_N2 inverting mechanism, generating sialosides[10] **(Figure 1.2)**.

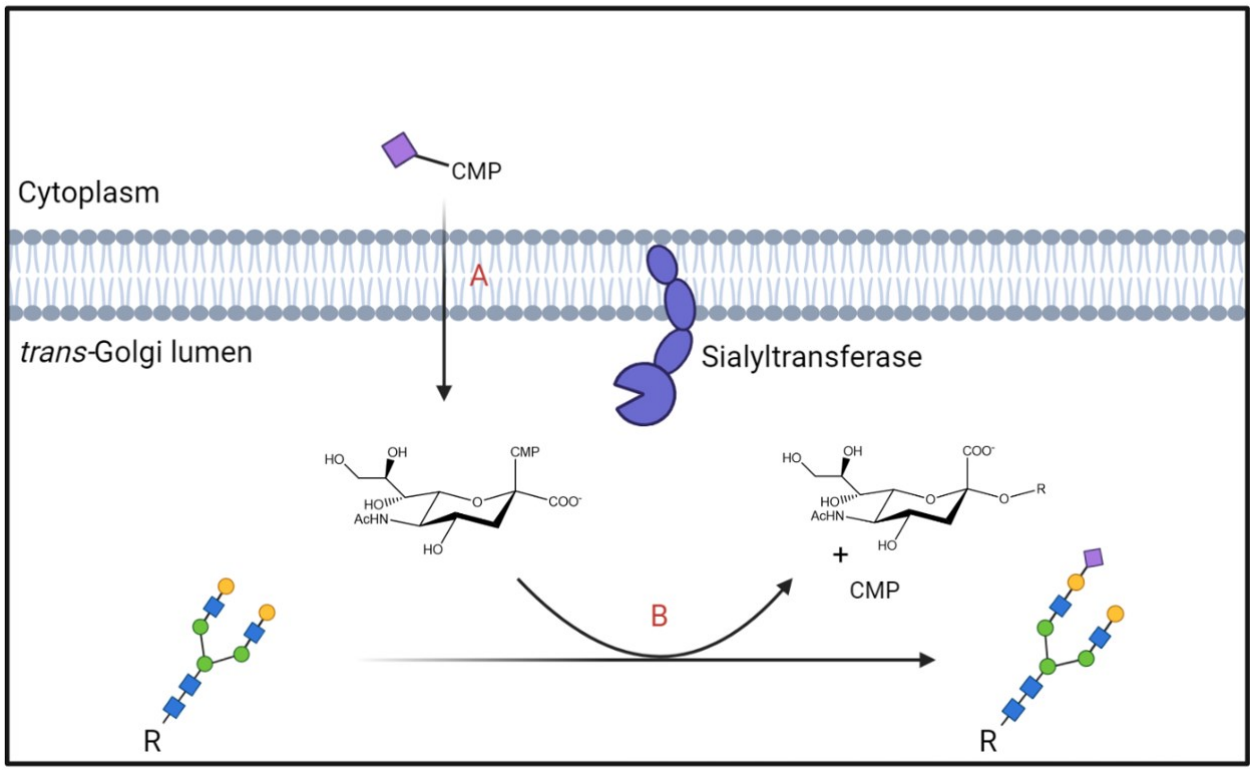

Figure 1.2: Generation of Sialylated Glycans by the Canonical Sialyltransferase Reaction in the trans-Golgi. Step A: CMP-Neu5Ac enters the *trans*-Golgi from the cytoplasm. **Step B**: Sialyltransferase anchored to the *trans*-Golgi membrane transfers Neu5Ac to an accepting *N*-glycan with inversion of stereochemistry, generating CMP and a sialylated *N*-glycan. R represents a general *N*-glycosylated glycoprotein.

Sialyltransferases expressed in humans represent the GT29 group of proteins in the CAZy database (carbohydrate active enzymes database) and are expressed as type II transmembrane proteins anchored to the *trans*-Golgi network[11]. The C-terminal domain possesses catalytic activity, with large conserved sequences referred as a sialyl-motif's L, S, and VS, which are involved in binding CMP-Neu5Ac[12]. The variable expression of these sialyltransferases across different tissues and cell types leads to a diverse array of sialosides in a tissue-dependant manner.

Four sub-families of mammalian sialyltransferase are evident by phylogenetics and observed function, including the: ST6Gal sub-family (2 members), the ST3Gal sub-family (6 members), the ST6GalNAc sub-family (6 members), and the ST8Sia sub-family (6 members)[12] **(Figure 1.3).** Therefore, in total there are twenty distinct sialyltransferases. While some members

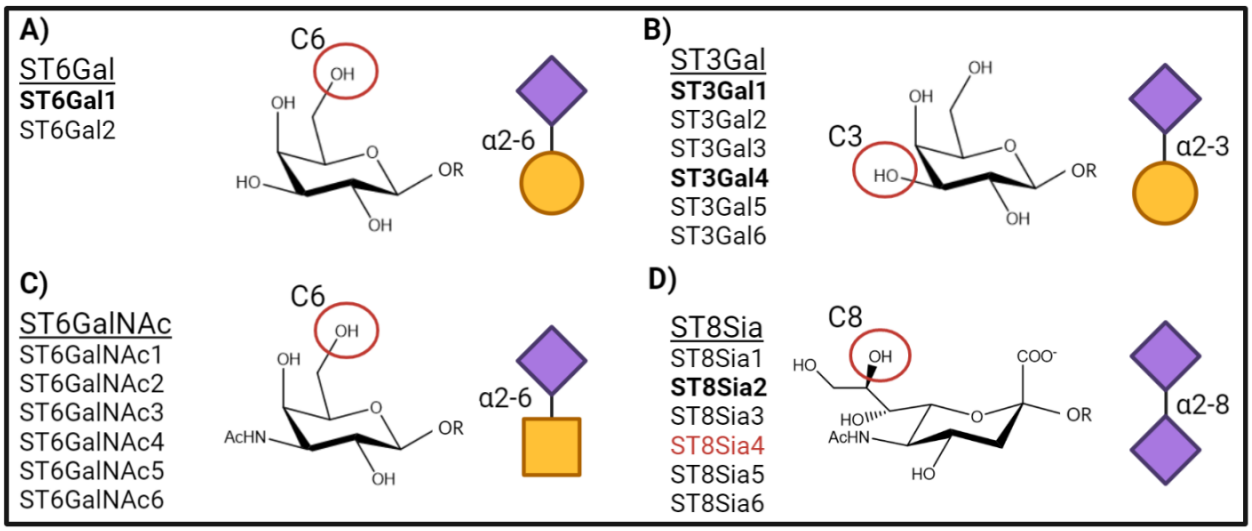

Figure 1.3: GT29 Family of Human Sialyltransferases Grouped by Family. A) Two members of the ST6Gal sub-family, characterized by addition of α2-6 linked Neu5Ac to underlying galactose residues. **B)** Six members of the ST3Gal sub-family, characterized by addition of α2-3 linked Neu5Ac to underlying galactose residues. **C)** Six members of the ST6GalNAc sub-family, characterized by addition of α2-6 linked Neu5Ac to underlying *N*-acetyl galactosamine residues. **D)** Six members of the ST8Sia sub-family, characterized by addition of α2-8 linked Neu5Ac to underlying Neu5Ac residues. **A-D)** Bolded sialyltransferases were successfully cloned and functionally verified in the Thesis. Red sialyltransferase (ST8Sia4) was successfully cloned but failed to express. Circles indicate hydroxy groups on glycan acceptors that form glycosidic linkages to Neu5Ac. R represents glycans underlying the monosaccharides.

within a sub-family have drastically different observed functions, others largely overlap, sialylating the same substrates with differential potency. Sialyltransferases within the same sub-family may produce identical linkages to different subsets of accepting glycan epitopes, which remain incompletely understood. The temporospatial action of sialyltransferases represents a key step of glycan processing pathways in mammals, but more advanced tools are required to study the biological roles of individual sialyltransferases. Studies using cells and mouse models have implicated sialyltransferases as key players in many different clinical conditions, ranging from obesity to schizophrenia[13,14]. The following subsections list the members of the GT29 family of sialyltransferases successfully expressed in this Thesis, as well as their preferred acceptors and enzymatic products.

***1.2.1: ST6Gal1*.** The ST6Gal sub-family contains only two members, ST6Gal1 and ST6Gal2, both of which catalyze the addition of Neu5Ac in an α2-6 linkage to an underlying galactose residue. ST6Gal1 is referred to in older literature as CD75, or Sialyltransferase-1, and was the first human sialyltransferase structurally elucidated by x-ray diffraction in 2013[10]. This work produced the structure in complex with CMP and phosphate at a resolution of 2.1 angstroms. As of 2020, a new structure has been elucidated both complexed with CMP-Neu5Ac and unliganded at a resolution of 1.7 angstroms[15]. ST6Gal1 has garnered the attention of many researchers, especially in the field of cancer, where aberrant glycosylation is observed in various pathologies. Review papers demonstrate upregulation of ST6Gal1 in colorectal, pancreatic, prostate, breast, and ovarian cancers[16,17]. Furthermore, ST6Gal1 overexpression in cancer is linked to downstream consequences including angiogenesis and immortalization[18–20].

N-linked glycoproteins serve as the major acceptor for ST6Gal1, and sialylation is typically extended from type II LacNAc (Gal β1→4GlcNAc)[21]. The C6 hydroxyl group of galactose and the *N*-acetyl functionality of the penultimate GlcNAc were crucial for ST6Gal1 substrate compatibility[22]. More recent findings demonstrated this, showing Type II LacNAc was

preferentially used as a substrate compared to Lactose (Galβ1→4Glc)[23]. The donor sugar CMP-Neu5Ac and CMP-Neu5Ac derivatives have been studied, finding that large modifications on the C5 acetyl functionality can be tolerated, such as the addition of an Alkyne or Biotin functionality[24,25]. When the desialylated glycoprotein asialofetuin was used as an acceptor, containing both *N*-linked and *O*-linked glycoproteins, ST6Gal1 demonstrated a strong preference towards *N*-glycan epitopes over *O*-linked epitopes[24]. ST6Gal1 demonstrates optimal activity at slightly acidic pH, near pH 6[26].

***1.2.2: ST3Gal1 & ST3Gal4*.** The ST3Gal sub-family has 6 members: ST3Gal1-6. As there are more members of this sub-family, there is notably more redundancy in the substrate specificities. In this work, ST3Gal1 and ST3Gal4 were studied and, therefore, will be introduced herein. ST3Gal1 was the first member of this family to be discovered, and originally named Sialyltransferase 4A. A crystal structure for the porcine ortholog ST3Gal1 complexed with a disaccharide and CMP was solved, making it the only member of the ST3Gal sub-family with a crystal structure to date[27]. Elevated ST3Gal1 expression has been observed pathologies including melanoma[28] and breast cancer[29]. ST3Gal1 prefers the Core 1 *O*-glycan (Galβ1→3GalNAc), but has also been demonstrated to tolerate glycolipids as substrates including Asialo-GM1 and GD1b[30]. More recent data collected using mass spectrometric techniques against CD55 glycans demonstrated that ST3Gal1 silencing only had a measurable effect on *O*-linked glycans, not *N*-linked glycans[31]. This work detected an increase in non-sialylated Core 1 *O*-glycans and mono-sialylated Core 2 O-glycans in response to ST3Gal1 silencing in cancer cell lines, which has been corroborated by recent literature using ST3Gal1 knockout cell lines[32].

ST3Gal4 has been referred to as multiple names in previous literature, including SAT-3, ST-4, STZ, and Sialyltransferase 4C. Initial work on ST3Gal4 demonstrated a substrate preference for type II LacNAc over Lactose[33]. However, other work found that Core 1 *O*-glycan motifs (Galβ1→3GalNAc) were preferential acceptors when compared to type II LacNAc[34]. This

work also demonstrated that LNnT (Galβ1→4GlcNAcβ1→3Galβ1→3Glc), a tetrasaccaride containing a terminal type II LacNAc, was a good substrate of ST3Gal4. These findings suggest that glycans underlying the terminal galactose of type II disaccharides may play a crucial in the substrate specificity of ST3Gal4. The enzymatic activity of human ST3Gal4 has been reported have a narrow substrate tolerance when compared to other members such as ST3Gal1[35]. Researchers have demonstrated that ST3Gal4 plays a key role in the biosynthesis of the Sialyl-lewis^x motif [Neu5Acα2→3Galβ1→4(Fucα1-3)GlcNAc][36]. This tetrasaccharide motif is a key player in leukocyte rolling and requires the sialylation of a type II disaccharide structure by an α2-3 sialyltransferase, prior to fucosylation[37]. Interestingly, another member of the ST3Gal subfamily, ST3Gal6, has been characterized showing redundant substrate specificity with ST3Gal4 especially in the context of the Sialyl-lewis^x motif[38,39].

1.2.3: ST8Sia2. The ST8Sia sub-family, consists of 6 members: ST8Sia1-6. Many reviews have covered the roles of these sialic acid polymers, also known as 'PolySia', including involvement in immune regulatory mechanisms[5,40]. Generally, the formation of PolySia has been observed both on glycoproteins and glycolipids, ranging from the Neu5Ac dimers to polymers longer than 200 residues. Perturbations in PolySia expression have been linked to disorders such as Schizophrenia, Alzheimer's, and Parkinson's disease[41]. In this Thesis, ST8Sia2 was studied. ST8Sia2 has previously been referred to in the literature as Sialyltransferase 8B and Sialyltransferase X (STX). ST8Sia2 contains a polybasic 'polysialyltransferase domain' and is associated with the formation of large PolySia chains, implicated in neural development[42,43]. Much of the work on polysialyltransferases is studied using the neural cell adhesion molecule (NCAM) as a substrate[44,45]. NCAM is a protein expressed on the surface of neurons known to express high levels of PolySia, crucial to the adhesion function of the protein. Initial work carried out using the murine ortholog of ST8Sia2 demonstrated a substrate specificity towards sialylated *N*-linked glycoproteins, with no activity against asialo-glycoproteins or glycolipids[46]. *In vitro* assessment of

ST8Sia2 overexpression demonstrated an increase of PolySia expression in both murine and human models[47]. While studies typically focus on the poly sialylation of the NCAM molecule, early studies measuring the activities of ST8Sia2 used fetuin as an acceptor and demonstrated that various other glycoproteins could act as substrates[48]. To further investigate the substrate specificity of ST8Sia2, researchers prepared substrates differing by the length of the Neu5Ac chains with polymer lengths of three and twelve to be studied against polysialyltransferases[49]. This work demonstrated a remarkable preference of ST8Sia2 towards the shorter polymer of three Neu5Ac residues compared to the 12-residue substrate. Furthermore, the researchers used various derivatives of sialic acid, replacing the methyl group of the C5 acetyl functionality with various aliphatic groups. They found that propyl, butyl, and pentyl groups were tolerated, but the canonical methyl group exhibited the best reaction rate for ST8Sia2. Accordingly, ST8Sia2 is a polysialyltransferase for which short Neu5Ac polymers on glycoproteins act as the preferred substrate. It is notable that ST8Sia2 also undergoes autopolysialylation, whereby the acceptor is a sialylated glycan on itself or a neighbouring molecule of ST8Sia2[50].

1.3: Sialyltransferase Enzymatic Assays

To study the activity of sialyltransferases, the ideal assay would possess a few key characteristics. First, it would not require the reaction to be stopped, and products of the reaction would not require separation. Instead, it would be capable of real time measurements. Second, the assay would use native reaction components in physiological conditions to allow comparisons to living systems. Lastly the assay would use cheap reagents, and accessible technologies, allowing for scalability and high-throughput applications. Many sialyltransferase assays have been established in the literature, but most of these techniques require quenching and/or separation of the reaction mixture prior to measurement. Few assays have been demonstrated to provide real-time measurements, and these assays are outlined below.

1.3.1: Stopped Radioactive Assays: Initial research in the field mainly used radiometric assessments after quenched reaction mixtures were separated by various techniques. One of the early papers using this technique focused on the function of ST6GalNAc2, cited widely by other researchers in the field[51]. The assay allowed for measurement of glycoprotein, glycolipid, and oligosaccharide acceptors by using radioactive CMP-[^{14}C]Neu5Ac as the donor sugar. For glycoprotein acceptors, reaction mixtures were subjected to SDS-PAGE and radioactivity was quantified. For oligosaccharide and glycolipid acceptors, HPTLC (High-Performance Thin Layer Chromatography) was used for separation instead. The researchers indicate that this technique was used to generate quantitative data by ensuring that measurements were taken during the linear phase of the enzyme kinetics. While this paper used the radiometric assay for the assessment of ST6GalNAc2, the same technique has been used extensively for the assessment of ST6Gal[52], ST3Gal[53], and ST8Sia[46] sub-families. In these assays, researchers indicate that the measurements were carried out after the reaction is terminated with either the addition of methanol or KCl for glycoprotein and glycolipid acceptors respectively. One of the key weaknesses of the early radiometric assays is the inability to measure the sialyltransferase reactions in real-time, requiring quenching and separation prior to measurement. In these assays, incomplete reaction termination or non-linear reaction conditions may lead to erroneous measurements. Furthermore, radiometric assays require the use of expensive reagents and laboratory classifications needed for handling radioactive waste.

1.3.2: Stopped HLPC Assays: The radiometric techniques that dominated the early literature have been largely phased out, replaced with other preferred assays. Functional parameters of the sialyltransferases such as the Michaelis-Menten constants K_M and V_{max}, are relevant in the study of enzyme kinetics. In the development of a putative assay, these constants should be consistent and parsimonious with established assays. Initial work that deviated from radiometric strategies was carried out by Christoph Schaub, with the goal of replacing radioactivity detection

with UV visualization[54]. In this work, the acceptor sugar LacNAc was converted to a p-nitrophenyl glycoside, thereby generating a UV-active acceptor for the reaction against ST6Gal1. Reactions were quenched and separated by reverse-phase HPLC. Using this strategy, K_M values for CMP-Neu5Ac and LacNAc were verified to match established literature values. Furthermore, K_i values were calculated for known competitive inhibitor CDP, found to be 10 μM. This same UV-detection reverse phase HPLC assay has been used by other researchers to quantify inhibitory potency of novel transition-state analog inhibitors against sialyltransferases[55]. The main drawbacks of this approach include the requirement of non-native accepting substrates, as well as requiring samples to be purified and separated prior to analysis.

1.3.3: Stopped Coupled Glo Assays: The CMP-Glo assay is a coupled luminescence-based assay capable of precise measurement of free nucleotide monophosphates UMP and CMP. This assay was developed in 2014 and commercialized by ProMega in 2016[56]. In this assay, both free UMP and CMP in a given solution is converted directly into ATP by the proprietary detection buffer, which then generates luminescence by a coupled luciferase reaction. A standard curve consisting of CMP can be used to directly relate luminescence values to concentration of CMP, allowing for direct quantification. If there is no other source of CMP generated in a sialyltransferase reaction mixture, all luminescent signal generated in the assay can be attributed to CMP freed from CMP-Neu5Ac by the action of the sialyltransferase. The key advantage of this approach is the ability to generate quantitative data, allowing for accurate calculations of reaction rate needed for enzyme kinetics. However, addition of the CMP-Glo kit components quenches the reaction, and as such real-time analysis is not possible with the technique. Researchers have demonstrated the effectiveness of the CMP-Glo assay, such as investigating the ‘ST3Gal’ sub-families substrate preferences[57], and assessment of ST6Gal1 inhibition with known transition-state analog inhibitors[58]. Another key benefit of this assay is the ease-of-use. While previous techniques have required radioactive components and post-reaction purification techniques such

as HLPC, or expensive mass spectroscopic instrumentation, the CMP-Glo Assay offers a single reagent kit that can be used to directly quench and quantify reaction products requiring only the use of a luminometer for measurement with negligible post-reaction processing.

1.3.4: Real-Time Mass Spectrometry Assays: Researchers aimed to address the shortcomings of the stopped assay strategies by looking to Mass Spectroscopy. Initially, these strategies were investigated for the assessment of the mammalian galactosyltransferase β-GalT[59]. Using electrospray ionization time-of-flight (ESI-TOF) mass spectroscopy, the formation of product and depletion of reactant were detected in real-time. The kinetic parameters calculated from this technique matched those of research using HPLC separation methods. One drawback of this technique was that the accepting substrate lacked underlying glycan structure. To addressing this, researchers published a similar strategy using gold colloidal nanoparticles of 100 nm diameter as a scaffold to mimic the shape of a globular protein[60].

In a modern application, researchers at the University of Alberta introduced CUPRA (Competitive Universal Proxy Receptor Assay). This method uses Electrospray Ionization Mass Spectrometry (ESI-MS) to assess binding interactions between glycans and glycan binding receptors, also called lectins[61]. Briefly, a library of various oligosaccharide acceptors was generated, each conjugated to a universal affinity tag kept constant between all acceptors. The affinity tag binds strongly to a protein referred to in the work as '$^{Uni}P_{proxy}$', or the universal proxy protein receptor. Thus, the acceptors generated are bifunctional, with the ability to bind $^{Uni}P_{proxy}$ via. the universal tag, or a glycan binding protein by the canonical glycan-binding interaction of the lectin tested. However, the binding interaction in one of these modes precludes binding in the other, thus leading to competition between the two bound states. Applying this to enzymatic reactions, the 'CUPRA-ZYME' protocol was introduced[62]. As the reactants and products of glycosyltransferase reactions differ in molecular weight, ESI-MS detected the relative

abundances of substrate and product over time. In this work, the technique was validated for ST6Gal1 and ST3Gal4.

1.3.5: Real-Time Fluorescence Polarization Assays: Florescence Polarization is a technique initially theorized by Francis Perrin in 1926, but technological limitations prevented practical applications[63]. The core concept underpinning this technique is the observation that an inverse relationship exists between molecular size and rotational speed. If a plane-polarized light source excites a fluorophore attached to a small molecule, the high rate of rotation inherent to small molecules leads to a depolarization of the light signal upon emission. Any given fluorophore can be characterized by its 'fluorescence lifetime', a time value in the nanosecond range that indicates the average time between excitation and emission of electromagnetic radiation[64]. Therefore, solutions containing small molecule fluorophores which rotate quickly will emit a depolarized signal when excited by a polarized source. However, large molecules rotate slowly, and a fluorophore on such a molecule will not fully depolarize the signal. To measure this, instruments must be configured with polarizing filters to detect the emission of the target fluorophore in two orientations, referred to as parallel (P) and perpendicular (S) **(Figure 1.4)**. As per the equation below, mP (milli-polarization) can be calculated in real time, with signal increasing as the average size of the conjugated-fluorophore in the solution increases. 'I' represents the intensity of light detected from the fluorophore.

$$mP = 1000 * \frac{I(para) - I(perp)}{I(para) + I(perp)}$$

This technique has been demonstrated to be highly effective at investigating binding interactions of small molecules to larger biomolecules. A representative example of this is the use of fluorescently tagged estradiol to investigate estradiol binding to the estrogen receptor[65]. The applications of FP assays can also be adapted to study enzymatic reactions in real-time, however there are notable considerations. Critically, the fluorophore must be conjugated to a small

molecule and the product of the enzymatic reaction must transfer the small molecule to a large substrate. For glycosyltransferases, this means that the donor sugar substrate of the enzyme cannot be directly assessed, as the fluorophore is required to generate an mP signal. The application of this technique in sialyltransferase reactions was first demonstrated in 2011 at the Scripps Research Institute, where researchers conjugated a FITC (Fluorescein isothiocyanate) fluorophore to the C9 position of CMP-Neu5Ac generating the donor sugar 9'FITC-CMP-Neu5Ac[66]. Herein the potencies of multiple classes of sialyltransferase inhibitors were calculated towards ST6Gal1, ST3Gal1 and ST3Gal3.

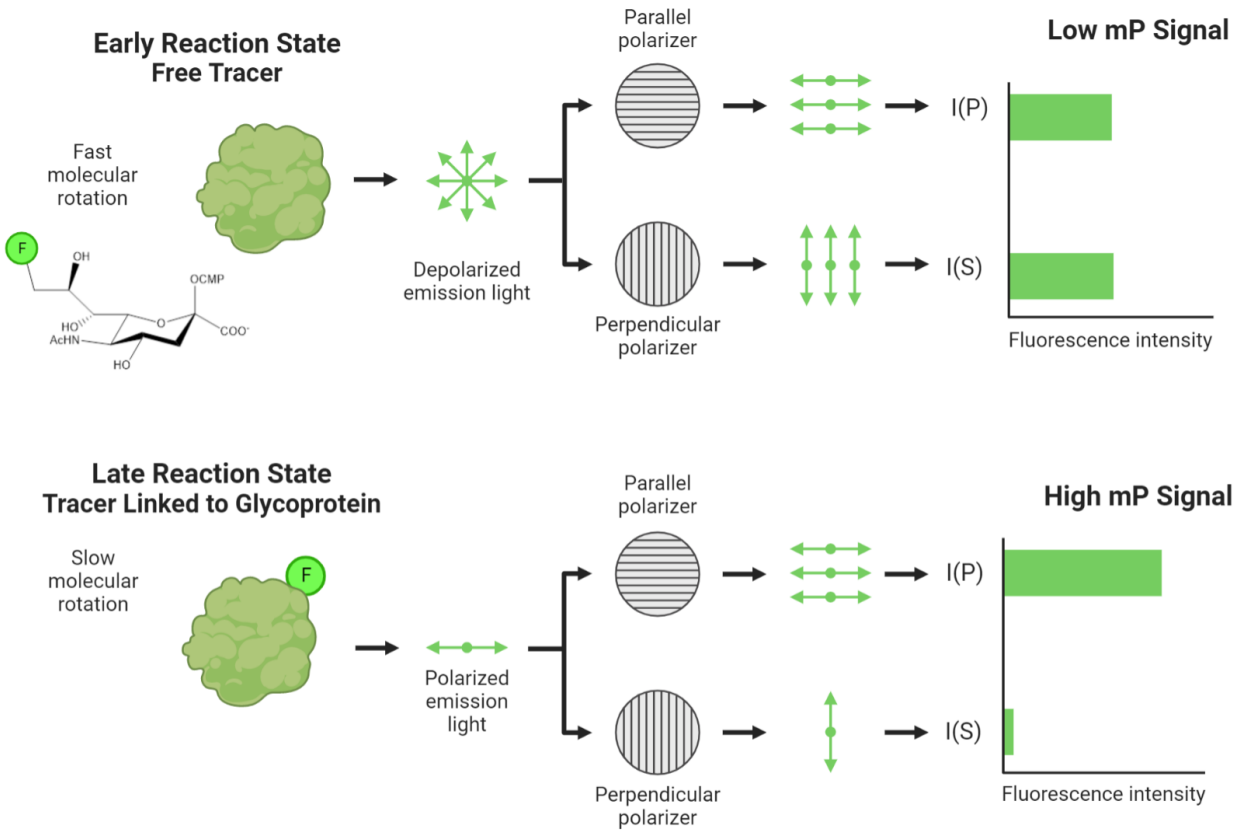

Figure 1.4: Overview of FP Assay Application for Sialyltransferases. Fundamental principles of Fluorescence Polarization assay. Early reaction state is characterized by free donor sugar (tracer), which rotates quickly. Depolarized emission leads to equivalent parallel (P) and perpendicular (S) signal (Low mP). Late reaction state is represented products of sialyltransferase reaction. Donor sugar is bound to a large glycoprotein, which rotates slowly. Polarized emission leads to inequivalent parallel and perpendicular signal (High mP). Green circle F represents conjugation of fluorescein.

1.4: Sialyltransferase Inhibitors

Modulating cell surface sialic acid with sialyltransferase inhibitors has the potential to advance fundamental understanding for the biological roles of sialic acid. This could also have a therapeutic potential in circumstances such as cancer, where it is desirable to decrease sialic acid levels. Several classes of ST inhibitors have been identified including cytidine analogs, and flavonoids, which has been reviewed extensively elsewhere[67,68]. Inhibitors that structurally mimic the transition state of an enzyme catalyzed reaction are known to exhibit higher affinity to the active site than the enzyme substrate. These inhibitors are called transition-state analogs, and as typically act as highly potent inhibitors. In the context of sialyltransferases, researchers have employed this technique to develop potent inhibitors with transition state features that are effective at low nanomolar concentrations *in vitro*[67,69]. These features include a planar, oxocarbenium-like motif commonly achieved using amides, as well as addition of aromatic or aliphatic rings used to mimic the structure of the Neu5Ac. Acting as competitive inhibitors, many of these bind to sialyltransferases with affinities 10-100 times stronger than CMP-Neu5Ac[70]. However, nearly all these inhibitors are ineffective in a cellular context, as they likely do not enter the cell and/or the *trans*-Golgi network. Inhibitor designs mimicking the natural substrate Neu5Ac have had more success in cells.

CMP-3F-Neu5Ac is a Neu5Ac-analog inhibitor which has shown promise in cell culture and flow cytometry-based assays[71]. CMP-3F-Neu5Ac is a structural analog of Neu5Ac, distinct only by a single fluorine on C3 as either the axial epimer ($3F_{ax}$) or the equatorial epimer ($3F_{eq}$)[72]. The fluorine atom is understood to withdraw electron density from the anomeric carbon of Neu5Ac, destabilizing the formation of an oxocarbenium-like transition state. Unlike a transition state analog, $3F_{ax}$-CMP-Neu5Ac can be recognized by host cell machinery due to its structural similarities to CMP-Neu5Ac. If provided to cells in a peracetylated form, the inhibitor can enter the same biosynthetic pathways as a normal Neu5Ac monosaccharide. As such, peracetylated $3F_{ax}$-

Neu5Ac is a prodrug that exerts no inhibitory effect until host cell processes it, leading to the generation of an active inhibitor and reduction of sialic acid on the cell surface **(Figure 1.5).**

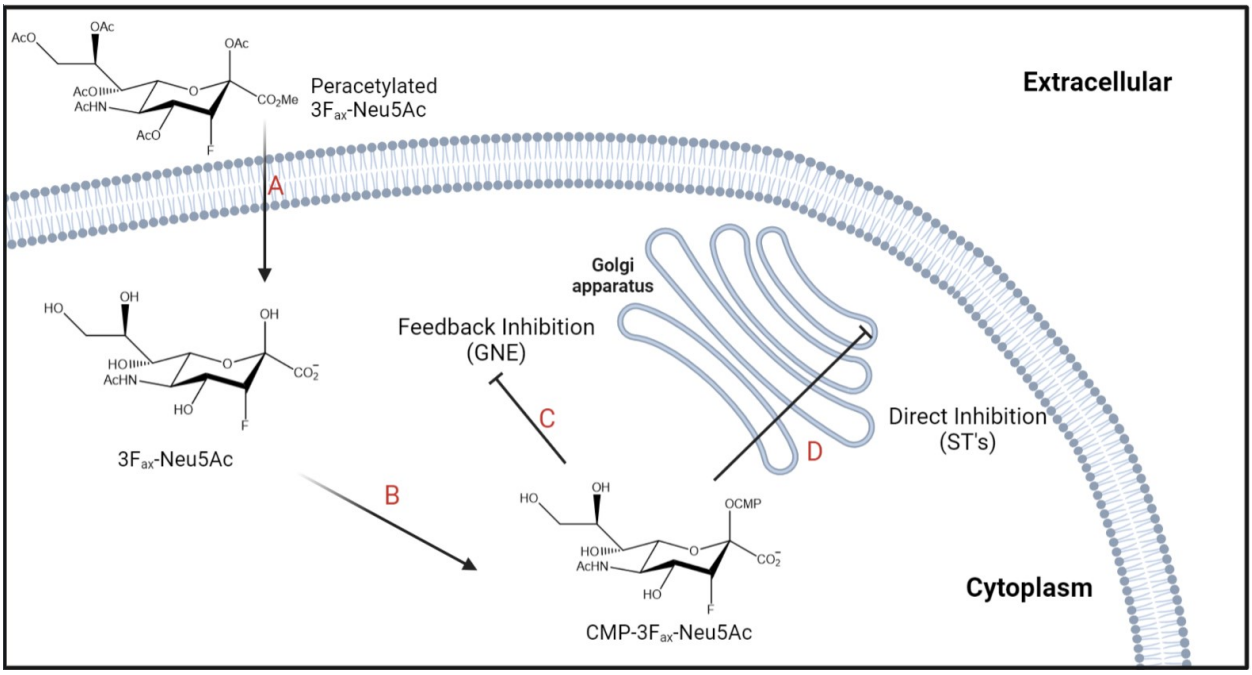

Figure 1.5: Cellular Processing of Peracetylated 3F$_{ax}$-Neu5Ac to Generate Global Sialyltransferase Inhibitor CMP 3F$_{ax}$-Neu5Ac. Step A: Peracetylated 3F$_{ax}$-Neu5Ac enters the cell and is processed by cytosolic esterase's and demethylases to generate 3F$_{ax}$-Neu5Ac. **Step B:** 3F$_{ax}$-Neu5Ac is charged with CMP by CMAS in the cell nucleus, generating active inhibitor CMP-3F$_{ax}$-Neu5Ac. **Step C:** Feedback inhibition of GNE by CMP 3F$_{ax}$-Neu5Ac reduces global production of Neu5Ac. **Step D:** CMP 3F$_{ax}$-Neu5Ac is translocation into the *trans*-Golgi, where it can directly inhibit sialyltransferases competitively.

Two mechanisms are proposed to account for how 3F$_{ax}$-CMP-Neu5Ac decreases cell-surface sialic acid [73]. The first mechanism is direct inhibition of ST's by 3F$_{ax}$-CMP-Neu5Ac **(Figure 1.4D)**. Indeed, it was reported that 3F$_{ax}$-CMP-Neu5Ac exhibits an IC_{50} of 9.5 μM towards ST6Gal1. A second mechanism was also proposed whereby CMP-3F$_{ax}$-Neu5Ac serves as an allosteric feedback inhibitor of GNE (UDP-GlcNAc 2-epimerase), which leads to decreased levels of endogenous CMP-Neu5Ac in cells **(Figure 1.4C)**. Notably, this mechanism does not require localization of CMP-3F$_{ax}$-Neu5Ac into the *trans*-Golgi as GNE localizes in the cytosol[74]. More

recent studies have suggested that this may be the major mechanism of action[75]. Nevertheless, it is not currently understood which of these effects is predominant. Studies focusing on the direct sialyltransferase inhibition mechanism indicated a K_i value of 5.7 μM for CMP-3F$_{ax}$-Neu5Ac inhibition of rat derived ST6Gal1 using a radiometric method[76]. For bacterial sialyltransferases, *Pm*ST1 was demonstrated to be strongly inhibited by CMP-3F$_{ax}$-Neu5Ac as evidenced by a K_i value of 25.7 μM compared to the K_M of its native substrate CMP-Neu5Ac (K_M = 430 μM)[77]. When researchers assessed another bacterial sialyltransferase, CstII, the K_i value was 657 μM, similar to the native CMP-Neu5Ac affinity (K_M = 460 μM)[78]. The current literature finds that CMP-3F$_{ax}$-Neu5Ac exhibits differential affinity towards mammalian sialyltransferases when compared to bacterial sialyltransferases. Demonstrating the *in vivo* application of 3F$_{ax}$-CMP-Neu5Ac inhibition, researchers observed reduction in tumor size for mice treated with peracetylated 3F$_{ax}$-Neu5Ac[79].

While promising for their ability to localize to cellular compartments required for inhibition of cell surface sialic acid, fluorinated Neu5Ac analog inhibitors possess a fundamental problem for applications in living systems that must be addressed. There are many sialyltransferases expressed differentially across tissues with variable tolerance for accepting glycan substrates. CMP-3F$_{ax}$-Neu5Ac is understood to act as a global inhibitor due to its inhibition of GNE, yet it's ability to competitively inhibit all 20 human sialyltransferases has not yet been established. When mice were injected with peracetylated 3F$_{ax}$-Neu5Ac, high levels of toxicity and death were observed[80]. The authors attributed this primarily to kidney dysfunction caused by loss of Neu5Ac on podocalyxin, a highly sialylated protein involved in glomerular filtration[81]. This demonstrates the importance of Neu5Ac expression across physiological systems in mammals, and the key drawback of global sialyltransferase inhibitors, toxicity. The observed global reduction of sialic acid on the cell surface may stem from the feedback inhibition of GNE. However, it cannot be ruled out that CMP-3F$_{ax}$-Neu5Ac also inhibits all sialyltransferases in the *trans*-Golgi, also leading to the observed global inhibition. In the former case, a modified inhibitor that did not cause

feedback inhibition to GNE may reduce the observed toxicity. In the latter case, this would not be sufficient, and the inhibitor would need to be designed to selectively interact with a subset of sialyltransferases. These approaches have the potential to develop sialyltransferase inhibitors that could modulate specific types of Neu5Ac expression without the toxic side-effects. As the field develops, many more sialyltransferase inhibitors emulating or modifying CMP-3F_{ax}-Neu5Ac will undoubtedly be generated and assessed to address these issues.

To help disentangle these complicating observations, a reductionist approach is appropriate. By assessing the potency of sialyltransferase inhibitors *in vitro*, the feedback inhibition is removed from the equation. To achieve this, researchers need recombinantly expressed sialyltransferases and robust enzymatic assays. These tools must be capable of assessing sialyltransferase reaction rates for various acceptors and must tolerate various inhibitory compounds without interference. Elucidating the relative inhibitory potencies of inhibitors against all human sialyltransferases is a critical step in characterizing the complicated interactions at play. These insights will pave the way for the development of next generation therapeutics, selective sialyltransferase inhibitors, which modulate the expression of Neu5Ac.

1.5: Overview of the Thesis

To comprehensively study the potency of inhibitors against various sialyltransferases, recombinant sialyltransferases and enzymatic assays are required to measure inhibition. Furthermore, recombinant sialyltransferases allow the use of chemoenzymatic approaches to generate Neu5Ac containing ligands that would otherwise require many protection and deprotection steps using tradition carbohydrate strategies. Thus, the major objective of this work is the development of a functional set of sialyltransferases to measure enzyme kinetics in the presence of inhibitors. A primary outcome is to provide evidence supporting the direct inhibition mechanism of action of CMP-3F_{ax}-Neu5Ac.

In Chapter 2, the generation a modular strategy is presented to obtain functional expression of GT29 family human sialyltransferases. The optimization of expression and purification for functional recombinant sialyltransferase constructs was achieved. In Chapter 3, the testing of inhibitors was carried out. Characterization of a sialyltransferase inhibition assay capable of assessing inhibitor potencies against glycoprotein acceptors enabled the quantification of IC_{50} values towards 5 different sialyltransferase inhibitors. The inhibitory potency of CMP-3F_{ax}-Neu5Ac as well as other CMP-Neu5Ac analog inhibitors were successfully quantified. Overall, this work demonstrates that CMP-3F_{ax}-Neu5Ac inhibits all tested sialyltransferases equally and provides new evidence that CMP-7F-Neu5Ac may be a more potent inhibitor *in vitro*.

Chapter 2

Development of a Mammalian Expression System for Sialyltransferases

2.1: Introduction and Objectives

In this chapter, an expression system to produce soluble and functional recombinant human sialyltransferases was developed. Cloning, expression, and purification of soluble recombinant sialyltransferases were carried out, followed by functional validation of sialyltransferase activity in an enzymatic assay. These soluble recombinant sialyltransferases are subsequently used in biochemical inhibition assays in Chapter 3.

Researchers have developed numerous strategies to generate soluble and functional sialyltransferases. Many of these strategies share common features, while some key differences are worth noting. GT29 Sialyltransferases share a type II transmembrane topology, with a C-terminal catalytic domain facing the intracellular compartment of the *trans*-Golgi network[82]. The N-terminal transmembrane domain anchors sialyltransferases to the Golgi apparatus, which poses a challenge when studying the proteins *in vitro*. In theory, clarified cell lysates of mammalian cells transfected with the full-length sequence of a sialyltransferase could be used as a source of enzyme, but this strategy possesses two main drawbacks. First, conditions required for cell lysis could negatively affect the function of the sialyltransferase. Second, cell lysates contain many other proteins, including other naturally expressed sialyltransferases. For this reason, it is preferable to use a recombinant strategy to produce soluble and secreted sialyltransferases, ideally with affinity tags for purification. To do this, the DNA encoding the N-terminal transmembrane domain is removed. However, this region is also used as the transcriptional signal sequence, and therefore recombinant cloning designs must replace the signal sequence to ensure the expressed protein ends up in the secretory pathway. By including purification tags on either the N- or C-terminus of the expressed protein construct, purification

column strategies can be employed to purify and concentrate the activity of expressed and secreted sialyltransferases[83]. Examples of common purification tag/column systems include the 6x His tag in conjugation with Nickel chelate chromatography as well as the IgG-Fc in conjugation and capture with Protein A. It is important to note that when using the IgG_1 Fc fragment as a purification target, extremely low pH or elevated temperatures are required for elution which may lead to losses in protein integrity[84].

The early literature demonstrating expression of soluble sialyltransferases commonly used transient transfection of COS-7 cells. In transient transfection, introduced vectors only exist in the cell for a short period, whereas a stable transfection strategy is characterized by integrating a DNA sequence into the host genome. One such strategy is the Flp-in system, where a cell line is generated with an integrated FRT (Flp Recombination Target) site. To integrate the DNA sequence, cells are co-transfected with pOG44 (a vector expressing the Flp-recombinase protein) and an expression plasmid containing the FRT site with linked hygromycin resistance gene. This leads to incorporation of the desired sequence into the host genome at the FRT site while conferring hygromycin resistance to allow for antibiotic selection[85]. Many of the early sialyltransferase constructs were based on work outlined in a review, characterized by an IgM signal sequence to replace transmembrane domain and native signal sequence allowing for soluble expression[82]. If required, the transfection plasmid pcD-SRα used would include the sequence for the IgG-binding region of Protein A located upstream of the truncated sialyltransferase catalytic sequence. This allowed for purification and concentration over an IgG-Sepharose column, a technique required for sialyltransferases that expressed poorly in their chosen expression system. At the time of the review, these researchers had cloned 13 sialyltransferases. Other early researchers used the pAMoA vector and transfected KJM-1 cells with the same protein A fusion and IgM signal sequence[86].

Another key consideration for expression of mammalian sialyltransferases is the glycosylation of the protein as sialyltransferases themselves are glycosylated proteins. Therefore, if the glycosylated structures are elaborated by other host glycosyltransferases and possess appropriate terminal residues, they are potential acceptors. Glycosylation of sialyltransferases may stabilize the folding, or impact of the function of the sialyltransferase when expressed recombinantly[87,88]. ST6Gal1 possesses three consensus sequence sites for *N*-linked glycosylation, with two being found experimentally to be elaborated with complex, sialylated glycans[89]. Researchers have also used bacterial expression systems for recombinant sialyltransferase expression due to their efficient yield and lower relative cost to mammalian cell expression[90]. However, without the eukaryotic capacity for glycosylation, these systems can often lead to poorly expressed protein due to an essential role for glycosylation in protein folding[91]. Nonetheless, the optimization bacterial expressions systems have been investigated to generate the high protein yields needed for x-ray crystallography structural assessments, as the direct function of the enzyme is not required for these experiments[92]. The use of baculovirus transfected insect cells to generate soluble sialyltransferases has also been explored. Glycosylation pathways of insect cells have been characterized well and do not generate similar glycans to mammalian cells[93,94]. As such, sialyltransferases expressed in insect cells may not possess the enzymatic activity and/or stabilization observed for mammalian systems.

To elucidate the impact of glycosylation on sialyltransferase function, researchers transfected various lines of Chinese Hamster Ovary (CHO) cells with ST6Gal1, each line possessing unique defects of glycosylation[87]. Here, it was found that glycosylation defects leading to truncation of the glycan structures on ST6Gal1 led to reduced activity of the enzyme. Other researchers demonstrated that abrogation of glycosylation on ST6Gal1 led to complete loss of *in vivo* catalytic activity measured by lectin binding[88]. These findings indicate that even if functionally expressed, the enzymatic activity of soluble sialyltransferases may depend on how well the

expression system used can mimic the natural glycan profile. HEK293 cells are another mammalian cell line used commonly for recombinant protein expression.

In this work, we aimed to use a stable mammalian transfection strategy to generate at least one functional recombinant isoform from each GT29 family (ST6Gal, ST3Gal, ST6GalNAc, ST8Sia). This could validate the expression system for use across the entire diversity of expressed human sialyltransferases. As each family uses a distinct set of acceptor substrates, it is crucial to generate tools that allow for assessment of all reactions that these enzymes can catalyze. To do this, we envisioned a vector with a non-native signal sequence and purification tags directly upstream of an NheI digestion site. With this vector, restriction double digestion would allow for direct and unidirectional ligation of the gene encoding the catalytic domain of mammalian sialyltransferases. Then, a library of cell lines stably transfected with the recombinant sialyltransferases would be stored and thawed for generation of functional sialyltransferases.

2.2: Results

2.2.1: Cloning Designs for Expression of Soluble Sialyltransferases

To clone the soluble portion of each human sialyltransferase requires removal of the DNA encoding the 5' signal sequence, transmembrane domain, and part of the stem region. Previous published work on all 20 human sialyltransferases established the required amino acids[95]. As an example, for hST6Gal1, amino acids 75-406 were used. Accordingly, PCR was used to amplify the desired coding region for each sialyltransferase including the appropriate restriction endonuclease sites for cloning into the appropriate vector.

Using this strategy, the native signal sequence requires replacement to ensure localization to the secretory pathway. For this purpose, the Interleukin-2 signal sequence was chosen, due to its widespread use in commercial protein production[96]. Therefore, a pcDNA5 vector was created with a 5' IL2 signal sequence and purification tags employing a compatible sticky end strategy **(Figure 2.1)**. Typically, only sticky ends produced by the same restriction enzyme can be ligated. However, there are rare cases in which a pair of restriction enzymes use different digestion sites, yet the generated sticky ends are identical. Pairs of restriction enzymes that fit this criterion are called 'compatible', and therefore have 'compatible sticky ends'. When the compatible sticky ends of NheI and XbaI ligate, a novel sequence is generated (TCTAGC), which is non-palindromic. By adding a 5' XbaI sequence and 3' NheI sequence to the initial insert containing the IL2 signal sequence and purification tags, the compatible sticky ends could then be ligated to an empty pcDNA5 vector, singly digested with NheI to generate a product with a single 3' NheI site.

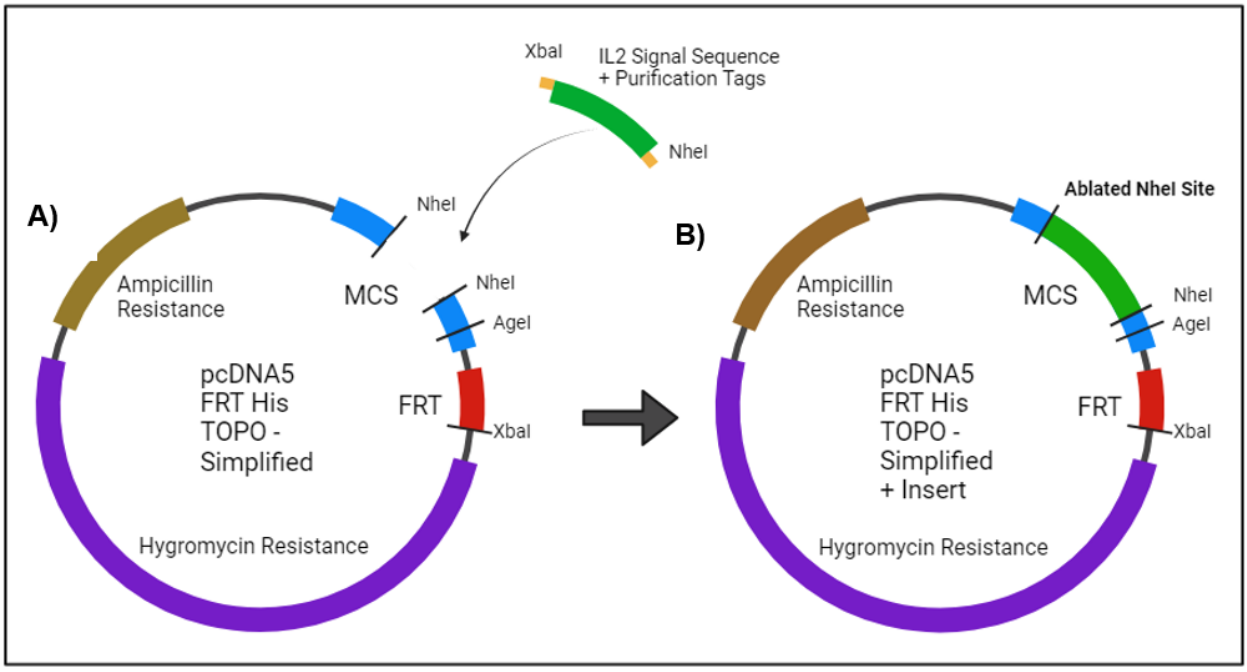

Figure 2.1: Generation of Modular Recombinant Sialyltransferase Vector using Compatible Sticky End Strategy. (A) linearized pcDNA5/FRT/V5 His TOPO vector digested with NheI with inclusion of antibiotic resistance genes, multiple cloning site, and FRT recombination region. **(B)** pcDNA5/FRT/V5 His TOPO post-ligation with insert sequence containing 5' XbaI sticky end and 3' NheI sticky end in multiple cloning site.

Once the vector was generated and doubly digested with NheI and AgeI, sialyltransferase sequences with 5' NheI and 3' AgeI restriction sites were double digested with the respective restriction enzymes. Then, ligations were carried out between the respective truncated sialyltransferase sequences to produce the complete vector for transfection into CHO Flp-In cells. However, when expression of hST6Gal1 was assessed using the initial cloning design, very little to no expression of the desired soluble sialyltransferases were detected. This led us to reassess the cloning design with the goal of improving expression yield by using a fusion strategy, as the Moremen group had previously demonstrated with GFP fusion strategies. Work published by the Anthony group demonstrated successful expression of hST6Gal1 constructs by fusing an IgG_1 Fc domain to the N-terminus of the catalytic domain of the sialyltransferase, which we emulated[97]. A new cloning strategy was developed using similar principles to that of the original design with

three notable changes. First, a DNA sequence encoding the constant domain of human IgG_1 (Fc) was added to the 5' end of the recombinant sialyltransferase sequence. Second, a TEV protease consensus sequence was added directly downstream of the IgG_1 Fc and upstream of the NheI digestion site. Finally, glycine spacers were added in-frame between the two purification tags, as well as 5' and 3' ends of the IgG_1 Fc sequence to allow for increased flexibility. All enzymes expressed in this work use this strategy and are referred to as 'Fc constructs'. The differences in the DNA templates and the final protein structures between the initial design and the final Fc construct design are outlined below **(Figure 2.2)**. The Fc-construct strategy led to successful expression of functional sialyltransferases in the CHO Flp-in mammalian expression system.

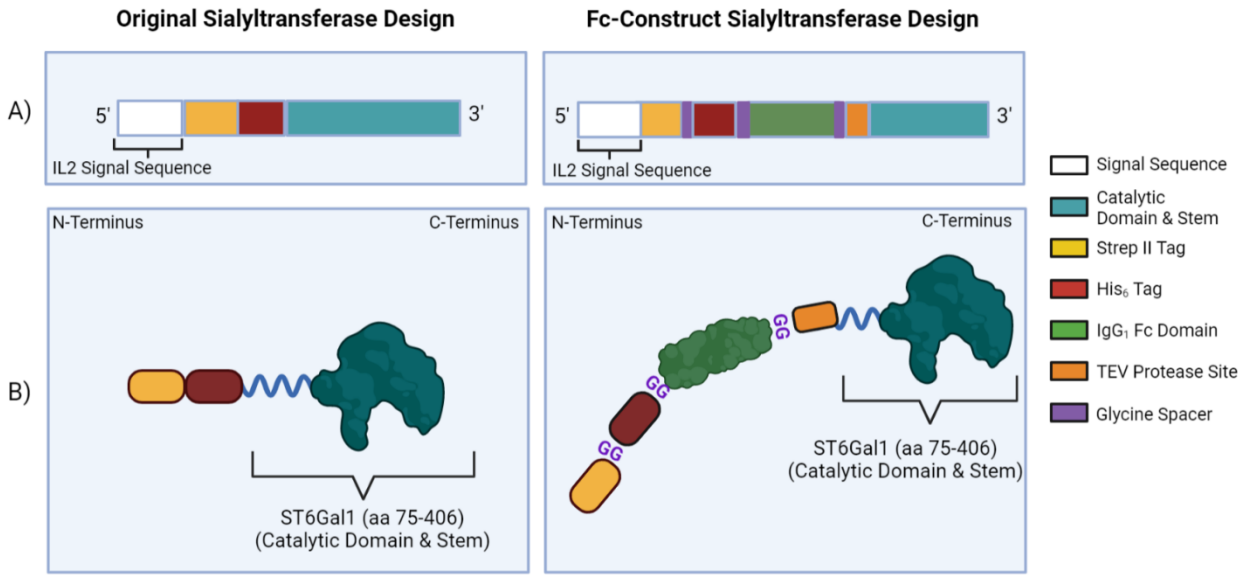

Figure 2.2: Cloning Strategies for Expression of Recombinant Sialyltransferases. A) Encoded DNA ligated into MCS of expression vector for original (left panel) and Fc-construct (right panel) cloning strategies for ST6Gal1. **(B)** Pictorial representation of expressed protein for original (left panel) and Fc-construct (right panel) cloning strategies for ST6Gal1

2.2.2: Quantitative Measurement of Fc-construct Expression by ELISA

To quantify the expression yield directly from cultured supernatants, an ELISA (Enzyme-Linked Immunosorbent Assay) was developed, wherein the capture antibody targeted the IgG_1 Fc present on the Fc-constructs. To detect the amount of target protein present in the plate well, a secondary Streptactin-HRP conjugate was used to bind the Strep-tag II **(Figure 2.3)**.

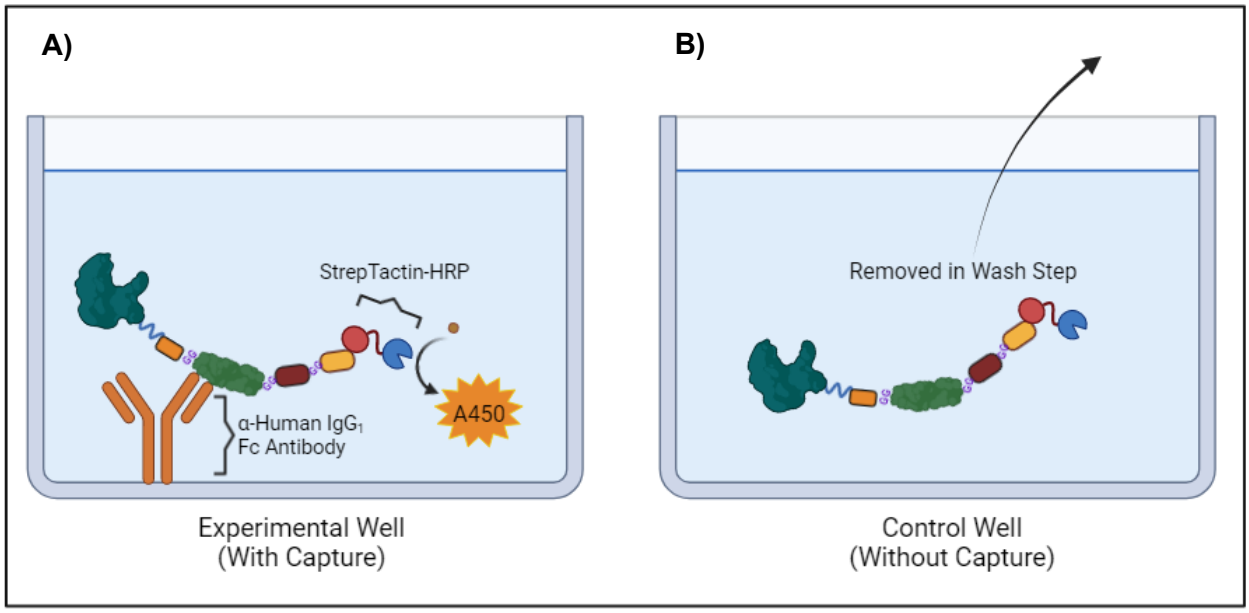

Figure 2.3: Experimental and Control Wells in ELISA Strategy. (A) Experimental well characterized by presence of α-Human IgG_1 Fc Antibody. Streptactin-HRP is retained through washing and produces a colorimetric signal at 450 nm. **(B)** Control well characterized by absence of α-Human IgG_1 Fc Antibody. Streptactin-HRP is not retained through washing and produces limited colorimetric signal at 450 nm.

To validate the assay, soluble Siglec proteins bearing both the Fc and Strep-Tag II were used as positive controls[98]. Initially, Siglec-5-Fc's signal generation was very high with a linear range between 0-5 µg/mL. However, the 'without capture' controls exhibited signal just as high as the 'with capture' wells (**Figure 2.4A)**. The Siglec-5-Fc used for establishing the ELISA was stored at -80°C after being lyophilized. However, CD33-Fc (Siglec-3 Fc) constructs that were stored at -80°C without lyophilization generated a specific signal in the assay **(Figure 2.4B)**. While the signal

generated against frozen target protein was lower than that generated by lyophilized protein, the signal generated in the 'no capture' control of the frozen protein remained at baseline. After tuning the ELISA conditions to increase the signal, a standard curve against Siglec-6-Fc (not lyophilized) was generated without background signal issue **(Figure 2.4C)**.

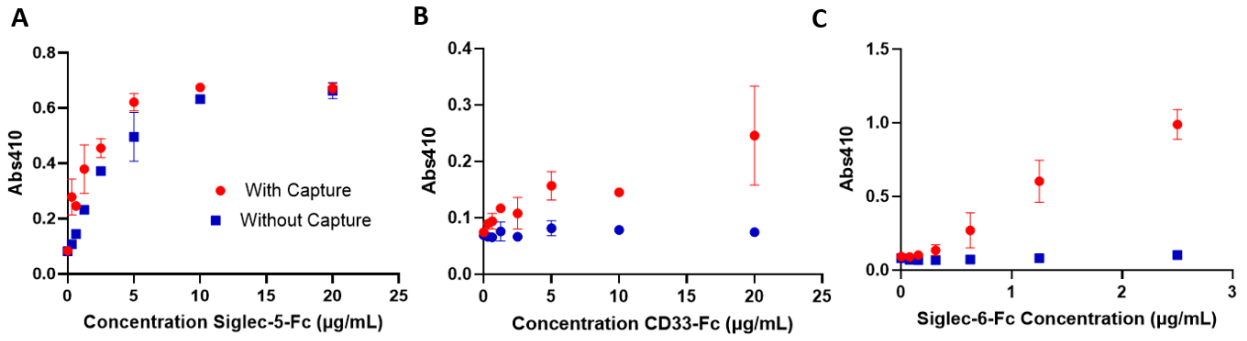

Figure 2.4: Siglec-Fc Constructs Generate Non-Specific Signal in ELISA. (A) Assessment of non-specific signal generation using Siglec-5-Fc (lyophilized) visualized at 410 nm. Error bars represent standard deviation (n=2). **(B)** Assessment of specific signal generation using CD33-Fc (non-lyophilized) visualized at 410 nm. Error bars represent standard deviation (n=2). **(C)** Representative standard curve of Siglec-6-Fc (non-lyophilized) after signal optimization visualized at 410 nm. Error bars represent standard deviation (n=3). **(A-C)** A410 represents raw absorbance at 410 nm.

With the optimized assay demonstrating specificity and quantifiability in the linear range of a standard curve between 0-5 µg/mL, the ELISA strategy was used to optimize the expression of the Siglec-7-Fc construct. Siglec-7 was used initially, as construction of the sialyltransferase Fc-constructs was being completed. Three variables were altered in the expressions to assess their effects on protein yield as measured by the ELISA: temperature of expression (32 °C vs. 37 °C), amount of FBS in media (5% vs. 2.5%), and amount of antibiotic pen-strep in media (100 µg/mL vs. 25 µg/mL). Quantified expression yields of all 8 expression conditions were calculated in triplicate **(Figure 2.5)**. These findings demonstrate ~two-fold improvements in recombinant protein expression yield at 32°C compared to 37°C when grown in media containing 5% or 2.5% FBS. While showing no significant difference between antibiotic and FBS concentrations tested.

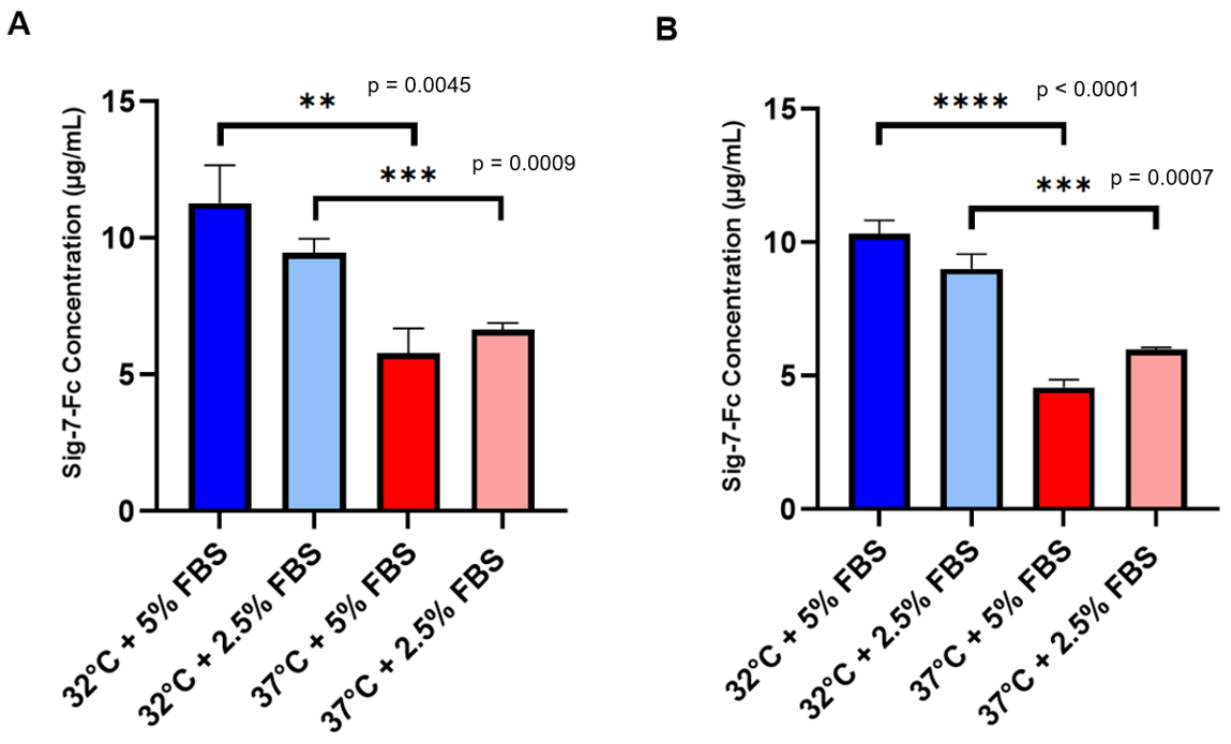

Figure 2.5: Titration of Temperature, Media Serum Protein, and Pen-Strep to Determine Optimal Expression Conditions for Soluble Recombinant Protein in CHO Flp-in Mammalian Expression System. (A) Quantified expression yield of Siglec-7-Fc measured directly from CHO cell supernatant containing 100 µg/mL Pen-Strep. **(B)** Containing 25 µg/mL Pen-Strep. **(A-B)** Grown for 7 days (post-confluence) in DMEM-F12 media supplemented with 10 mM HEPES. Post-expression supernatants were diluted 24-fold prior to incubation. Quantification was multiplied by the concentration factor for final quantification. Error bars represent standard deviation (n=3). P-values calculated from unpaired two-tailed t-test (degrees of freedom = 4).

Using this ELISA strategy, the expression yields of sialyltransferase Fc-constructs were measured. Despite using the same protocol, an issue appeared when testing supernatant derived from Fc-construct hST6Gal1. The background signal generated in the 'no capture' control wells were identical to the signal generated from wells which contained capture antibody. Absorbance signal from experimental and control wells for ST6Gal1 expressed at both 32 °C and 37 °C are outlined below **(Figure 2.6)**. Protein concentration was not calculated as the non-specific signal prevented accurate quantification. From Bradford assays performed post-purification, ST6Gal1 Fc-construct expressed at 32 °C was quantified at ~1.5 mg/L. These findings could not be

corroborated with the ELISA strategy, as Fc-construct sialyltransferases generate non-specific background signal. However, the ELISA can quantify the expression of Siglec-Fc constructs directly from media. When expressed in the 32 °C condition, both the signal and background of the ST6Gal1 Fc-construct were three-fold higher than the 37 °C condition, suggesting increased expression that could not be converted to absolute concentration due to the background issue.

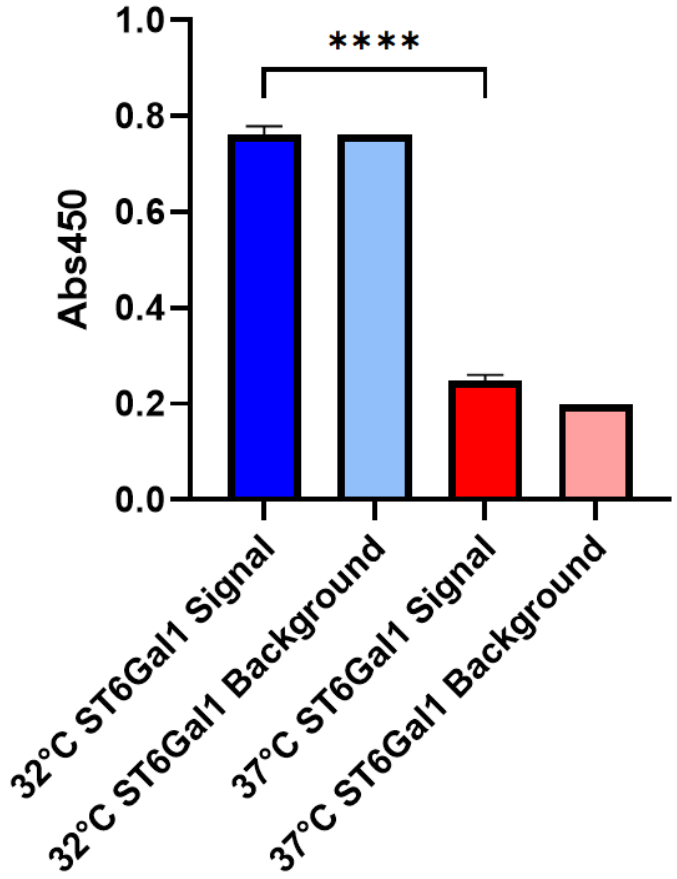

Figure 2.6: Non-Specific Signal in ELISA for Sialyltransferase Fc-Constructs. CHO cells transfected with hST6Gal1 Fc-construct were expressed for 7 days (post-confluence) in DMEM-F12 media supplemented with 5% FBS, 10 mM HEPES, and 100 µg/mL pen-strep. Post-expression supernatants were diluted three-fold prior to incubation. Error bars represent standard deviation (n=3). p-values calculated from unpaired two-tailed t-test ($p<0.0001$). Abs450 represents the raw absorbance signal at 450 nm. Background signal is a single replicate (n=1).

2.2.3: Purification of Sialyltransferase Fc-Constructs

Once expression of soluble sialyltransferases was established, a purification strategy was optimized. A two-step purification strategy was employed to take advantage of the His_6 and Strep-Tag II tags, with a Nickel affinity and Streptactin column, respectively. For the first step a Nickel-Sepharose column was used because media contains biotin, which could affect purification of supernatants directly over a StrepTactin column. Eluted protein from the Nickel column was diluted in StrepTactin Column Buffer (Buffer W) and run over the StrepTactin column. Eluted protein was dialysed into 20 mM Tris, 150 mM NaCl, pH 8 buffer. This buffer was chosen due to its capability with commercial sialyltransferase assays and previous work on glycosyltransferase assays[99]. After dialysis, the protein was concentrated by spin filtration and protein concentration was assessed by Bradford assay. Finally, 10% glycerol was added to the total volume as a cryoprotectant, and the solution was distributed into aliquots varying from 10-20 µl for long-term storage at -20°C. SDS-PAGE was run on samples collected during various time points of the purification to assess purification efficiency **(Figure 2.7)**.

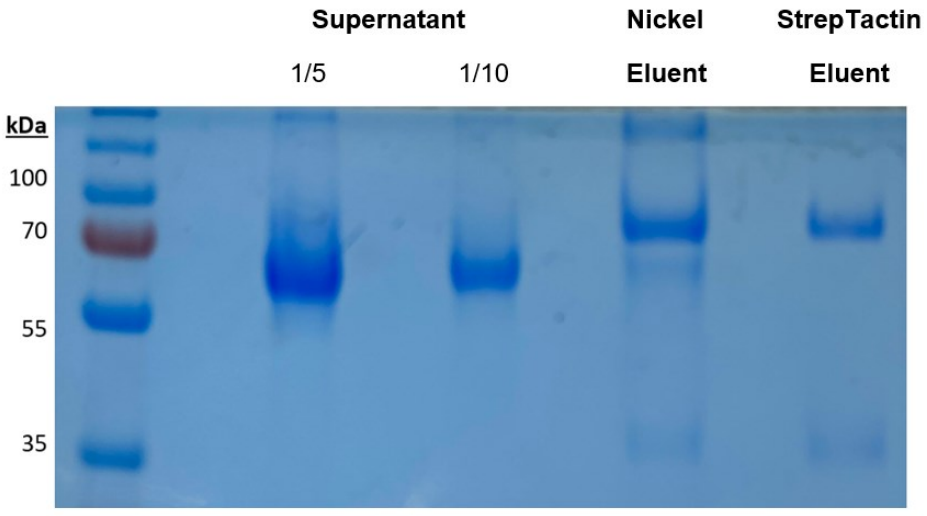

Figure 2.7: Validation of Dual-Purification Strategy to Purify ST6Gal1 Fc-construct. Wells were loaded with 20 µL of post-expression supernatant diluted five and ten-fold, or 20 µL of undiluted eluent from Nickel or StrepTactin purification. Protein ladder for size assessment in kDa loaded in the left lane.

Lanes containing diluted supernatant demonstrated the presence of a strong contaminant band at ~60 kDa corresponding to the BSA (bovine serum albumin). After elution from the Nickel column, a strong band representing the sialyltransferase Fc-construct appeared at ~80 kDa but contaminant bands remained. After elution from the StrepTactin column, all contaminant bands were undetectable demonstrating efficient purification of Fc-construct hST6Gal1. Using this purification strategy, four of the twenty GT29 family sialyltransferases have been successfully purified from expression supernatant, as shown on an SDS-Page Gel with 2.3 µg of each purified sialyltransferase loaded per lane **(Figure 2.8)**. ST8Sia4 was the only enzyme that was transfected successfully but failed to express in the mammalian CHO system used in this work.

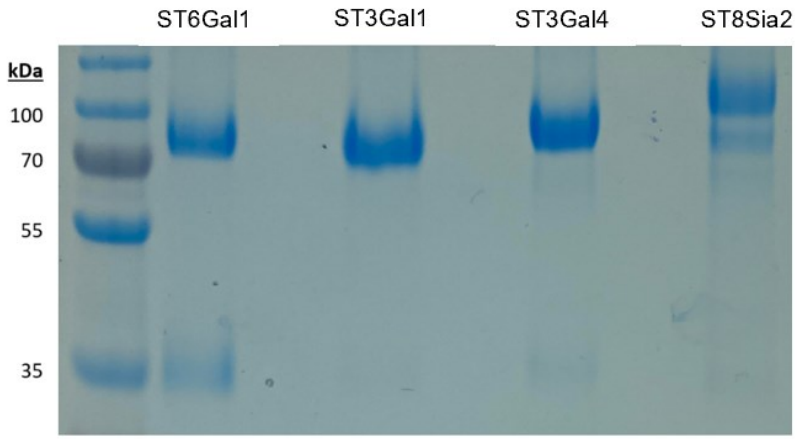

Figure 2.8: Sialyltransferase Fc-constructs Successfully Expressed in CHO Flp-in Expression System. Wells were loaded with 2.3 µg of protein as calculated from Bradford assay. SDS-PAGE was run in reducing conditions and were visualized with Coomassie staining. Protein ladder for size assessment in kDa loaded in the left lane.

2.2.4: Functional Validation of Sialyltransferase Constructs

To assess the function of the expressed and purified recombinant sialyltransferases, a UMP/CMP-Glo Assay was initially used. This luminescence-based coupled assay measures the amount of free nucleotide monophosphate CMP with high sensitivity[56]. Specifically, CMP is enzymatically converted to ATP, which serves as a substrate for a luciferase reaction. As all

sialyltransferases use CMP-Neu5Ac as a donor, one catalytic cycle leads to production of one molecule of CMP. A standard curve of CMP is used to convert luminescence values (RLU) to concentration of CMP-Sia transferred by the ST. It is important to note that this assay must be stopped prior to measurement. The addition of the coupled components from the commercial kit not only converts the CMP to luminescence, but also stops the ST reaction.

As a preliminary test prior to optimization and quantification of the assay, the activity of hST6Gal1 was measured against two disaccharide acceptors. Based on previously reported literature, hST6Gal1 is expected prefer LacNAc as an acceptor compared to Lactose[23]. Reaction mixtures were prepared with various concentrations of hST6Gal1, 100 µM CMP-Neu5Ac and 1 mM LacNAc or 1 mM Lactose acceptor. Reactions were incubated at 37°C for 15 minutes and quenched by addition to the CMP-Glo detection buffer. The luminescent signal generated was quantified for the various enzyme conditions, demonstrating that the hST6Gal1 was providing a signal in the assay, and that the signal was far greater when incubated with a LacNAc acceptor at all concentrations tested (**Figure 2.9).**

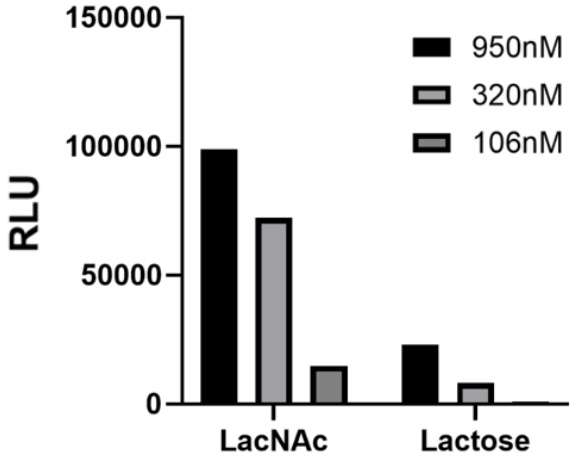

Figure 2.9: ST6Gal1 Fc-construct Exhibits Preferential Activity to LacNAc. Reaction was quenched at 15 minutes after enzyme incubation at 37 °C in 166 mM MOPS, MES, and Tris Buffer (pH 6). Reaction mixtures contained LacNAc or Lactose acceptors (1 mM), donor sugar CMP-Sia (100 µM), and various concentrations of hST6Gal1. RLU represents background subtraction from wells containing only CMP-Sia (100 µM). Each reaction condition was assessed in singlicate (n=1).

To convert the relative luminescent signal (RLU) to a concentration of CMP, a standard curve was generated from 0-50 µM CMP **(Figure 2.10)**. The assay demonstrated clear linearity in this CMP range and was used for all subsequent quantification. To assess the function of hST6Gal1, a series of reaction mixtures were prepared with an asialo-glycoprotein acceptor (asialofetuin), and 3 concentrations of native donor sugar CMP-Neu5Ac. To assess linearity of reactions over time, reaction mixtures were incubated at 37 °C and quenched at various time points by incubation with the CMP-Glo detection buffer components**.** A linear rate of luminescent signal generation over time was observed, which was then converted to CMP-Sia generated as per the standard curve for each condition **(Figure 2.10)**. Based on the quantification, reaction progress appeared to be <20% for all tested conditions at 20 minutes. This was desired, as reactions approaching completion lose linearity due to a combination of substrate depletion and product inhibition.

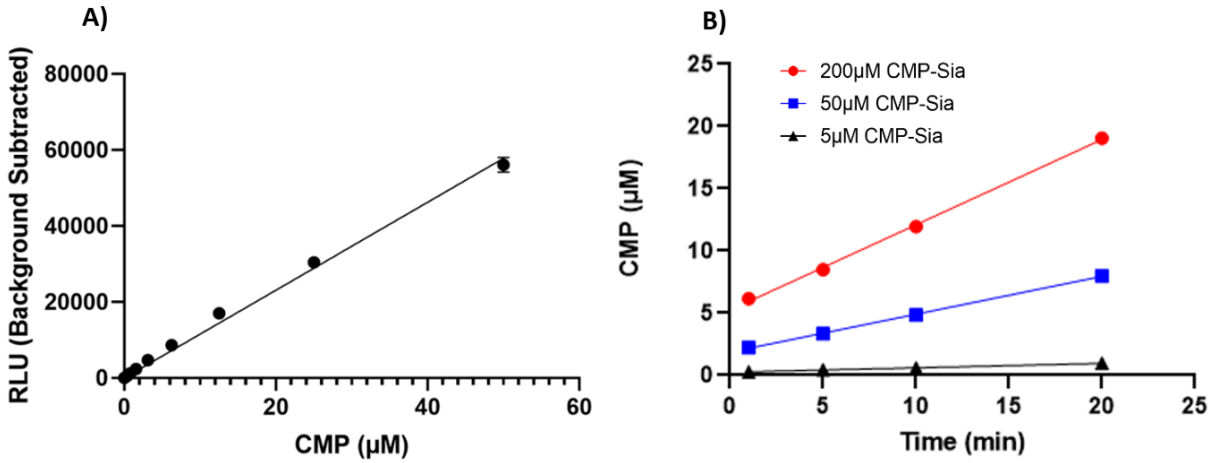

Figure 2.10: CMP-Glo Standard Curve Generation for Quantification of Sialyltransferase Reaction Progress. (A) Standard curve generated using CMP at 0-50 µM. Each concentration was tested in triplicate (n=3). Wells containing 20 mM Tris 150 mM NaCl buffer (pH 8) were used for background subtraction **(B)** Quantified hST6Gal1 reaction stopped at various timepoints for linearity assessment. Reaction was quenched at 1, 5, 10 and 20 min after incubation at 37 °C in 20 mM Tris 150 mM NaCl buffer (pH 8). All reaction mixtures contained 50 µM asialofetuin (glycoprotein acceptor), 33 nM ST6Gal1 and a variable concentration of donor sugar CMP-Sia. Each point represents a well in singlicate (n=1). Trendlines represent simple linear regression plotted in PRISM (R^2 > 0.99 for all conditions). RLU signal was converted to CMP concentration using standard curve. Background wells containing 200, 50 and 5 µM CMP-Sia were used for background subtraction of each condition.

With reaction rates in a linear across the wide range of donor sugar CMP-Sia concentrations, assays were carried out with eight concentrations of CMP-Neu5Ac in triplicate and quenched after 20 minutes. Rates were converted to µmoles of substrate produced per minute per mg of ST6Gal1. The data was fit to a nonlinear regression (Michaelis-Menten) curve using GraphPad PRISM **(Figure 2.11)**. A K_M value (95% C.I) for CMP-Neu5Ac was calculated to be 140 µM (99 µM – 210 µM). The maximal catalytic efficiency $V_{max}/[E_0]$, the y-axis asymptote, was calculated as 0.37 µmol min^{-1} mg^{-1}. Dividing $Vmax[E_0]$ by the K_M value provided the $V_{max}/[E_0]K_M$ value of 0.0026 µmol μM^{-1} min^{-1} mg^{-1}.

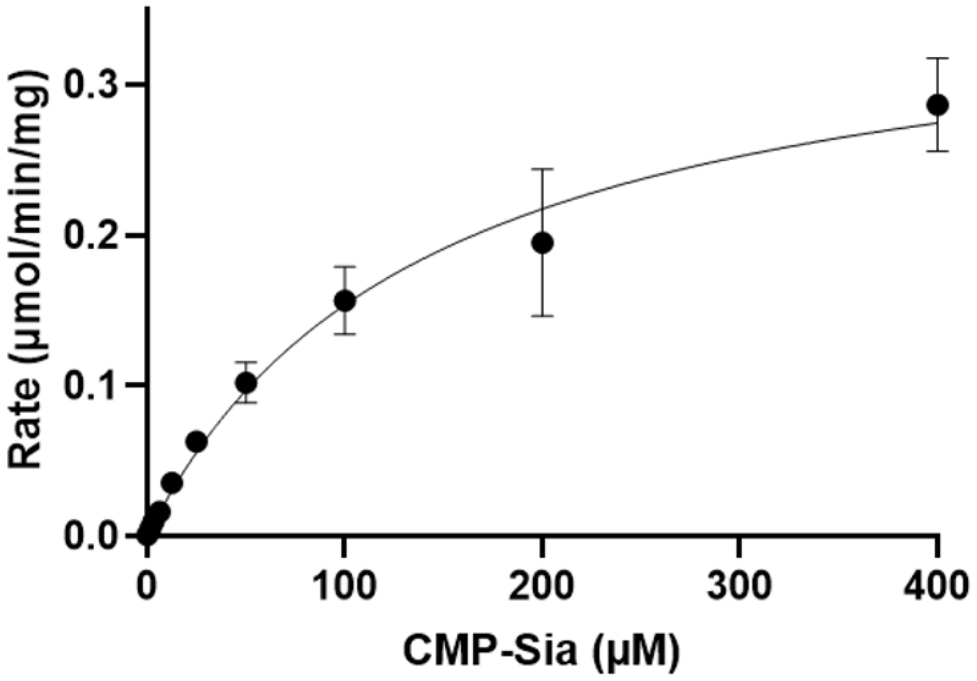

Figure 2.11: Michaelis-Menten Curve for Assessment of CMP-Sia K_M for ST6Gal1. Reaction was quenched at 20 minutes after 37 °C incubation in 20 mM Tris, 150 mM NaCl buffer (pH 8). Reaction mixtures contained 50 µM asialofetuin (glycoprotein acceptor), 33 nM ST6Gal1, and various concentrations of donor sugar CMP-Sia. RLU values collected were converted to specific activity by converting RLU to CMP (µmol) and dividing by both time (min) and total enzyme (mg)**.** Wells containing each concentration of CMP-Sia were incubated in singlicate and used for background subtraction for each condition. Each concentration was tested in triplicate, error bars represent standard deviation (n=3).

2.3: Discussion

2.3.1: Cloning Designs for Expression of Soluble Sialyltransferases

A primary goal of this work was to express functional sialyltransferases from all 4 subfamilies of the GT29 enzymes. ST6Gal1, ST3Gal1, ST3Gal4, and ST8Sia2 have been functionally expressed using the Fc-construct design strategy outlined, representing 3 of the 4 subfamilies. As the first sialyltransferase to be successfully expressed and functionally verified in this work, ST6Gal1 will be treated as the prototypical example. Based on the post-purification quantification of total protein, the expression yield of the ST6Gal1 Fc-construct was ~1.5 mg/L. While our cloning strategy and workflow has successfully expressed the enzymes listed above, it is important to note that ST8Sia4 was also transfected into CHO Flp-in cells and no detectable recombinant protein expression was observed. The potential causes of this failure to express as well as potential strategies to address them will be discussed here.

One consideration is the signal sequence chosen to replace the native signal sequence in the recombinant design. We elected to use the IL2 (Interleukin-2) signal sequence for this purpose, but it is important to note that this may not be optimal in our expression system. As previously mentioned, published work by the Moremen group was used to guide the cloning designs. In their work, they used the *Trypanosoma cruzi* lysosomal α-mannosidase signal sequence and were able to express ST6Gal1 at over 100 mg/L yield using HEK-293 cells and Gateway cloning[95]. This represents a >50-fold secretion efficiency when compared to the expression system developed in this work. It is also important to note that they cloned all members of the GT29 family with variable efficiency, except for ST8Sia5 which failed to express. While the expression systems and vectors used are different, it is possible that the chosen IL2 signal sequence may not be a sufficient driver of expression for certain sialyltransferases, such as ST8Sia4. To elucidate this effect, comparing the expression of identical constructs with various signal sequences would be required. It is possible other signal sequences would improve the yield

of poorly expressed sialyltransferases. Another potential strategy would be mutation of the wild type IL2 signal sequence, as previous research has indicated that mutations that increase hydrophobicity early in the signal sequence may lead to significantly higher expression of recombinant protein in mammalian culture[96]. Using the initial sialyltransferase design without the IgG_1 Fc fusion protein expression was not detected with either signal sequence. It may be interesting to compare the two signal sequences with the Fc-construct, as it is functionally expressed, and therefore differential expression may be observed.

Other considerations for optimizing expression include altering the fusion protein strategy and changing the expressing cells. Fusion protein strategies such as the IgG_1 Fc fusion used in this work have been used to increase protein production of especially hard-to-express recombinant proteins. Other fusion proteins have been used including super folder GFP (sfGFP) and Maltose Binding Protein (MBP). Exploring other fusion protein tags may be an avenue worth exploring to increase the expression yield. While the CHO Flp-in cells have been successfully utilized for my recombinant expression strategy it is important to note that other Flp-in cell lines are available. These cell lines also express the FRT recombination site needed to generate stable transfectants and could therefore be transfected directly with the vector generated in this work and compared to CHO. Another consideration is that these cell lines are adherent, limiting the expression yield due to confluence of cells during the expression. Other cell lines such as the HEK293-Freestyle line are grown in shaking incubators as a suspension, typically leading to far greater recombinant protein yield. For future optimization of expression both the fusion protein and cell types used for expression should be assessed, especially for those sialyltransferases which fail to express in the current strategy.

2.3.2: ELISA Strategy for Optimization of Soluble Sialyltransferase Expression

As a method used to determine recombinant protein expression directly from cultured cell supernatant, it was important that the assay generated a highly specific signal. However, the use of lyophilized Siglec-5-Fc as a standard did not satisfy this requirement. This finding suggested that the likely cause of the non-specific signal observed was a consequence of lyophilization. I hypothesize that lyophilization of recombinant IgG_1 Fc-tagged proteins may lead to the formation of protein aggregates upon resuspension, leading to generation of the observed non-specific signal in the assay. This hypothesis was not investigated any further in this work and is therefore not conclusive. However, the impact of lyophilization-storage strategies in the context of quantitative assays is a question that does warrant further investigation.

The initial motivation for developing the strategy was for the quantification of Fc-construct sialyltransferases directly from supernatant. However, the supernatant containing recombinant ST6Gal1 exhibited a background issue like that observed for lyophilized Siglec-5-Fc**.** Sialyltransferase Fc-constructs were not lyophilized, so the cause of this background signal must be related to the inherent properties of the construct itself. One potential cause of this may be aggregation during purification or storage. Another cause may be that ST6Gal1 may adhere to the blocking proteins used or remove them to allow for nonspecific plate binding. This issue prevented quantification of absolute concentration for the Fc-construct of ST6Gal1. Despite this, ST6Gal1 Fc-construct supernatant grown at 32 °C demonstrated a four-fold increase in absorbance at 450 nm when compared to 37 °C. It was expected that increased signal correlates with protein concentration, and therefore this temperature was chosen for all future expressions. Given the poor expression yields of sialyltransferase constructs generated in this work, identifying the source of this non-specific signal will be critical. Addressing this will allow for quantification of sialyltransferase constructs directly from cultured supernatant, allowing for direct measurements of expression efficiency.

2.3.3: Purification of Sialyltransferase Constructs

To illustrate the effectiveness of the two-step purification, samples from various steps of the purification were collected and separated by SDS-Page to assess their purity. Lanes ran with cultured supernatants possessed a strong band at ~60 kDa, expected to be the serum protein BSA present in the media used to culture the cells. After the Nickel-Sepharose column purification, a weak band representing BSA is still present at ~60kDa, while a large band appeared at ~75 kDa. The presence of a residual band at 60 kDa indicates that the use of a Nickel column may not be sufficient for thorough purification. After the StrepTactin column purification, the weak band at ~60 kDa was no longer detectable, indicating successful purification of the recombinant protein from the serum protein components. Interestingly, the StrepTactin eluent lane clearly demonstrated the formation of a band at ~35 kDa, not present in the previous stages of purification. This may be due to the presence of a β-secretase site present in the primary structure of the hST6Gal1 catalytic domain as previously described[97]. It is also possible that the protein is being degraded by another mechanism, such as cleavage at the TEV protease site.

With the two-step purification strategy presented, successful purification of ST6Gal1, ST3Gal1, ST3Gal4 and ST8Sia2 was demonstrated**.** The predicted weights of the recombinant sialyltransferases were 66.9 kDa, 61.6 kDa, 61.9 kDa, and 64.6 kDa for ST6Gal1, ST3Gal1, ST3Gal4 and ST8Sia2 respectively. However, the bands observed for each expressed construct ran higher than the 70 kDa ladder band. This difference may be explained by the presence of elaborated glycosylation sites present on the enzymes themselves. Based on information gathered from UniProt, hST6Gal1 possesses two N-linked glycosylation consensus sequences, ST3Gal1 and ST3Gal4 possess four, and ST8Sia2 possesses six. Therefore, the increased observed weight on SDS-PAGE may be due to the presence of elaborated N-glycans at these sites. ST8Sia2 is found at a much higher size when compared to the other sialyltransferases. This is not unexpected, as ST8Sia2 is known to use its own glycan’s as acceptors for formation of

poly-sialic acid chains. This feature of ST8Sia2 (and ST8Sia4) is known as 'auto-polysialylation' and has been demonstrated *in vivo* and *in vitro*[100,101]. It is then reasonable to assume that in a cell overexpressing active ST8Sia2 constructs, the enzymes will be able to generate long poly-sialic acid chains on themselves leading to an increased weight on SDS-PAGE. This could be assessed by the application of glycosidases such as PNGase F, which catalyze the removal of N-linked glycans on glycoproteins. This has not been performed in this work but is a common enzymatic strategy which would address the observed weight discrepancies.

2.3.4: Functional Validation of Sialyltransferase Constructs

To initially validate the function of ST6Gal1, Lactose and LacNAc were compared as accepting substrates. While the disaccharide acceptors are structurally similar, the N-acetyl functionality on LacNAc is not present on Lactose and has been demonstrated to significantly alter the reaction rate of ST6Gal1[23]. Observing the same selectivity in the CMP-Glo assay gave us confidence that the expressed construct was functional. It is important to note that the donor sugar CMP-Sia used in the assay is capable of hydrolyzing during the reaction. CMP generated by CMP-Sia hydrolysis provides a signal in the CMP-Glo assay, which was accounted for by background subtracting wells containing only CMP-Sia. This initial work was performed at pH 6, and in acidic environments the rate of hydrolysis is expected to increase, causing an elevated background signal. These observations motivated a change to a pH 8 Tris buffer for subsequent experiments, due to its use in commercial applications. However, looking back this may not have been a good choice, as recent literature studying bacterial sialyltransferases *Nm*CSS and *Pm*ST1 have demonstrated that Tris buffer can act as an acceptor[102], however this has not been demonstrated with GT29 family sialyltransferases.

To assess reaction linearity, various reactions were performed over a range of CMP-Sia concentrations. Interestingly, the slopes generated were linear with respect to enzyme, but did not start at the origin. This is a concerning observation as the slope of the reaction progress

should ideally intersect with the origin. The source of this issue is not due to background, as background subtractions were carried out appropriately. One explanation is that sialyltransferases may undergo a process known as “burst kinetics” whereby the initial rate of an enzymatic reaction is very high, stabilizing at a normal rate shortly after the start of the reaction. More work needs to be done to elucidate this observed ‘burst’ and identify if the observation is accurate to the action of the enzyme, or if it represents a problematic artefact in the assay.

As a final characterization of the ST6Gal1 generated in this work, a Michaelis-Menten plot was plotted to calculate the enzymatic parameters of ST6Gal1 against a range of CMP-Sia concentrations. Ideally, the Fc-construct would generate a similar K_M value to those previously described in the literature for human ST6Gal1. By converting the RLU data in the linearity assessment to a concentration CMP using the standard curve, we determined that reaction progress was <20% complete for all tested CMP-Sia conditions (5, 50 and 200 μM). This was important to verify, as robust Michaelis-Menten curves require many concentrations of substrate but must be assessed during the early stage (linear stage) of reactions to capture initial rates. Eight different CMP-Sia concentrations were assessed in reaction mixtures and plotted in units of specific activity (μmol/min/mg enzyme) to generate the Michaelis-Menten Plot. A K_M value of 140 μM was calculated, which is larger than but reasonably close to previous values collected for recombinant hST6Gal1 (50-120 μM)[103–105]. This difference may be due to the use of asialofetuin as the acceptor in the assay or the use of slightly alkaline pH 8 buffer instead of slightly acidic pH 6 buffers. Most literature citing a K_M value for donor sugar CMP-Sia does so using LacNAc or other oligosaccharides as an acceptor, not a glycoprotein such as asialofetuin. It is important to note that when the highest concentration of CMP-Sia was removed from the fit, the K_M calculated was within the literature range at 86 μM. It is important to note that the exact molar concentration of ST6Gal1 Fc-construct was not accurately characterized. Primarily, this is due to the presence of the uncharacterized ~35 kDa band observed on SDS-PAGE for ST6Gal1 Fc-construct. When

calculating catalytic efficiency of any enzyme (V_{max}/K_M), the molar concentration of enzyme active sites must be known. Due to uncertainty regarding the concentration and activity of ST6Gal1, approximations using the mass of the enzyme were preferred over moles. $V_{max}/[E_0]$ represents the maximal specific activity and was calculated to be 0.37 μmol min^{-1} mg^{-1}. Dividing this value by the K_M calculated yields an approximation of the second-order rate constant ($V_{max}/[E_0]K_M$) for ST6Gal1 against CMP-Sia, 0.0026 μmol μM^{-1} min^{-1} mg^{-1}. These values cannot be directly compared to literature to assess the reaction rate. Assuming accurate enzyme concentrations, the reaction rate was plotted in units of μM/min and a V_{max} value was calculated at 0.87 μM/min. Dividing by the concentration of ST6Gal1, 0.033 μM, k_{cat} was found to be 26.4 min^{-1}. These values compare favorably to previous literature, with k_{cat} values of 11 min^{-1} for human ST6Gal1[105] and 35.6 min^{-1} for rat ST6Gal1[106]. Notably, rates and catalytic efficiencies will depend on reaction conditions such as the pH of the reaction buffer and identity of the ST acceptor. The reaction rate presented in this work was expected to be lower than literature values, due to the different reaction conditions used. The use of asialofetuin as an acceptor compared to the literatures use of LacNAc and other disaccharide derivatives may play a factor. The reaction was performed in pH 8 Tris buffer, which may also explain reduced rates as optimal ST6Gal1 activity has been observed near pH 6[26].

2.4: Conclusions

This chapter demonstrates the successful cloning and purification of recombinant sialyltransferases ST6Gal1, ST3Gal1, ST3Gal4, and ST8Sia2. The development and optimization of an ELISA strategy allowing for quantification directly from cultured supernatant to assess protein expression is also presented. Lastly, the function of ST6Gal1 was validated by CMP-Glo assay and confirmed to exhibit kinetic parameters and substrate specificities with previously established cloning strategies existing in the literature.

2.5: Materials and Methods

2.5.1: Cloning and Expression Materials Tables and Methods

Amplification of Recombinant DNA Sequences (PCR).

To perform PCR, 50 µl reactions were prepared as follows. 10 µl of 5X HF buffer was added to a PCR tube, followed by the addition of 1 µL of each primer from 100 µM stocks purchased from IDT. Then, 1 µL of dNTP's purchased from NEB at 10 mM per NTP was added to the reaction mixture. Volume of DNA template stock depended on initial concentration, and ~250 ng of DNA template was added to the reaction mixture. Finally, the volume was brought up to 49.5 µl with nuclease-free water. Recommended temperature and times for the thermocycler were used as suggested by NEB. Once the thermocycler reached the initial temperature, 0.5 µl of Phusion DNA Polymerase was added into each reaction tube and vortexed to mix completely. Finally, PCR tubes were placed in the thermocycler for ~1 hour to complete the cycling protocol. Complete PCR mixtures were either used directly in Gel Electrophoresis, or stored at 4°C **(Table 2.1).**

Forward primers were generated with variable overlap (16-24 bp) to the truncated 5' end of the native ST sequence. This design included a 5' overhang encoding for the NheI restriction site (G/CTAGC) as well as 6 non-complementary bases (AGCAGC) added upstream of the NheI site. Reverse primers were generated as the reverse compliment of the 3' end of the native sialyltransferase sequence with variable overlap (16-24bp). This design included a 5' overhang encoding for the AgeI (A/CCGGT) restriction site, as well as the 6 non-complementary bases (AGCAGC).

Table 2.1: Amplification of Recombinant DNA Sequences (PCR) Materials

Primer	Target Sequence (5'-3')	Manufacturer
ST6Gal1-F (5'NheI)	AGCAGCGCTAGC**CGCCAGACCCTCGGCAGTCTC**	IDT
ST6Gal1-R (3' AgeI)	AGCAGCACCGGT**TCAGCAGTGAATGGTCCGG**	IDT
ST3Gal4-F (5'NheI)	AGCAGCGCTAGC**GAGAAGAAGGAGCCGTGCCTC**	IDT
ST3Gal4-R (3' AgeI)	AGCAGCACCGGT**TCAGAAGGACGTGAG-GTTCTTGATAG**	IDT
ST3Gal1-F (5'NheI)	AGCAGCGCTAGC**AGACTGATCAAGCACAGG**	IDT
ST3Gal1-R (3' AgeI)	AGCAGCACCGGT**TCATCTCCCCTTGAAGATCC**	IDT
ST8Sia2-F (5'NheI)	AGCAGCGCTAGC**AACGGCTCCTCATCACCAG**	IDT
ST8Sia2-R (3' AgeI)	AGCAGCACCGGT**CTACGTGGCCCCATCGCAC**	IDT
ST8Sia4-F (5'NheI)	AGCAGCGCTAGC**AAAATCATTCGAAAGGCTG**	IDT
ST8Sia4-R (3' AgeI)	AGCAGCACCGGT**TTATTGCTTTACACACTTTCC**	IDT
N-Vector Block-F (5' XbaI)	AGCAGCTCTAGAATGTACAGGATGCAGC-TGCTGAGCTGC**ATCGCCCTGAGCCTG**	IDT
N-Vector Block-R (3' NheI)	GCTGCTGCTAGC**CCCCTGGAAG**	IDT
5x HF Buffer	E0553S	New England Biolabs
dNTP's	E0553S	New England Biolabs
Phusion Polymerase	E0553S	New England Biolabs

Agarose Gel Electrophoresis.

For large polynucleotides, such as pcDNA5 vectors, 0.8% agarose gels were prepared by mixing 0.32 g agarose with 40 mL 1X TAE Buffer. For smaller polynucleotides, 2.0% agarose gels were prepared by mixing 0.8 g agarose with 1X TAE Buffer. The mixture was then heated in a microwave until the agarose was fully dissolved. Then, 4 µL of SYBR Safe was added and mixed into the agar solution via. gentle swirling. Gels were then poured into a gel rack with a comb to

provide the wells of the agarose gel. Gels were left at R.T to set before use for at least 30 minutes. To load the gel, DNA samples were combined with the appropriate amount of 6x DNA Loading buffer to a final concentration of 1X, and the dyed PCR product was added to wells via. pipette. 1X TAE Buffer was used to cover the gel in a running chamber. Once loaded, the gels were run at 110-130 V for 30 minutes to allow for sufficient separation of the bands. The gels were then visualized under UV light and desired bands were excised via. razor for gel extraction **(Table 2.2).**

Table 2.2: Agarose Gel Electrophoresis Materials

Reagent	Detail	Manufacturer
UltraPure Agarose	0.8-2% in 1X TAE Buffer 16500-500	ThermoFischer Scientific
1X TAE Buffer	40 mM Tris Base 57.1 mL Glacial Acetic Acid 1 mM EDTA (S311-500)	ThermoFischer Scientific Fischer Chemical
SYBR Safe DNA Gel Stain	1:10000 dilution S33102	ThermoFischer Scientific
Gel Running Apparatus	Powerease 300W (PS0300)	Life Technologies
6X DNA Loading Dye Purple	B7024A	New England Biolabs
GeneRuler 1kb Plus Ladder	SM1333	ThermoFischer Scientific

DNA Purification from Agarose - Gel Extraction.

To perform Gel Extraction, excised gel fragments containing target genes were transferred to microcentrifuge tubes. To these tubes Binding buffer (ThermoFischer Scientific, K0691) was added in a 1 µL:1mg agarose gel ratio. Tubes were then incubated at 55 °C and periodically vortexed until the gel was completely dissolved. Then, 800 µL of the solubilized gel was loaded onto a GeneJET purification column. Purification columns were spun at 10,000 RCF for 1 min and the flowthrough was discarded. Then, 700 µL of Wash Buffer (ThermoFischer, K0691, diluted with 96% EtOH) was added to the column and spun at 10,000 RCF for 1 min. After discarding flowthrough, columns were spun empty for 1 minute at 10,000 RCF to remove residual wash buffer. To elute, 40 µL of water was added to the purification column and spun for 1 minute at 10,000 RCF. This flowthrough was collected in a microcentrifuge tube, containing the desired DNA, and extraction yields were calculated on a Nanodrop microvolume spectrophotometer.

Double Restriction Digestion of DNA using Restriction Endonucleases.

To perform restriction digestion, a 50 µL reaction mixture was prepared in a PCR tube. First, 5 µL of 10X CutSmart buffer was added, as well as 1-2 µg of DNA containing endonuclease sites. The remaining reaction volume is filled with Nuclease-free water. The reaction was initiated when 0.5 µL of restriction endonucleases were added. Multiple restriction enzymes can be added to a single reaction, leading to cleavage at multiple restriction sites. In this work, the 'double-digestion' strategy was frequently utilized with NheI and AgeI, for the digestion of both NheI sites (GCTAGC) and AgeI sites (ACCGGT). The reaction was then mixed by vortex and incubated at 37°C for 1 hour in a thermocycler. Once complete, the digested polynucleotides were removed, processing and size verification were carried out via agarose gel electrophoresis, and the DNA was then purified via. gel extraction **(Table 2.3).**

Table 2.3: Double Restriction Digestion of DNA with Restriction Endonucleases Materials

Enzyme	Recognition Site	Manufacturer
NheI-HF	G/CTAGC	New England Biolabs
AgeI-HF	A/CCGGT	New England Biolabs
BamHI	G/GATCC	New England Biolabs
XbaI	T/CTAGA	New England Biolabs
CutSmart Buffer	B7024	New England Biolabs

Ligation of DNA into Sialyltransferase Expression Vector.

To perform DNA Ligation, a 20 µL reaction mixture was prepared in a microcentrifuge tube. Digested insert and digested target vector were added in a molar ratio of 1:3, using 50 ng or 100 ng target vector. Nuclease-free water was used to bring the reaction volume to 17µL. To the reaction mixture, 2 µL of 10X T4 DNA Ligase Buffer (New England Biolabs, B0202A) was added, as well as 1 µL of T4 DNA Ligase (New England Biolabs, M0202L) to reach the final reaction volume of 20 µL. Once mixed thoroughly with a pipette, the mixture was incubated at room temperature for 10 minutes and used directly for transformation.

Transformation of DNA into competent DH5(Alpha) Cells.

To transform 5-α competent *E. coli,* the competent cells were first removed from -80°C and allowed to thaw on ice for 20 minutes. While thawing, LB Agar plates containing Ampicillin (0.01% w/v) were removed from 4°C and allowed to equilibrate to room temperature. Once competent cells mixtures were thawed, 25 µL was transferred to a microcentrifuge tube gently with a pipette. To this, 5 µL of ligation mixture was added and mixed gently by agitating the tube. This mixture was then incubated on ice for 25 minutes. After incubation on ice, the competent cell mixtures were then placed on a 42 °C heat block for 45 seconds, the promptly moved back to ice for another 2 minutes. 200 µL of SOC Outgrowth media was then added, and the putatively transformed cells were incubated at 37 °C for 30 minutes. After this, 50 µL of the SOC solution is added to the LB Agar plates containing ampicillin and spread thoroughly using the flat portion of a glass pipette. These plates were then incubated overnight at 37 °C to allow for colony growth of successful transformants. One day post-transformation, individual colonies were transferred to LB media containing Ampicillin and once again incubated at 37 °C overnight. Day 2 post-transformation, 500 µL the liquid cultures containing successful transformants was then combined with a 250 µL of glycerol and 250 µL of water. After thoroughly mixing, glycerol stocks were labelled and promptly stored at -80°C. Remaining bacterial growth culture was typically used to extract and purify the DNA Plasmid **(Table 2.4).**

Table 2.4: Bacterial Transformation and Selection Materials

Reagent	**Details**	**Manufacturer**
5-α competent *E. coli*	C2987H	New England Biolabs
SOC Outgrowth Media	B90205	New England Biolabs
Bacto Agarose	20 g/L (214010)	BD
Bacto Tryptone	10 g/L (211705)	BD
Yeast Extract	5 g/L (212750)	BD
Sodium Chloride	10 g/L (S9625)	Sigma-Aldrich
Ampicillin	BP1760-25	Fischer BioReagents
Glycerol	G33-1	Fischer Chemicals

Plasmid Collection from Bacteria – Miniprep.

ThermoScientific's 'GeneJET Plasmid Miniprep Kit' was used in this work (ThermoScientific, K0502). To begin the procedure, 10 mL tubes containing 3 mL of highly turbid LB Media containing desired bacterial cells were spun at ~3,000 RCF for 10 minutes. Bacterial cells formed a pellet at the bottom of the tubes, and all liquid was then decanted followed by removal of remaining media via. Pipette. To the pellet, 250 µL of Resuspension solution was added. The tube was then vortexed at top speed until the pellet was entirely resuspended. Resuspended cells were then transferred into microcentrifuge tubes for the subsequent steps. To the tubes, 250 µL of Lysis solution was added followed by inversion of the tube 5 times to mix gently. Then, 350 µL of Neutralization solution was added followed by inversion of the tube 5 times to mix gently. Addition of Neutralization solution causes precipitation of the cells genomic DNA as evidenced by the formation of a white precipitate. The tubes were then spun at 10,000 RCF for 5 minutes. After centrifugation, 700-800 µL of the clear liquid was decanted into a GeneJET Spin Column. The column was then spun at 10,000 RCF for 1 minute. Flowthrough was then discarded. To wash the column, 500 µL of Wash solution (diluted with 96% EtOH) is added followed by 1 minute centrifugation at 10,000 RCF, repeated twice. To remove excess wash solution, the columns are then spun empty for 1 minute at 10,000 RCF. Finally, 40-50 µL of nuclease-free water is added to the columns, freeing the bound DNA from the silica resin, and spun again at 10,000 RCF for 1 minute. The flowthrough of this step is collected as purified DNA plasmids and stored at -20 °C.

Preparing Samples for Sanger Sequencing.

To confirm the sequence identity of plasmids prior to use, it is crucial to verify the sequencing using Sanger sequencing. Using a single primer and a template, Sanger sequencing allows for the base-to-base characterization the bases present in a DNA sequence. This process was carried out by the Molecular Biology Facility (MBSU) at the University of Alberta. Sanger

sequencing samples were prepared as per the requirements of the MBSU. A microcentrifuge was used, adding 575 ng of the desired plasmid (final concentration: 57.5 ng/μL) and 2.5 pmoles of desired sequencing primer (final concentration: 0.25 μM). Nuclease-free water was then added to bring the final reaction volume to 10 μL. The solution was thoroughly mixed via. Pipette prior to submission the MBSU for sequencing. Forward sequencing primer was pCMV (5'-CGCAAATGGGCGGTAGGCGTG-3'). Reverse sequencing primer was BGH (5'-TAGAAGGCACAGTCGAGG-3'). Both sequencing primers were ordered from IDT (Integrated DNA Technologies.

Stable Transfection of Flp-in CHO Cells and Storage.

The pcDNA5 vector used in this work contains an FRT region. In this system, a pcDNA5-FRT plasmid is co-transfected with the pOG44 vector. The pOG44 vector encodes a Flp recombinase, leading to a recombination event in which the pcDNA5-FRT template is integrated into the host genome of Flp-in cells, conferring resistance to hygromycin.

A day prior to transfection, Flp-in CHO cells are split into a 6 well plate at ~750,000 cells/well and incubated at 37°C overnight in DMEM F-12 supplemented with 10% FBS and 1% pen-strep (growth media). The next day, 3.6 μg of pOG44 Flp recombinase vector, and 0.4 μg of the desired plasmid for transfection were added to Opti-MEM Serum Free Media to a final volume to 500 μL in a microcentrifuge tube. Note that typically a tube is made containing all components except the desired DNA Plasmid, to act as a negative transfection control. Then, 4.70 μL of the Lipofectamine PLUS reagent was added and mixed by gently inverting the tubes. This mixture was left to incubate at room temperature for 15 minutes. After this, 15.7 μL of the Lipofectamine LTX reagent is added, and left to incubate at room temperature for 30 minutes after gentle inversion. During this incubation, the media present in the 6 well plate was aspirated, and the cells were washed with 1.5 mL of Opti-mem two times to remove serum present in growth media. After 30-minute incubation the Opti-mem/Lipofectamine complex was added to the cells in the 6 well plate, and

left to incubate at 37°C overnight. The next day, 2 mL of growth media is added to the well, and returned to overnight incubation at 37°C. On the second day post-transfection all cells were lifted from the 6 well plate using trypsin. Cells were moved into T-25 cell culture dishes, in growth media supplemented with 0.5mg/mL of hygromycin. Every 2 days the media supplemented with hygromycin was replaced, until it was observed that all control cells in the negative transfection control were dead. Cells successfully transfected were then lifted using trypsin and split into T-75 cell culture dishes in standard growth media at 37 °C. Once successfully transfected, cells in the T-75 dish were grown to confluency and 1 mL of cell suspensions were moved into cryo-vials in growth media containing 10% DMSO v/v. This was followed by immediate freezing at -80 °C or liquid nitrogen for long-term storage.

Table 2.5: Stable Transfection of Flp-in CHO Cells and Storage Materials

Reagent	Detail	Manufacturer
Lipofectamine Plus Reagent	10964-021	Invitrogen
Lipofectamine LTX Reagent	94756	Invitrogen
pOG44 Vector	V600520	Invitrogen
Opti-MEM Media	31985-070	Gibco
Hygromycin B	0.5 mg/mL (10687010)	Invitrogen
DMEM/F12 (1:1) Media	11320-033	Gibco
Pen Strep	15140-122	Gibco
Fetal Bovine Serum	12483020	Gibco

2.5.2: Expression Quantification and Optimization Materials

ELISA (Enzyme-Linked Immunosorbent Assay).

To perform the ELISA, a clear flat-bottom 96-well plate coated in MaxiSorp coating was incubated with the capture antibody overnight at 4 °C while covered. For this step, the capture antibody utilized was Mouse α-Human IgG1 Fc Secondary Antibody (Clone: HP6070) purchased from Invitrogen. The initial 0.5 mg/ml solution was diluted 1:250 in a 50 mM sodium carbonate buffer

at pH 9.4. Then, 50 µl of the solution was added to each well for overnight incubation (final concentration, 2 µg/ml). For each well with capture antibody, a well was loaded with only the carbonate buffer, to act as a negative control and assess for non-specific signal. The following day, the antibody solution was removed and washed 3 times with 1x PBS. Then, a 1% BSA solution (blocking solution) was prepared by dissolving 0.5 g of pure Bovine Albumin in 50 ml 1x PBS and agitating lightly to allow complete solvation. To each well, 100 µl of blocking solution was added and incubated for 1 hour at room temperature. This step was crucial to prevent non-specific binding to the plate, leading to false positive colorimetric signal generation. During the incubation, samples and standards were prepared by dissolving desired constructs (containing an IgG_1 Fc fragment as well as a Strep II tag) in supernatant. This was collected from transfected WT CHO Flp-in cells to control for other secreted proteins and spiked with 0.05% Tween-20 prior to use in the assay. After this step, the blocking solution was removed, and the plate was washed 3 times with PBS-Tween (0.05%). Samples and standards were then loaded at 50uL per well as desired and incubated on the plate at room temperature for 2-3 hours. After this incubation, the supernatant was removed, and the plate was again washed 3 times with PBS-Tween. Then, a 1 mg/mL solution of Streptactin-HRP from IBA Sciences was diluted 1/10000 in PBS-Tween, to a final concentration of 0.1 µg/ml. Then, 50 µl of the diluted Streptactin-HRP solution was applied to all wells at room temperature for 15 minutes with a multi-channel pipette. To quench the reaction, 50 µL of 8.5% phosphoric acid was quickly added and a yellow color change was observed. The plate was then measured for absorbance at 450 nm by a spectrophotometer. Raw absorbance values of wells without capture antibody present were subtracted from the absorbance values of wells containing the capture antibody to subtract background signal and account for impact of non-specific interactions on generated signal **(Table 2.6)**.

Table 2.6: ELISA Materials

Reagent	Detail	Manufacturer
Clear Flat-Bottom Immuno Nonsterile 96-Well Plate	Coating: MaxiSorp 439454	ThermoFischer Scientific
Sodium Carbonate	S263-500	Fischer Chemical
Sodium Bicarbonate	S233-500	Fischer Chemical
Mouse α-Human IgG_1 Fc Secondary Antibody	Clone: HP6070 Isotype: Mouse IgG_1: κ 0.5 mg/mL (MH1015)	Invitrogen
Albumin, Bovine	>99% Purity via. HPLC A-0281	Sigma-Aldrich
Streptactin-HRP	1 mg/mL (2-1502-001)	IBA Life Sciences
KPL TMB Peroxidase Substrate System (2-C)	5120-0047	Seracare Life Sciences
Phosphoric Acid (85%)	A242-500	Fischer Chemical

Expression in Mammalian Cell Culture using Stably Transfected Flp-in CHO Cells.

To perform expressions, Flp-in CHO cells stably transfected with desired DNA sequences were grown in liquid culture under typical growth conditions in a T-175 cell culture flask. Expression media was prepared as DMEM-F12 supplemented with 5% FBS, 1% Pen-Strep, and 10 mM HEPES. When confluent, cells from the T-175 were lifted and split equally into four T-175 cell culture flasks with 50 mL of expression media per flask, such that each flask was seeded by a quarter of the confluent T-175 cells. For sialyltransferase constructs, these flasks were initially incubated at 37 °C to consistently reach confluency by the following day. The next day, expressions were moved to a 32 °C incubator and left undisturbed until day 7 of expression. On day 7 the supernatant was transferred to multiple 50 mL falcon tubes and spun at 3,400 RCF for 5 minutes to pellet cells and cell debris. After spinning, the supernatant was combined and filtered into a sterile container for further purification **(Table 2.7).**

Table 2.7: Expression of Stably Transfected Flp-in CHO Cells Materials

Reagent	Detail	Manufacturer
DMEM/F12 (1:1) Media	11320-033	Gibco
Pen Strep	15140-122	Gibco
Fetal Bovine Serum	12483020	Gibco
HEPES	15630-080	Gibco

2.5.3: Purification and Functional Validation of Sialyltransferases Materials

Nickel-Sepharose Purification Column (for 6x His Tag).

To perform Nickel column purification, three buffers are prepared. The equilibrium buffer contains 20 mM sodium phosphate and 500 mM sodium chloride at pH 7.4. The washing buffer contains 20 mM sodium phosphate, 500 mM sodium chloride, and 30 mM imidazole at pH 7.4. The elution buffer contains 20 mM sodium phosphate, 500 mM sodium chloride, and 500 mM imidazole at pH 7.4. Buffers were filtered (0.22uM pore size) and stored at 4 °C. To facilitate purification, an ÄKTA start chromatography system was used to automate the addition of the buffers to the 1 mL HisTrap HP column. All following steps were run at a flow rate of 1 mL/min. Initially, 20 mL of equilibrium buffer was flowed through the column into waste. Then, the filtered supernatant containing desired protein was flowed through the column into waste (e.g 200 mL = 200 minutes). After the sample, 20 mL of washing buffer was flowed through the column into waste to allow for the elution of non-specific and weakly binding mixture components from the column. Finally, 10 mL of elution buffer was run through the column to elute all His-tagged protein, which was then collected in 1mL fractions by the ÄKTA start chromatography system. Fractions containing high amounts of protein (characterized via. Nanodrop) were combined for the next step of purification. The column was then washed with 20% ethanol and stored at 4 °C for future purification **(Table 2.8).**

Table 2.8: Nickel-Sepharose Column Purification Materials

Reagent	Detail	Manufacturer
HisTrap Excel Column	1 mL Column Volume 17524701	Cytiva Lifesciences
Sodium Chloride	500 mM (S271-3)	Fischer Chemical
Sodium Phosphate	20 mM (S374-500)	Fischer Chemical
Imidazole	30 mM or 500 mM (O3196-500)	Fischer Chemical

StrepTactin Purification Column (For Strep II Tag).

To perform StrepTactin column purification, three buffers are prepared. The washing buffer (Buffer W) contains 100 mM Tris-HCl, 150 mM sodium chloride, and 1 mM EDTA at pH 8.0. The elution buffer (Buffer E) contains 100 mM Tris-HCl, 150 mM sodium chloride, 1 mM EDTA, and 2.5 mM desthiobiotin at pH 8.0. The regeneration buffer (Buffer R) contains 100 mM Tris-HCl, 150 mM sodium chloride, 1 mM EDTA, and 1 mM HABA at pH 8.0. Buffers were filtered (0.22 µM pore size) and stored at 4°C. The column used was a 1 mL Strep-Trap HP, and the flow rate for all steps was 1 mL/minute. As per the manufacturer's protocols, biotin can interfere the StrepTactin – Strep tag II binding interaction and lead to losses in purification yield. As such direct cultured supernatant requires pre-treatment prior to running over the column. First, 2 mL of buffer W was flowed through the column into waste. Then, the sample was loaded through the column into waste. If the sample was eluent from a nickel column it was first diluted five-fold with Buffer W to reduce the concentration of imidazole. After the sample ran through the column, 5 mL of Buffer W was flowed through the column into waste to allow for the elution of non-specific mixture components present in the column. Then, 4 ml of Buffer E was flowed through the column and collected in eight 0.5 mL fractions. Fractions were then characterized via. Nanodrop and fractions putatively containing the desired protein were combined for the next step of purification. The column was then washed with Buffer R until a deep red color was observed throughout the column, indicating successful regeneration of the Strep-Tactin resin. Buffer R was then removed by washing with Buffer W until the column was colorless, and the column was stored at 4 °C for future purification **(Table 2.9)**.

Table 2.9: StrepTactin Column Purification Materials

Reagent	Detail	Manufacturer
StrepTrap HP	1 mL Column Volume 2-1239-001	Cytiva Lifesciences
Tris-HCl	100 mM (10812846001)	Roche Diagnostics GmBH
Sodium Chloride	150 mM (S271-3)	Fischer Chemical
EDTA	1 mM (S311-500)	Fischer Chemical
Desthiobiotin	2.5 mM (2-1000-002)	IBA-Lifesciences

Dialysis of Purified Protein.

To perform dialysis, 2 L of the desired buffer was prepared in a large beaker with a magnetic stir-bar (for sialyltransferase constructs: 20 mM Tris Base, 150 mM NaCl, at pH = 8). Then the sample for desired buffer exchange was added into a piece of Snakeskin dialysis tubing (ThermoScientific, 68035). Both ends of the tubing were sealed, and the tubing was monitored to ensure the fidelity of the seals. A piece of Styrofoam was clipped onto the dialysis tubing, providing buoyancy, and preventing the snakeskin from sinking in the beaker. The sample was then placed into the large beaker at 4 °C on a stir plate set to the lowest speed. Every 4-12 hours, the sample was removed from the beaker, and placed into 2 L of fresh buffer. This process was repeated 2-3 times depending on desired buffer exchange efficiency. Finally, the sample was carefully transferred from the Snakeskin into microcentrifuge tubes.

Concentration of Protein Samples (Ultracentrifugation).

To concentrate samples post-dialysis, 400 µL of dialysis buffer alone was initially loaded into the 400 µL Amicon centrifugal filter unit (Millipore Sigma Aldrich, UFC501024, 10 kDa Cut-off). Filter units were placed into a centrifuge and spun at maximum speed (~13,000 RCF) for 4 minutes. This washing process was then repeated twice to prepare the filter for dialyzed protein. After washing, 400 µL of post-dialysis liquid containing the desired protein at low concentration was added. The filter units were then spun at maximum speed for 4 minutes. 400 µL of post-dialysis liquid was continually added and spun until the entire volume was added. Once all liquid was

added, the liquid was agitated via. pipetting and transferred to a 1 mL microcentrifuge tube for quantification by Bradford assay.

Bradford Assay.

To perform a Bradford protein assay, a standard curve is prepared using a bovine serum albumin (BSA) standard (Bio-Rad,, 5000206). A serial dilution is performed as per the manufacturer's recommendations from 2 mg/ml to 0.125 mg/ml. 5 µL of each standard was then loaded in triplicate into a clear flat-bottom 96-well plate for use as a standard curve to compare experimental samples to. Then, 5 µL of sample for measurement was loaded into the plate in triplicate. Then, 250 µL of the Quick-Start Bradford reagent (Bio-Rad, 5000205), warmed to room temperature, is added to each well and mixed with a pipette. The plate was then incubated at room temperature for 5 minutes. After incubation, the 96-well plate was loaded into a spectrophotometer and absorption measurements were carried out at 595 nm. Once measured, a standard curve was generated and fitted to a second-order polynomial, which was then used to calculate the concentration of the unknown sample.

Protein Size Analysis - SDS-PAGE.

To perform SDS-PAGE electrophoresis, two gel solutions were prepared. A resolving gel (10% polyacrylamide) was prepared to a volume of 8 ml containing: 2 ml of 40% SureCast Acrylamide, 2 mL of SureCast Resolving Buffer, 80 µL of 10% APS, and 3.9 mL of distilled water. A stacking gel (4% polyacrylamide) was prepared to a volume of 3 mL containing: 0.30 mL of 40% SureCast Acrylamide, 0.75 mL of SureCast stacking buffer, 30 µL of 10% APS, and 1.92 mL of distilled water. To the resolving gel, 8 µL of Surecast TEMED was added and mixed quickly with vortex. The resolving gel was transferred between the front and back plate of the SureCast Handcast station, up to the fill line, as per the manufacturer's instructions. The resolving gel was then left to polymerize at room temperature for 10 minutes. Once solidified the isopropyl alcohol was decanted and 3 µL of TEMED was added to the stacking gel, mixed, and added above the

solidified resolving gel. Quickly, a 12-well comb was placed into the liquid stacking gel, to form the wells for addition of protein. The stacking gel was then left to polymerize at room temperature for 15 minutes. Once solidified the comb was removed, and the gel was ready for electrophoresis and placed in the mini-gel tank. The mini-gel tank was then filled with a 1X MOPS running buffer containing Tris Base, SDS, EDTA, and MOPS.

To prepare protein samples, a 6x loading buffer containing SDS, DTT, and Bromophenol blue was added to the sample to a final concentration of 1x. The samples were then incubated at 95 °C on a tube heater for 5 minutes. After incubation, samples were transferred into the wells of the prepared SDS-PAGE gel. A pre-stained protein ladder was loaded on one, or both ends of the gel. Once prepared, the mini-gel tank was connected to a PowerEase 300 W Gel running apparatus. A two-step voltage protocol was used, whereby a 90 V voltage was applied for 15 minutes, followed by a 150 V voltage applied for 45 minutes. Once the gel was finished running, the gel was carefully removed from the mini-gel tank and transferred to a small plastic container with a lid for visualization. To visualize the gel, a Staining solution containing Coomassie Brilliant Blue G-250 was added to the container until the gel was fully submerged. This solution was then heated in the microwave for 30 seconds and left to incubate on a platform shaker for 10 minutes. The Staining solution was then removed, and a Destaining solution containing ethanol and glacial acetic acid was then added to the container until the gel was fully submerged. This solution was then heated in the microwave for 30 seconds and left to incubate on a platform shaker for 10 minutes. This step was then repeated 2-3 times, or until the protein bands were visible. For storage, the container was filled with distilled water, and stored at 4 °C **(Table 2.10).**

Table 2.10: SDS-PAGE Materials

Reagent	Detail	Manufacturer
Surecast Acrylamide	40% w/v (HC2040)	Invitrogen
Surecast APS Ammonium Persulfate	HC2005	Invitrogen
Surecast TEMED	HC2006	Invitrogen
Surecast Stacking Buffer	HC2112	Invitrogen
Surecast Resolving Buffer	HC2212	Invitrogen
Tris Base	50 mM (BP152-5)	Fischer Chemical
MOPS	50 mM (BP308-500)	Fischer Chemical
SDS	3.4 mM (BP166-100)	Fischer Bioreagents
EDTA	1.025 mM (S311-500)	Fischer Chemical
PageRuler Prestained Protein Ladder	26619	Thermoscientific
Dithiothreitol (DTT)	BP172-25	Fischer Chemical
Coomassie Brilliant Blue G-250	161-0406	Bio-Rad
Destaining Solution	600 mL EtOH, 200 mL Acetic Acid, 1.2 L H_2O	-

Sialyltransferase Reactions for CMP-Glo Assay (Time-Course Assessment).

To perform the CMP-Glo assay for a time-course assessment of linearity, sialyltransferase reaction mixtures were prepared as follows. To microcentrifuge tubes, 100 µL of 2X sialyltransferase buffer (40 mM Tris, 150 mM NaCl, pH = 8) was added. Then, 25 µl of 8X acceptor solution and 25 µL 8X donor sugar solution was added to the microcentrifuge tubes. Then, 25 µl of water was added to each reaction tube, which could be replaced with extra components if required. Prior to the addition of enzyme to start the reaction, the reaction mixtures were incubated at 37 °C for 10 minutes to prevent temperature changes during the reaction. Reactions were initiated by addition of 25 µL 8X sialyltransferase solution. During incubation, 20 µL of CMP-Glo Enzyme was added to 500 µL of CMP-Glo detection buffer and thoroughly mixed. To wells of a white opaque 96-well plate, 25 µL of CMP-Glo detection reagent + CMP-Glo enzyme was added as required. At various time points, 25 µL of reaction mixture was added to each plate well as required. Addition of reaction mixture to CMP-Glo detection buffer quenches the reaction, allowing for a time-course to be assessed for the stopped assay. After the final time point, the opaque

plate was stored in a dark environment for 1 hour as per manufacturer's instruction and read on a ID5 SpectraMax plate reader with 1000 ms integration time for total luminescence. Background subtraction was carried out in wells containing identical reaction conditions with the addition of water instead of enzyme. Signal generated in background controls was subtracted from total luminescence for final assessment and quantification **(Table 2.11)**

Sialyltransferase Reaction for CMP-Glo Assay (Single-Time Point Assessment).

To perform the CMP-Glo Assay for a single time point measurement, reaction mixtures were prepared to 25 µL in the wells of a 96-well white opaque plate. To each plate well, 12.5 µL of 2X sialyltransferase buffer (40 mM Tris, 150 mM NaCl, pH = 8) was added. Then, 2.5 µL of 10X acceptor solution and 2.5 µL of 10X donor sugar solution were added to respective wells. Then, 2.5 µl of water was added to each reaction tube, which could be replaced with extra components if required. The 20 µL reaction mixture without enzyme was placed in a 37°C incubator for at least 10 minutes to equilibrate the plate and reaction components. During the plate incubation, a 5X sialyltransferase solution was prepared in a microcentrifuge tube and heated on a block heater for at least 5 minutes. Once both incubations were completed, a multi-channel pipette was then used to transfer 5 µL of the 5X sialyltransferase solution to respective wells of the plate and the plate was left in the 37 °C incubator for the chosen reaction duration. While the reaction was incubating, 500 µL CMP-Glo Detection Buffer and 20 µL CMP-Glo Enzyme were thawed and combined. Once the reaction time was completed, a multi-channel pipette was then used to add 25 µL of combined CMP-Glo Detection Reagent to each well. The addition of CMP-Glo Detection Reagent quenched the sialyltransferase reactions. After the final time point, the opaque plate was stored in a dark environment for 1 hour as per manufacturer's instruction and read with ID5 SpectraMax plate reader at a 1000 ms integration time for total luminescence. Background subtraction was carried out in wells containing identical reaction conditions with the addition of

water instead of enzyme. Signal generated in background controls was subtracted from total luminescence for final assessment and quantification **(Table 2.11).**

Table 2.11: CMP-Glo Sialyltransferase Assay Materials

Reagent	**Detail**	**Manufacturer**
Opaque White 96-well Plate	781965	Cole-Parmer
CMP-Glo Detection Buffer	VA1131	Promega
CMP-Glo Glo-Enzyme	VA1131	Promega
Tris Base	BP152-5	Fischer Chemical
MES	BP300-100	Fischer Biotech
Sodium Chloride	S9625	Sigma-Aldrich
N-Acetyl-D-Lactosamine	OA08244	Carbosynth
Galacto-*N*-Biose	OA01686	Carbosynth
Asialofetuin	A4781	Sigma-Aldrich
CMP-Neu5Ac	3063-71-6	Nacalai USA
Cytosine Diphosphate	C9755	Sigma-Aldrich

Chapter 3

Assessing the Potency of Sialyltransferase Inhibitors

3.1: Introduction and Objectives

Many assays are available for measuring the activity of sialyltransferases. Broadly, these strategies can be grouped into 'stopped' and 'continuous' assays. The former requires reaction mixtures to be quenched prior to measurement to convert the product into something that can be measured, while the latter enables the progress of reaction to be monitored in real time, which is more desirable. The CMP-Glo assay used in the previous chapter represents a stopped assay. It was initially used due to its high sensitivity (able to detect nM amounts of CMP), commercial availability, and its compatibility with native donor sugars and acceptors (no special compounds need to be synthesized). Furthermore, the assay does not require sophisticated instrumentation other than a plate reader capable of measuring luminescence. Other techniques typically require modifications to the donor or acceptor, or sophisticated instrumentation (e.g., a mass spectrometer) to detect product formation. As a continuous assay offers greater precision for determining reaction rates, such an assay was ultimately pursued in this Chapter.

The type of continuous assay used in this work is based on fluorescence polarization, which has been developed previously to monitor sialyltransferase activity[66]. To do so, researchers used a non-native donor sugar conjugated to a fluorophore, which rotates rapidly in solution due to Brownian motion but rotates less rapidly when transferred to a larger glycoprotein acceptor through the action of a sialyltransferase. The presence of the fluorophore on the donor requires some forethought as sialyltransferases may have different substrate preferences when comparing the fluorophore conjugated donor sugars to native CMP-Neu5Ac, which could cause changes in reaction rates. Notably, a previous application of this technique for sialyltransferase reaction monitoring used a fluorophore conjugated to the C9 position of CMP-Neu5Ac[73]. However,

structural research has pointed to the C5 donor modifications being tolerated preferentially by sialyltransferases[24,25]. Additionally, the mP (milli-polarization) value is a direct measurement of molecular rotation, and therefore only indirectly measures the progress of sialyltransferase reactions. Accordingly, the rates calculated in the FP-based assay cannot be compared to a standard curve for determination of absolute rate of product formation. This limitation prevents the calculation of absolute Michaelis-Menten kinetic parameters. However, the ability to assay inhibitors is unaffected, allowing for continuous monitoring of sialyltransferase reactions in the presence of various inhibitors.

The CMP-Neu5Ac analog inhibitor CMP-3F_{ax}-Neu5Ac has been preliminarily investigated in the literature, as it is biologically relevant inhibitor that reduces sialic acid on the cell surface when provided to cells *in vitro*[75] or *in vivo*[80] but there are still questions as to its major mechanism of action. Cell-based assays have demonstrated that peracetylated 3F_{ax}-Neu5Ac derivatives inhibit cell surface sialic acid, as demonstrated by work that assessed various derivatives of the inhibitor, the most potent of which had a calculated IC_{50} value < 5 μM[107]. However, these studies do not measure the direct inhibition using sialyltransferase assays. The direct inhibitory potency of CMP-3F_{ax}-Neu5Ac against the twenty members of the GT29 family of human sialyltransferases has not been investigated, as only inhibition towards human ST6Gal1 and ST3Gal1 have been quantified to date[73,76].

In this chapter, an inhibition assay is established for the measurement of sialyltransferase inhibitor potency. A primary outcome was measuring the inhibitory potency of CMP-3F_{ax}-Neu5Ac against multiple human sialyltransferases. The CMP-Glo assay demonstrated assay interference of inhibitors on the downstream steps that convert CMP to light, preventing use of the assay. Accordingly, a fluorescence polarization-based assay was developed. Using this assay, IC_{50} values for five different inhibitors were calculated towards ST6Gal1 and ST3Gal1. CMP, CDP, and CTP can act as inhibitors of sialyltransferase representing product inhibition, and were used

for validation **(Figure 3.1A).** Once the assay was established, CMP-Neu5Ac analog inhibitor CMP-3F$_{ax}$-Neu5Ac was assessed for inhibitory potency to address gaps in the literature. Another CMP-Neu5Ac analog inhibitor, CMP-7F-Neu5Ac, was assessed which represents a novel measurement of inhibitory potency using the FP-based assay towards two human sialyltransferases **(Figure 3.1B)**. To further characterize the assay, reaction conditions including buffer composition, buffer pH, and acceptor glycoprotein concentration were investigated and found to significantly impact the measured *IC*$_{50}$ values. Finally, ST8Sia2 activity was detected using the FP-based sialyltransferase inhibition assay and preliminary results quantified its ability to be inhibited by CTP.

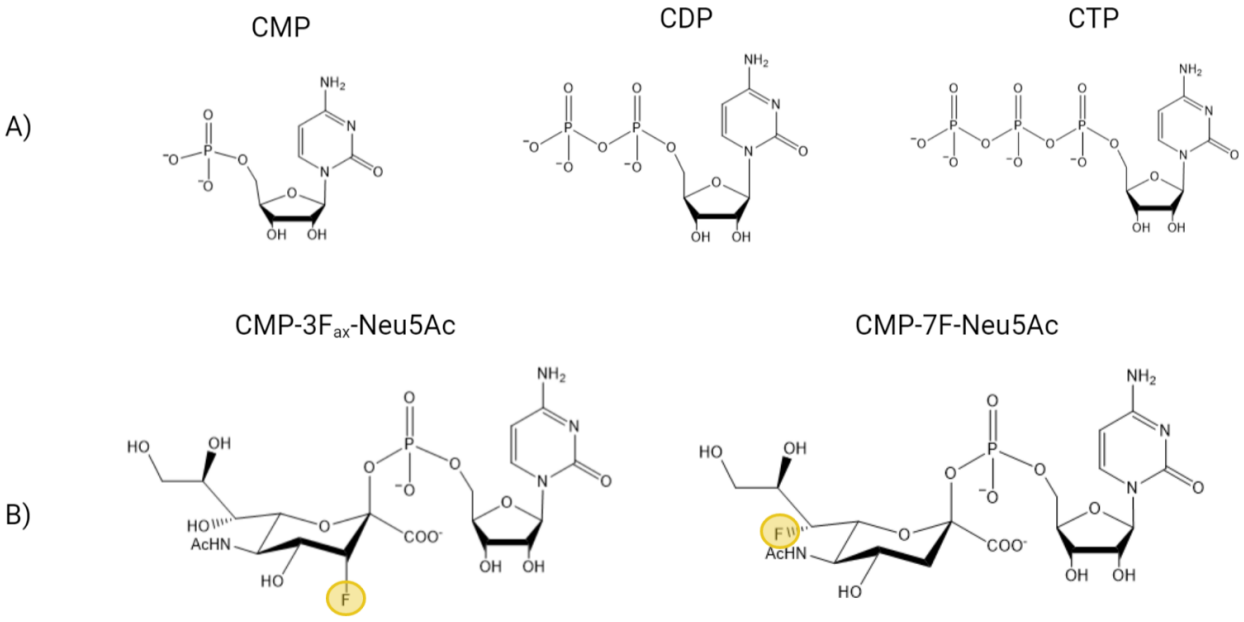

Figure 3.1: Sialyltransferase Inhibitors Assessed in this Work. A) Nucleotide inhibitors used to validate the FP-based inhibition assay. CMP (cytidine monophosphate), CDP (cytidine diphosphate) and CTP (cytidine triphosphate). **B)** CMP-Neu5Ac analog inhibitors studied in this work, with yellow circles indicating position of fluorine CMP-3F$_{ax}$-Neu5Ac and CMP-7F-Neu5Ac were both synthesized and purified by PhD candidate Dhanraj Kumawat in the Macauley Lab.

3.2: Results

3.2.1: Assessment of Inhibitor Potency with the CMP-Glo Assay

As the CMP-Glo assay had already been used to validate the activity of the ST6Gal1 Fc-construct in Chapter 2, it was chosen as the first assay to test inhibition. However, what emerged was an inverse relationship between inhibitor concentration and raw luminescent signal in background wells without any sialyltransferase present for certain inhibitors. This did not make sense, as the observed inhibition of signal could not be attributed to sialyltransferase inhibition in these conditions.

To confirm the cause of the background inhibition, another experiment was performed with only 10 μM CMP instead of the reaction components. This was done to test if inhibitors were inhibiting the components of the CMP-Glo kit, involved in converting CMP to luminescent signal. A titration the nucleotide inhibitor CDP was performed and found to interfere with components of the CMP-Glo assay at concentrations higher than 50 μM **(Figure 3.2A)**. This motivated the use of a dilution strategy, where the reaction mixtures were diluted prior to incubation of the kit components, such that the final concentration would not lead to assay interference. To assess inhibition, CDP was titrated from 200 μM to 5 μM in reaction mixtures containing 100 μM CMP-Sia, 1 mM LacNAc, and 0.3 μM ST6Gal1. After a four-fold dilution of the reaction mixtures at various time points, the highest concentration of CDP available to interfere with the CMP-Glo kit was 50 μM. Reactions were stopped at various time points to calculate reaction rate, and all conditions demonstrated linearity at 20 minutes post enzyme incubation **(Figure 3.2B).** Reaction rates were then plotted against CDP concentration to generate an IC_{50} curve fitted by non-linear regression in PRISM **(Figure 3.2C)**. The calculated IC_{50} was 180 μM, but it was clear that higher concentrations were needed to plot points on the IC_{50} curve. Due to the kit interference and high cost, the CMP-Glo kit was determined to be a poor inhibition assay, which motivated the development of a fluorescence polarization assay.

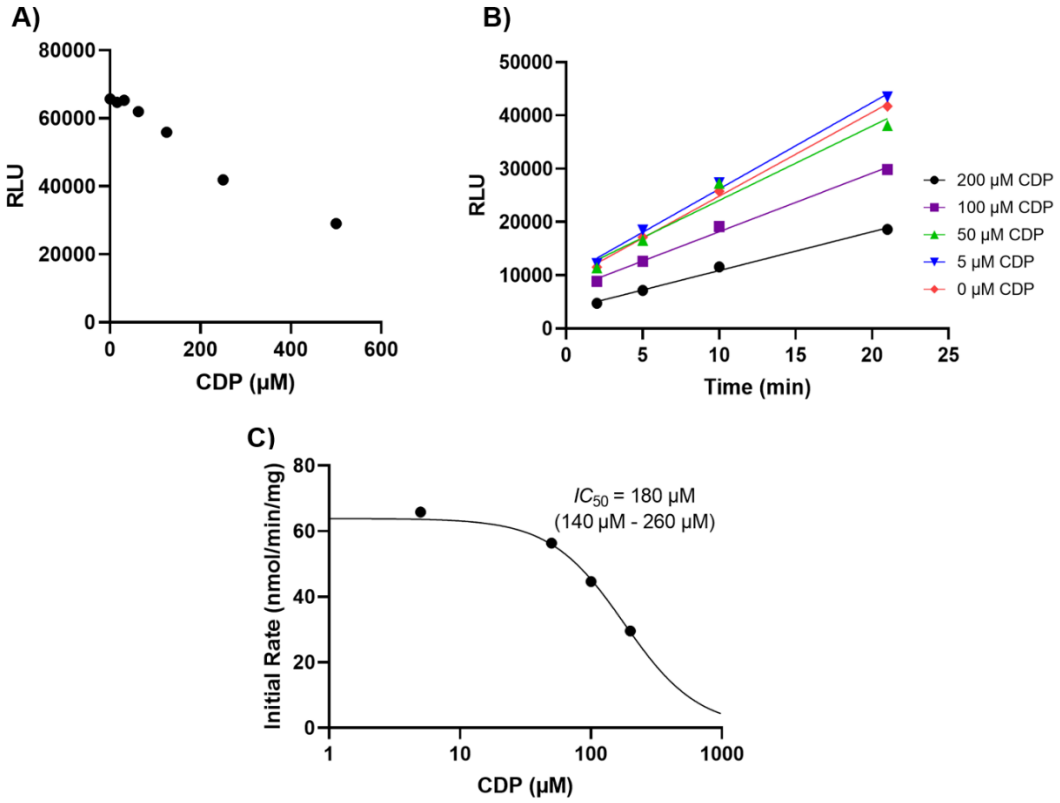

Figure 3.2: Inhibition of ST6Gal1 with CDP in the CMP-Glo Assay. (A) Titration of CDP (cytidine diphosphate) in wells containing 10 μM CMP. RLU represents raw luminescent signal from one well. **(B)** Time course experiment for calculation of ST6Gal1 reaction rate with various concentrations of CDP. Reaction volume was removed at 2-, 5-, 10-, and 21-minutes post-enzyme incubation and diluted four-fold into CMP-Glo kit for quenching and signal generation. **(C)** Plotted IC_{50} curve for CDP Inhibition of ST6Gal1. Bracket values represent 95% confidence interval calculated from non-linear regression in PRISM. RLU was converted to CMP (nmol) using standard curve and divided by total enzyme (mg) for rate quantification. **(B-C)** Reactions were carried out in Tris reaction buffer (20 mM Tris, 150 mM NaCl, pH = 8) containing 100 μM CMP-Sia, 1 mM LacNAc, and 0.3 μM ST6Gal1. RLU represents background subtracted values from wells containing 100 μM CMP-Sia and variable inhibitor concentrations.

3.2.2: Establishing and Optimizing a Fluorescence Polarization Based Assay

The enzymatic application of fluorescence polarization assays requires a change in the rotational rate of a fluorophore over the course of a reaction. To accomplish this, PhD candidate Dhanraj Kumawat synthesized several versions of CMP-Sia with a fluorophore **(Figure 3.3)**. The

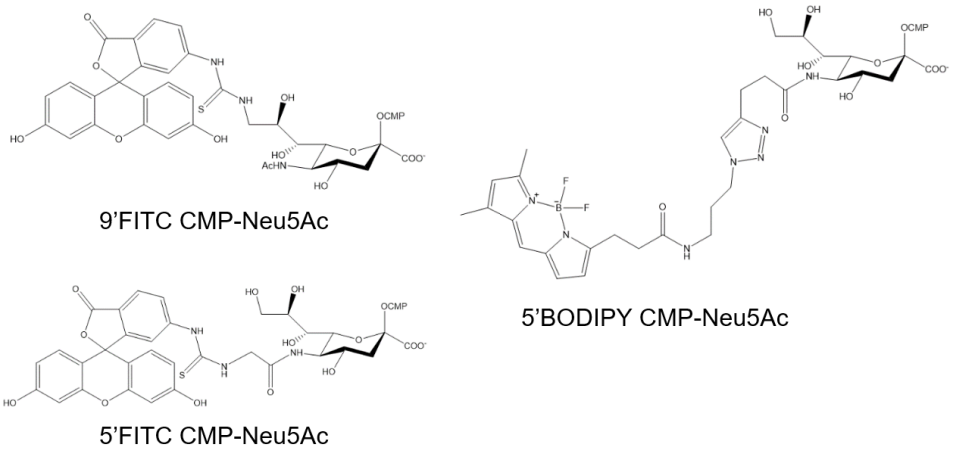

Figure 3.3: Tracers Used in Florescence Polarization Sialyltransferase Assay. 5'FITC CMP-Neu5Ac and 9'FITC CMP-Neu5Ac are conjugated using thiourea linkages. 5' BODIPY CMP-Neu5Ac is conjugated using a triazole linkage. All tracers were synthesized and purified by PhD Candidate Dhanraj Kumawat in the Macauley Lab.

conjugates of the donor-sugars and fluorophores are referred to as the 'tracers', as they generate the mP signal in the assay. The tracers used in the FP assay were 5'-BODIPY CMP-Neu5Ac, 9'-FITC CMP-Neu5Ac, and 5'-FITC CMP-Neu5Ac. 9'-FITC CMP-Neu5Ac was used in previous literature, but 5'-BODIPY CMP-Neu5Ac was expected be preferential due to its conjugation on C5 instead of C9[24,25]. 5'FITC CMP-Neu5Ac was synthesized later, after the 9'-FITC and 5'-BODIPY tracers were exhaustively tested, and results using 5'FITC are presented at the end of the chapter. The FITC compounds were created by reacting an amine-containing CMP-Neu5Ac with FITC, which resulted in a thiourea linkage. Notably, the final tracers do not contain isothiocyanate, but we have kept FITC in the name of the final compound. First, reaction rates were measured in real-time at various concentrations of ST6Gal1 with 3.1 μM ASF and 250 nM tracer to assess if the assay demonstrated linearity with respect to enzyme concentration **(Figure 3.4A,C).** Both 5'-BODIPY and 9'-FITC tracers were observed to demonstrate linearity with respect to enzyme concentration. The difference between the starting and maximal mP value of the assay an be described as the ΔmP, and 9'-FITC tracer had a ΔmP of ~100 mP compared to 5'-BODIPY's ΔmP of ~20 mP **(Figure 3.4B,D).**

With linearity established with respect to enzyme concentration, a titration of the glycoprotein asialofetuin, as the acceptor, was performed to determine if reaction rates varied with respect to acceptor. This was demonstrated with the 9'-FITC CMP-Sia tracer for both ST6Gal1 and ST3Gal1 Fc-constructs. ST6Gal1 demonstrated linearity between 0 – 15.6 μM asialofetuin, and when fitted to a Michaelis-Menten plot in PRISM, a K_M of 9.6 μM was calculated **(Figure 3.5A,B)**. ST3Gal1 demonstrated linearity across all asialofetuin concentrations tested, but notably the ST3Gal1 required four-fold increased concentration relative to ST6Gal1 to increase the reaction rate at pH 8 **(Figure 3.5C,D).**

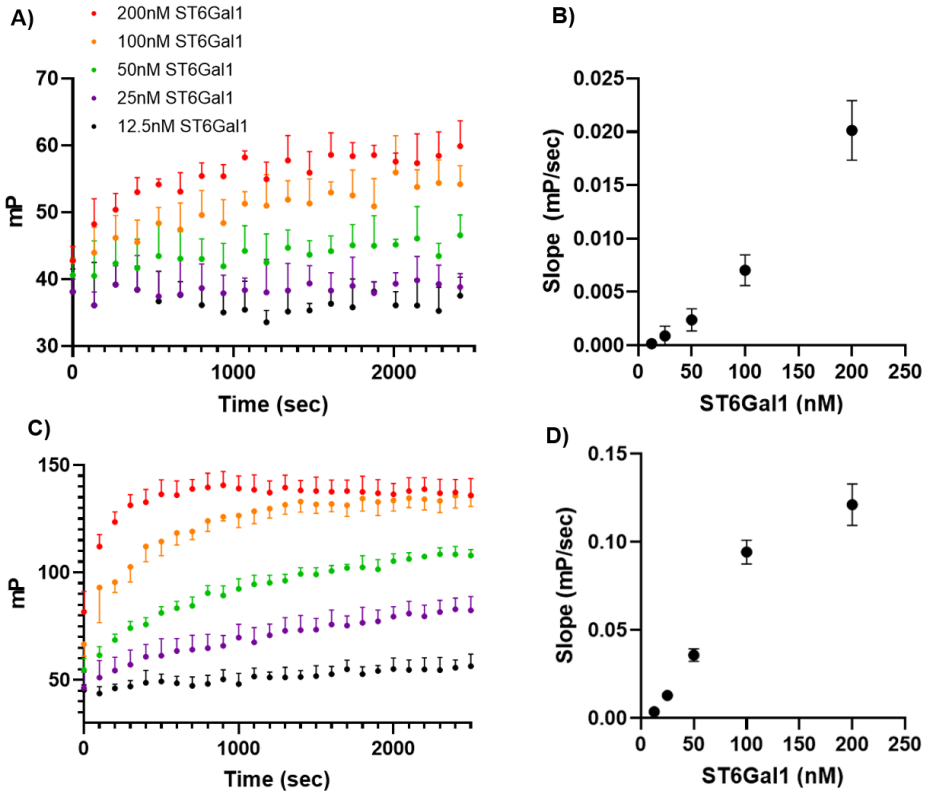

Figure 3.4: FP Assay Demonstrates Linearity with Respect to Enzyme Concentration. (A) Enzyme titration of ST6Gal1 using donor-sugar 5'-BODIPY CMP-Neu5Ac. **(B)** Slopes of linear ranges for each enzyme concentration in (A). Error bars represent standard deviation (n=5). **(C)** Enzyme titration of ST6Gal1 using donor-sugar 9'-FITC CMP-Neu5Ac. **(D)** Slopes of linear ranges for each enzyme concentration in (C). Error bars represent standard deviation (n=5) **(A-D)** Reactions were carried out at room temperature in Tris reaction buffer (20 mM Tris, 150 mM NaCl, pH = 8). Reaction mixtures contained 3.1 μM Asialofetuin, 250 nM donor-sugar, and variable amounts of ST6Gal1. Error bars represent standard deviation (n=5).

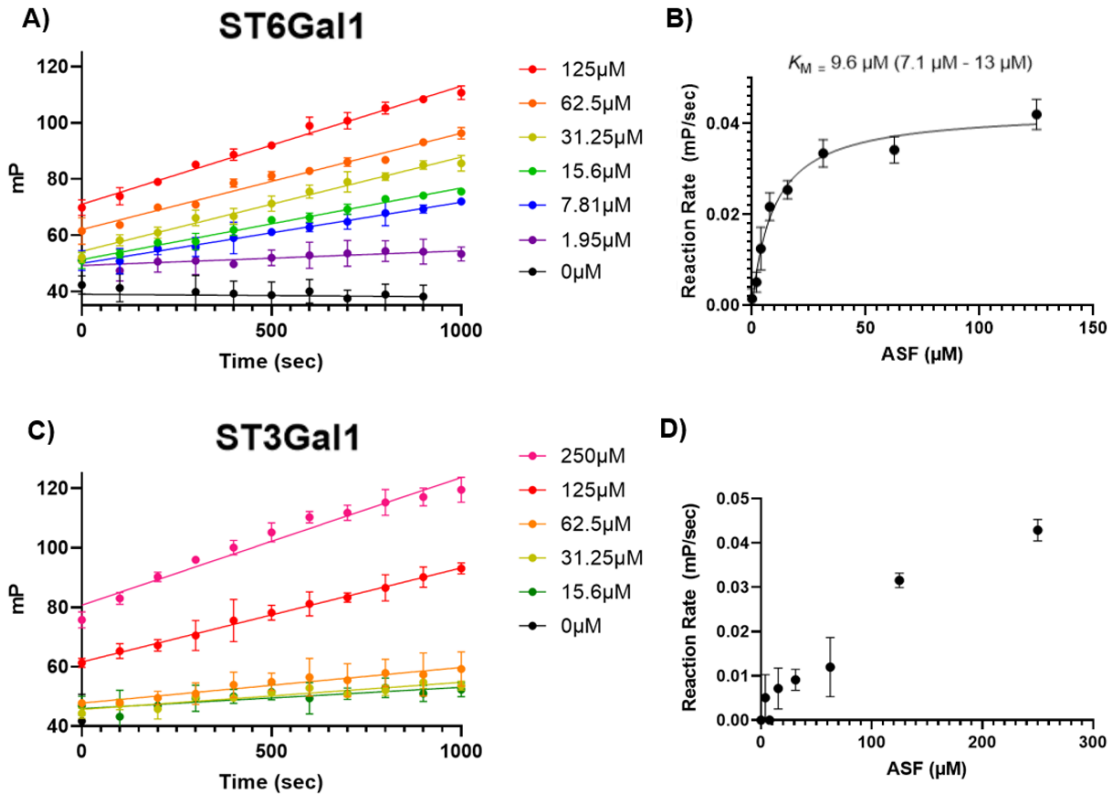

Figure 3.5: FP Assay Demonstrates Linearity with Respect to Glycoprotein Acceptor. (A) Raw Data for titration of asialofetuin against ST6Gal1. **(B)** Initial reaction rate across various concentrations of asialofetuin for ST6Gal1. Bracket values represent 95% confidence intervals calculated from non-linear regression in PRISM. Error bars represent standard deviation (n=3) **(C)** Raw FP Data for titration of asialofetuin against ST3Gal1, and a variable amount of glycoprotein acceptor asialofetuin. **(D)** Initial reaction rate across various concentrations of asialofetuin for ST3Gal1. Error bars represent standard deviation (n=3). **(A-D)** Reactions were carried out at room temperature in Tris reaction buffer at room temperature. Reaction mixtures contained 250 nM Tracer (9'-FITC CMP-Neu5Ac), 50 nM ST6Gal1 or 200 nM of ST3Gal1, and a variable amount of glycoprotein acceptor asialofetuin.

3.2.3: Initial Sialyltransferase Inhibition with FP-Based Assay

With preliminary characterization of the assay completed, the ability of the FP-based assay to assess inhibition of sialyltransferase activity was tested. Reaction mixtures containing 62.5 µM asialofetuin, 250 nM of either 5'BODIPY or 9'FITC tracer, and 33 nM ST6Gal1 were incubated with various amounts of CDP **(Figure 3.6A,C)**. The inhibition curves generated using 9'-FITC tracer had far greater statistical significance than the curve generated using 5'-BODIPY tracer, but both tracers generated similar IC_{50} values (100 and 110 µM respectively) **(Figure 3.6B,D)**. As the FP-based assay with the 9'-FITC tracer generated IC_{50} curves with high precision, due to the increased signal-to-noise with this tracer, it was chosen to assess the differential inhibitory potencies of nucleotide and CMP-Neu5Ac inhibitors against ST6Gal1 and ST3Gal1.

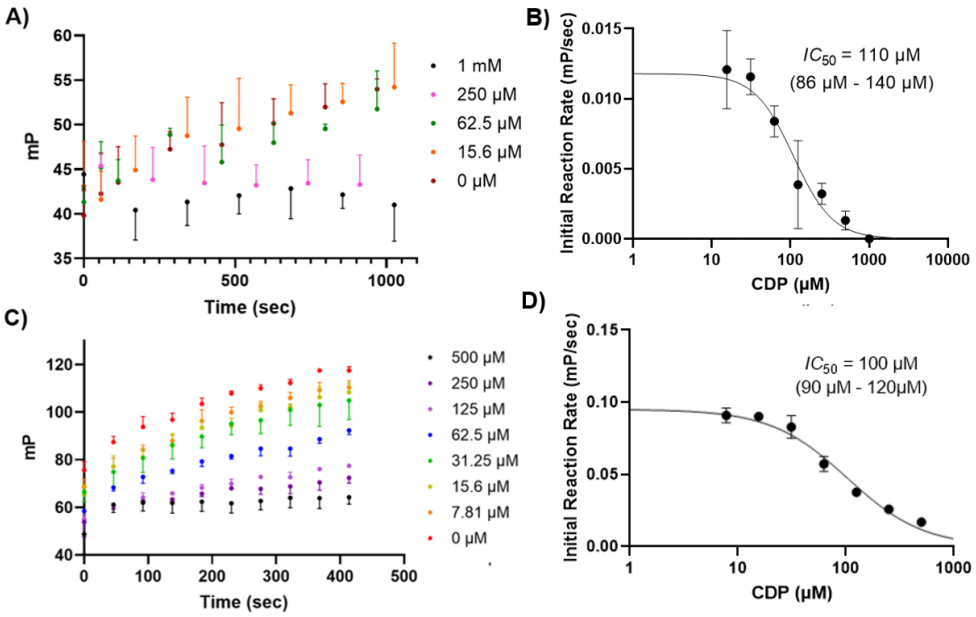

Figure 3.6: CDP Inhibits ST6Gal1 in FP Assay. (A) 5'-BODIPY CMP-Neu5Ac donor-sugar. Reaction mixtures contained 100 nM ST6Gal1, 250 nM donor-sugar, and 3.1 µM Asialofetuin with various concentrations of CDP. Error bars represent standard deviation (n=3) **(B)** IC_{50} curve plotted from (A). Error bars represent standard deviation (n=3). **(C)** 9'-FITC CMP-Neu5Ac donor-sugar. Reaction mixtures contained 33 nM ST6Gal1, 250 nM donor-sugar, and 62.5 µM Asialofetuin with various concentrations of CDP. Error bars represent standard deviation (n=3). **(D)** IC_{50} curve plotted from (C). Error bars represent standard deviation (n=3). **(A+C)** Reactions carried out at room temperature in Tris reaction buffer. **(B+D)** Data fitted using PRISM, setting bottom constraint to 0 and top constraint to the uninhibited reaction rate.

To establish enzymatic inhibition assays, compounds that represent the product or product analogs are useful as positive inhibition controls. For sialyltransferases, CMP is a reaction product which may bind the active site residues involved in nucleotide binding for the native CMP-Neu5Ac substrate. This is evidenced by liganded crystal structures of human ST6Gal1, ST3Gal1 and ST8Sia3, where CMP and CDP have been demonstrated to bind into the active site[10,11]. It is important to note that nucleotide inhibitors are only useful as positive inhibition controls to establish inhibition assays. First, ST6Gal1 inhibition was assessed for nucleotide inhibitors CMP, CDP, and CTP. Reaction mixtures were prepared with various concentrations of the inhibitors with 62.5 μM asialofetuin, 250 nM 9'-FITC CMP-Neu5Ac tracer, and initiated with the addition of 50 nM ST6Gal1. The slopes of the initial linear reaction were calculated and plotted against inhibitor concentration using non-linear regression on PRISM to generate three IC_{50} curves. The IC_{50} calculated for CMP was 250 μM **(Figure 3.7A).** The IC_{50} calculated for CDP was 190 μM **(Figure 3.7B).** The IC_{50} calculated for CTP was 160 μM **(Figure 3.7C).**

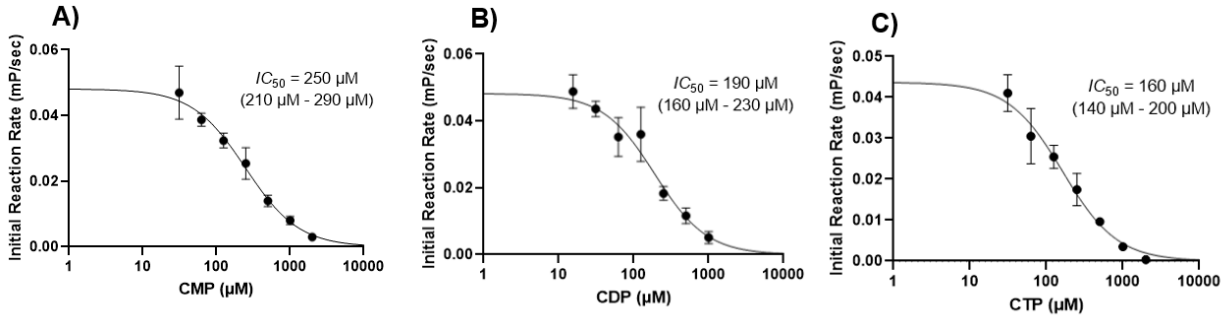

Figure 3.7: FP Assay IC_{50} Curves for Nucleotide Inhibitors of ST6Gal1. (A) Cytidine monophosphate inhibition of ST6Gal1. **(B)** Cytidine diphosphate inhibition of ST6Gal1. **(C)** Cytidine triphosphate inhibition of ST6Gal1 **(A-C)** Reactions were carried out in Tris reaction buffer (pH 8) at room temperature on the same plate and incubated in parallel. Rates for the linear regions were plotted with error bars representing standard deviation (n=3). Bracket values represent 95% confidence intervals calculated from non-linear regression in PRISM, setting bottom constraint to 0 and top constraint to the uninhibited reaction rate. Reaction mixtures contained 250 nM 9'FITC CMP-Neu5Ac, 62.5 μM asialofetuin, 33 nM ST6Gal1 and variable amounts of inhibitor.

Observing differential inhibition of ST6Gal1 with the nucleotide inhibitors tested, ST3Gal1 was subsequently assessed. As ST3Gal1 did not generate high reaction rates with the conditions used for ST6Gal1, the concentration of enzyme and asialofetuin were increased. Reaction mixtures were prepared with 200 nM ST3Gal1, 125 µM asialofetuin, 250 nM 9'-FITC CMP-Neu5Ac tracer, and various concentrations of the inhibitors. The slopes of the initial linear reactions were calculated and plotted against inhibitor concentration using non-linear regression on PRISM to generate three IC_{50} curves. The IC_{50} calculated for CMP was 110 µM **(Figure 3.8A).** The IC_{50} calculated for CDP was 53 µM **(Figure 3.8B).** The IC_{50} calculated for CTP was 13 µM **(Figure 3.8C).**

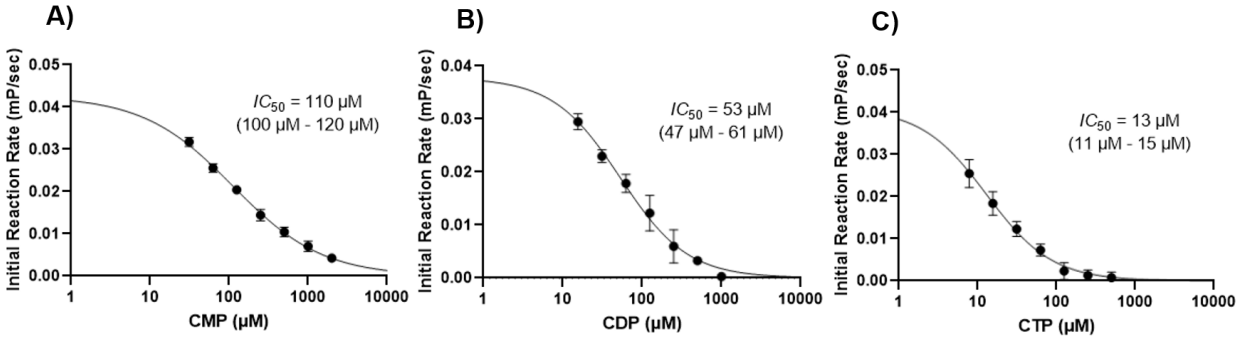

Figure 3.8: FP Assay IC_{50} Curves for Nucleotide Inhibitors of ST3Gal1. (A) Cytidine monophosphate inhibition of ST3Gal1. **(B)** Cytidine diphosphate inhibition of ST3Gal1. **(C)** Cytidine triphosphate inhibition of ST3Gal1 **(A-C)** Reactions were carried out in Tris reaction buffer (pH 8) at room temperature. Rates for the linear regions were plotted with error bars representing standard deviation (n=3). Bracket values represent 95% confidence intervals calculated from non-linear regression in PRISM, setting bottom constraint to 0 and top constraint to the uninhibited reaction rate. Reaction mixtures contained 250 nM 9'FITC CMP-Neu5Ac, 125 µM asialofetuin, 200 nM ST3Gal1 and variable amounts of inhibitor.

After the nucleotide inhibitors were assessed, the assay appeared to demonstrate consistent performance across various inhibitors without observable interference. The inhibitory potency of the biologically relevant inhibitor CMP-3F_{ax}-Neu5Ac was then assessed. Plotting the initial linear slopes against the concentration of CMP-3F_{ax}-Neu5Ac using a non-linear regression on PRISM generated an IC_{50} curve for ST6Gal1 and ST3Gal1**.** The IC_{50} calculated for CMP-3F_{ax}-

Neu5Ac towards ST6Gal1 was 660 μM **(Figure 3.9A)**. This value was far greater than 9.5 μM, the literature value generated using a similar assay[73] The IC_{50} calculated for CMP-3F$_{ax}$-Neu5Ac towards ST3Gal1 was 550 μM **(Figure 3.9B)**. Therefore, CMP-3F$_{ax}$-Neu5Ac demonstrated a similar inhibitory potency to both ST6Gal1 and ST3Gal1 Fc-constructs.

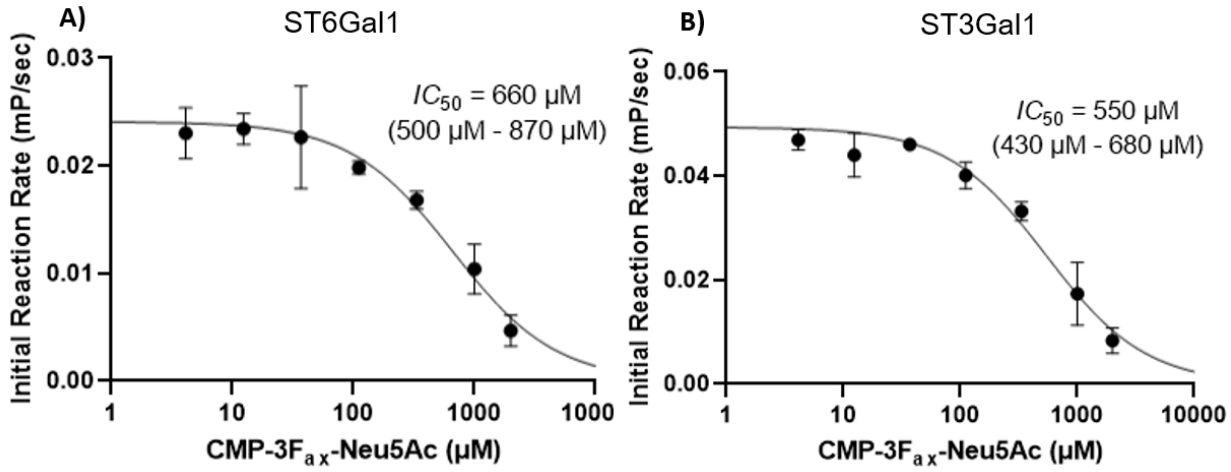

Figure 3.9: Initial FP Assay IC_{50} Curves for Inhibitor CMP-3F$_{ax}$-Neu5Ac. (A) Inhibition curve for ST6Gal1 (33 nM) with 62.5 μM asialofetuin. **(B)** Inhibition curve for ST3Gal1 (200 nM) with 125 μM ASF. **(A-B)** Reactions were carried out in Tris reaction buffer (pH 8) at room temperature. Rates for the linear regions were plotted with error bars representing standard deviation (n=3). Bracket values represent 95% confidence intervals calculated from non-linear regression in PRISM, setting bottom constraint to 0 and top constraint to the uninhibited reaction rate. Reaction mixtures contained 250 nM 9'FITC CMP-Neu5Ac, and variable amounts of CMP-3F$_{ax}$-Neu5Ac.

Another putative CMP-Neu5Ac was assessed in the FP assay. CMP-7F-Neu5Ac was synthesized by PhD candidate Dhanraj Kumawat in the Macauley lab and is characterized by the substitution of the hydroxyl group on C7 of Neu5Ac with fluorine. This inhibitor has not been directly assessed in an enzymatic inhibition assay in the literature, but ongoing work in the Macauley lab has demonstrated that it is effective at reducing cell surface α2-6 linked sialic acid in cells. Furthermore, preliminary data in collaboration with the Klassen lab demonstrated that it binds to ST6Gal1 stronger than CMP-3F$_{ax}$-Neu5Ac by a mass spectrometry-based binding assay

(not shown). To determine its inhibitory potency *in vitro*, reaction mixtures were prepared in identical conditions to those used for CMP-3F_{ax}-Neu5Ac and various concentrations of CMP-7F-Neu5Ac were added to the mixtures. Plotting the initial linear slopes against the concentration of CMP-7F-Neu5Ac using a non-linear regression on PRISM, IC_{50} curves were generated for both ST6Gal1 and ST3Gal1**.** The IC_{50} calculated for CMP-7F-Neu5Ac towards ST6Gal1 was 150 μM **(Figure 3.10A)**. The IC_{50} calculated for CMP-7F-Neu5Ac towards ST3Gal1 was 190 μM **(Figure 3.10B)**. Therefore, CMP-7F-Neu5Ac demonstrated a similar inhibitory potency to both ST6Gal1 and ST3Gal1, while appearing inhibit with greater potency compared to CMP-3F_{ax}-Neu5Ac, which is consistent with affinity measurements from the Klassen lab.

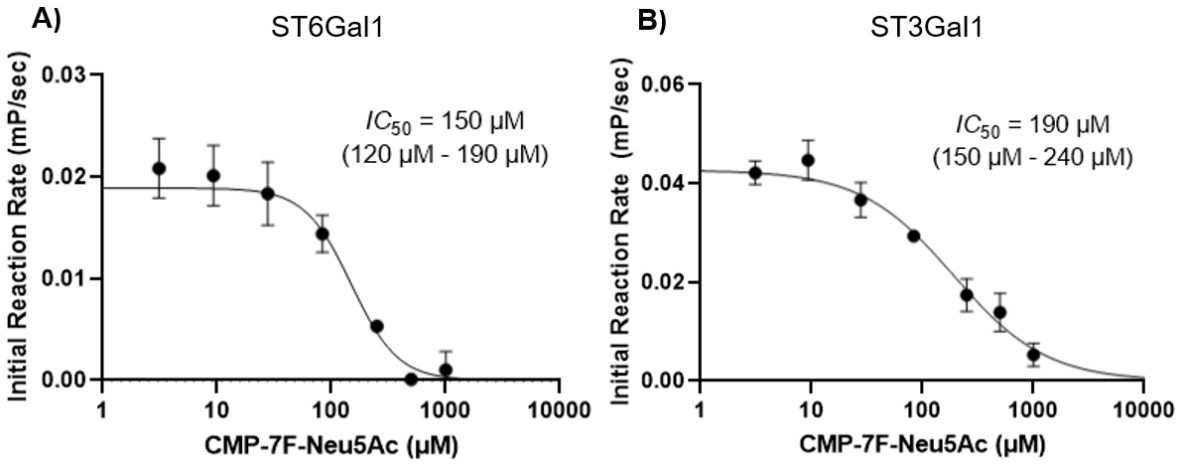

Figure 3.10: Initial FP Assay IC_{50} Curves for Inhibitor CMP-7F-Neu5Ac. (A) Inhibition curve for ST6Gal1 (33 nM) with 62.5 μM asialofetuin. **(B)** Inhibition curve for ST3Gal1 (200 nM) with 125 μM ASF. **(A-B)** Reactions were carried out in Tris reaction buffer (pH 8) at room temperature. Rates for the linear regions were plotted with error bars representing standard deviation (n=3). Bracket values represent 95% confidence intervals calculated from non-linear regression in PRISM, setting bottom constraint to 0 and top constraint to the uninhibited reaction rate. Reaction mixtures contained 250 nM 9'FITC CMP-Neu5Ac, and variable amounts of inhibitor.

The FP-based inhibition assay generated IC_{50} values for ST6Gal1 and ST3Gal1 using the initial reaction conditions characterized by Tris pH 8 buffer and high concentrations of acceptors. The assay demonstrated an ability to measure potency of all inhibitors tested, ranging from ~10 μM to ~660 μM **(Table 3.1)**.

Table 3.1: Initial IC_{50} Values for ST6Gal1 and ST3Gal1

	CMP	CDP	CTP	CMP-3F$_{ax}$-Neu5Ac	CMP-7F-Neu5Ac
ST6Gal1	250 µM	190 µM	160 µM	660 µM	150 µM
ST3Gal1	110 µM	53 µM	13 µM	550 µM	190 µM

3.2.4: Factors that Affect Observed Inhibition Potency

As the FP-based assay is not widely used, IC_{50} values calculated could not be directly compared to literature. However, CMP-3F$_{ax}$-Neu5Ac demonstrated a ~60-fold increase in IC_{50} to literature values using a similar assay. As this inhibitor is biologically relevant, the finding motivated a series of experiments to determine if reaction conditions impact the calculated IC_{50} values in the FP-based assay. There were three notable differences between reaction conditions used in the previous section and the literature: (i) pH , (ii) concentration of acceptor glycoprotein, and (iii) buffer composition. To disentangle the effects of these factors, four IC_{50} curves were plotted for CMP-3F$_{ax}$-Neu5Ac against ST6Gal1. The reaction pH was assessed using a HEPES buffer at pH 8 and compared to an MES buffer at pH 6.5, in order to avoid Tris as a buffer since recent studies have demonstrated that is unsuitable for use in sialyltransferase assays[102]. Moreover, these reaction mixtures carried either 55.6 µM or 2.7 µM asialofetuin. At pH 8, the 55.6 µM asialofetuin condition generated an IC_{50} of 46 µM while the 2.7 µM asialofetuin concentration generated an IC_{50} of 300 µM **(Figure 3.11A,B).** At pH 6.5, the 55.6 µM asialofetuin condition generated an IC_{50} of 15 µM while the 2.7 µM asialofetuin concentration generated an IC_{50} of 110 µM **(Figure 3.11A,B).**

It is noteworthy that the pH 8 experiment with 55.6 µM asialofetuin produced an IC_{50} value of 46 µM, a value ten-fold lower than the one calculated previously in Figure 3.10. The only difference between these experiments was the use of HEPES buffer instead of Tris. To investigate the potential effect of buffer composition on the activity of ST6Gal1 as detectable in the FP assay, reactions were prepared in pH 8 buffers (Tris or HEPES) at concentrations of 15 and 150 mM to

determine if reaction rates depended on the buffer used. At 15 mM, real time raw mP measurements demonstrate a reduced reaction rate in Tris buffer when compared to 15 mM HEPES buffer at equivalent pH **(Figure 3.12A).** These values were found to be significantly reduced at both 15 and 150 mM as determined by unpaired *t*-test **(Figure 3.12B).** Therefore, it was confirmed that Tris buffer is unsuitable for use in the FP-based sialyltransferase assay, as it leads to reduced reaction rates.

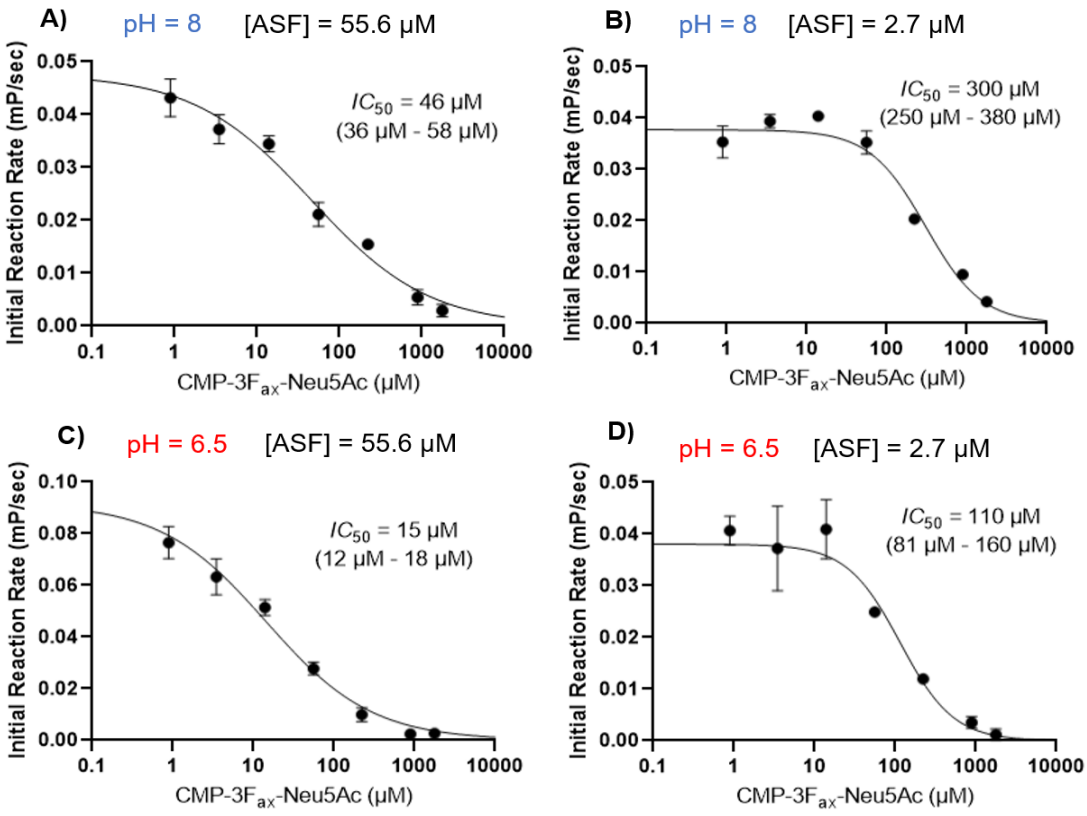

Figure 3.11: IC_{50} Values for CMP-3F$_{ax}$-Neu5Ac against ST6Gal1 Depend on pH and Acceptor Concentration. (A) Inhibition curve using 55.6 µM asialofetuin and pH 8 HEPES buffer (20 mM HEPES, 150 mM NaCl, 0.01% Triton X-100). **(B)** Inhibition curve using 2.7 µM asialofetuin and pH 8 HEPES buffer. **(C)** Inhibition curve using 55.6 µM asialofetuin and pH 6.5 MES buffer (20mM MES, 150 mM NaCl, 0.01% Triton X-100). **(D)** Inhibition curve using 2.7 µM asialofetuin and pH 6.5 MES buffer. **(A-D)** Reactions were carried out at room temperature. Rates for the linear regions were plotted with error bars representing standard deviation (n=3). Bracket values represent 95% confidence intervals calculated from non-linear regression in PRISM, setting bottom constraint to 0 and top constraint to the uninhibited reaction rate. Reaction mixtures contained 250 nM 9'FITC CMP-Neu5Ac, 29.3 nM ST6Gal1 and variable amounts of CMP-3F$_{ax}$-Neu5Ac.

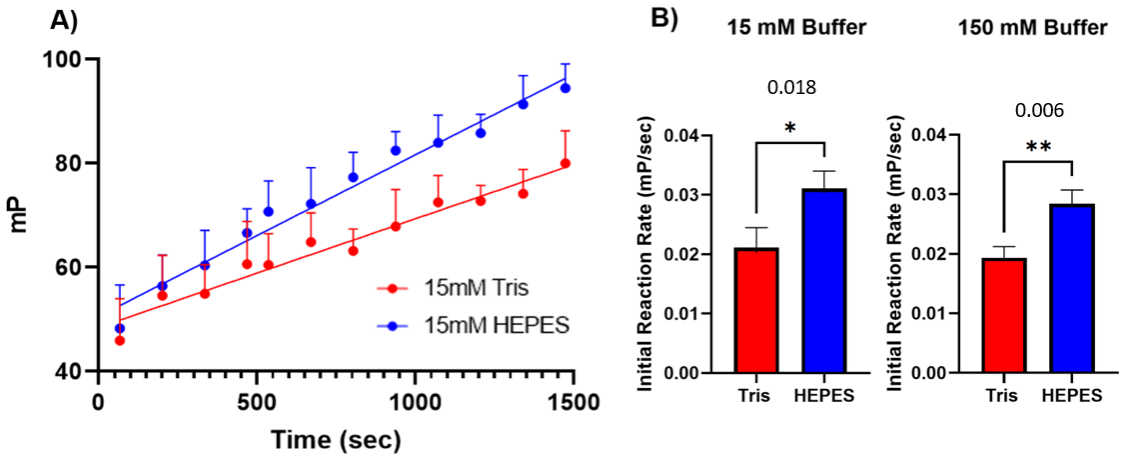

Figure 3.12: Tris Buffer Reduces ST6Gal1 Reaction Rates in FP Assay. (A) Raw ST6Gal1 reaction data for 15 mM buffer concentrations. Error bars represent standard deviation (n=3). **(B)** Slope of linear reaction rate in Tris or HEPES buffer at 15 mM and 150 mM. Error bars represent standard deviation (n=3). P-values from two-tailed *t*-test are presented above each comparison. **(A-B)** Reactions were carried out at room temperature in various buffers. All buffers contained 150 mM NaCl with 0.01% Triton X-100, and were adjusted to pH 8. Reaction mixtures contained 250 nM 9'FITC CMP-Neu5Ac, 3.1 µM asialofetuin and 33 nM ST6Gal1.

The IC_{50} values calculated in the FP assay were determined to deviate with reaction pH acceptor concentration, and buffer composition for CMP-3F_{ax}-Neu5Ac. To verify that these factors played a role for pairs of inhibitors and sialyltransferases, IC_{50} curves for CMP-7F-Neu5Ac were prepared in pH 6.5 MES buffer. ST6Gal1 and ST3Gal1 were both assessed in conditions similar to Figure 3.11. ST3Gal1 demonstrated far greater activity at pH 6.5, and as such the asialofetuin concentration was reduced from 125 to 62.5 µM and the ST3Gal1 concentration was reduced from 200 nM to 100 nM. Various concentrations of CMP-7F-Neu5Ac were added to the reaction mixtures, and the initial linear slopes were plotted to a non-linear regression in PRISM to generate IC_{50} values for CMP-7F-Neu5Ac towards ST6Gal1 and ST3Gal1. The IC_{50} value generated towards ST6Gal1 was 48 µM **(Figure 3.13A).** The IC_{50} value generated towards ST3Gal1 was 15 µM **(Figure 3.13A).** CMP-7F-Neu5Ac appeared to inhibit ST3Gal1 with three-fold greater potency than ST6Gal1.

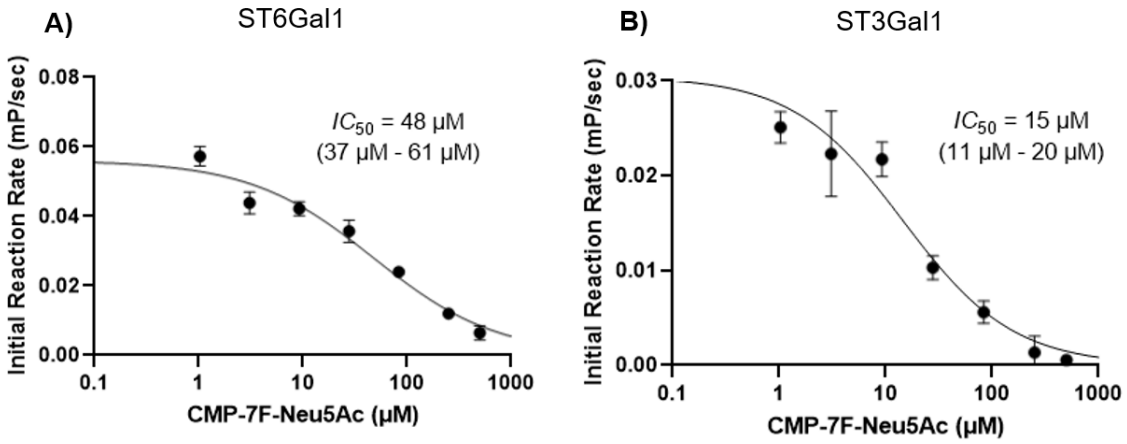

Figure 3.13: IC_{50} Values for CMP-7F-Neu5Ac at pH 6.5. (A) Inhibition curve for ST6Gal1 (33 nM) **(B)** Inhibition curve for ST3Gal1 (100 nM) **(A-B)** Reactions were carried out in MES reaction buffer (20 mM MES, 150 mM NaCl, 0.01% Triton X-100, pH 6.5) at room temperature. Rates for the linear regions were plotted with error bars representing standard deviation (n=3). Bracket values represent 95% confidence intervals calculated from non-linear regression in PRISM, setting bottom constraint to 0 and top constraint to the uninhibited reaction rate. Reaction mixtures contained 250 nM 9'FITC CMP-Neu5Ac, 62.5 μM asialofetuin, and variable amounts of inhibitor.

Using the 9'-FITC tracer, the FP-based assay was shown to be capable of measuring IC_{50} values, although the precise values we obtained varied depending on conditions used in the assay. One condition that had not been assessed was the identity of the tracer sugar. In early optimization, the 5'-BODIPY tracer was used and did not generate good signal-to-background. The cause of this issue may be due to the use of the BODIPY fluorophore, or the position of the fluorophore on the donor sugar CMP-Neu5Ac. To investigate this, a new tracer was, again, synthesized by Dhanraj Kumawat: 5'-FITC CMP-Neu5Ac. To determine the effect of the tracer in calculation of IC_{50} values, 5'-FITC CMP-Neu5Ac was used in reaction conditions identical to those outlined in Figure 3.12. Plotting the initial linear slopes against the concentration of CMP-3F_{ax}-Neu5Ac generated four IC_{50} curves for each set of reaction conditions. At pH 8, the 55.6 μM asialofetuin condition generated an IC_{50} of 43 μM while the 2.7 μM asialofetuin concentration generated an IC_{50} of 440 μM **(Figure 3.14A,B).** At pH 6.5, both the 55.6 μM and 2.7 μM asialofetuin conditions generated an IC_{50} of 29 μM **(Figure 3.11A,B).**

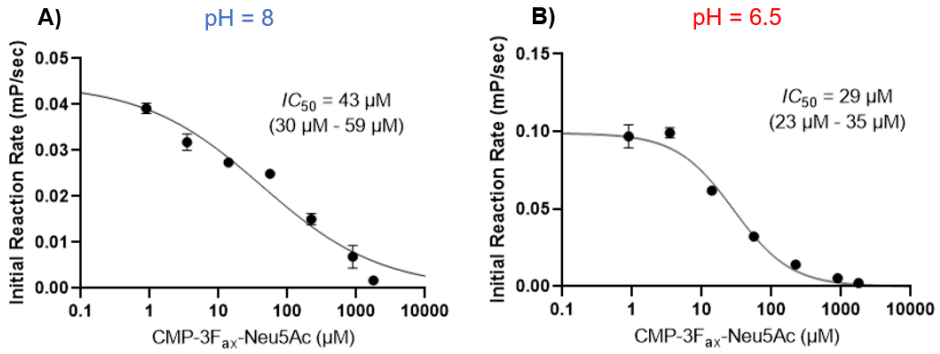

Figure 3.14: CMP-3F$_{ax}$-Neu5Ac Inhibition of ST6Gal1 with 5'FITC CMP-Neu5Ac Donor-Sugar. (A) Inhibition curve using 55.6 µM asialofetuin and pH 8 HEPES buffer. **(B)** Inhibition curve using 55.6 µM asialofetuin and pH 6.5 MES buffer. **(A-B)** Reactions were carried out at room temperature. Rates for the linear regions were plotted with error bars representing standard deviation (n=3). Bracket values represent 95% confidence intervals calculated from non-linear regression in PRISM, setting bottom constraint to 0 and top constraint to the uninhibited reaction rate. Reaction mixtures contained 250 nM 5'FITC CMP-Neu5Ac, 29.3 nM ST6Gal1 and variable amounts of CMP-3F$_{ax}$-Neu5Ac.

The IC_{50} values generated varied by up to twenty-fold across the conditions tested. Notably, the uninhibited rates detected in the FP assay were very similar when comparing the 5'-FITC tracer to the 9'-FITC tracer. All calculated IC_{50} values for CMP-3F$_{ax}$-Neu5Ac and CMP-7F-Neu5Ac towards ST6Gal1 and ST3Gal1 are broken down by reaction condition below **(Table 3.2).**

Table 3.2: Conditional IC_{50} Values for CMP-Neu5Ac Analog Inhibitors

*bracket values indicate use 5'FITC Tracer instead of 9'FITC Tracer

ST6GAL1	**pH 8 HEPES High Acceptor 9'FITC Tracer**	**pH 8 HEPES Low Acceptor 9'FITC Tracer**	**pH 6.5 MES High Acceptor 9'FITC Tracer**	**pH 6.5 MES Low Acceptor 9'FITC Tracer**
CMP-3F$_{ax}$-Neu5Ac	46 µM (43 µM)*	300 µM	15 µM (29 µM)*	110 µM
CMP-7F-Neu5Ac	-	-	48 µM	-
ST3GAL1	**pH 8 HEPES High Acceptor 9'FITC Tracer**	**pH 8 HEPES Low Acceptor 9'FITC Tracer**	**pH 6.5 MES High Acceptor 9'FITC Tracer**	**pH 6.5 MES Low Acceptor 9'FITC Tracer**
CMP-7F-Neu5Ac	-	-	15 µM	-

3.2.5: Assessing Inhibition of Polysialylation for Polysialyltransferase ST8Sia2

After thoroughly assessing the inhibition of ST6Gal1 and ST3Gal1-Fc constructs using the FP based assay, another Fc-construct cloned in the Thesis was considered. ST8Sia2 was initially assessed against the literature glycoprotein acceptor fetuin. When tested at pH 8, there was not any detectable activity in the assay. When tested in pH 6 buffer with ST8Sia2 concentrations below 250 nM, there was also no detectable activity. However, when 500 nM ST8Sia2 was used in pH 6 MES buffer, activity was detectable. Intriguingly the reaction rate was not affected by the concentration of Fetuin and, curiously, was still detected with no Fetuin **(Figure 3.15).** This could be explained by the process of autopolysialylation, in which polysialyltransferases such as ST8Sia2 use their own glycans as acceptors. As the highest rate was exhibited without fetuin present, the mP signal generated over time in the assay likely represents the transfer of the tracer sugar 9'-FITC CMP-Neu5Ac to the glycans of ST8Sia2.

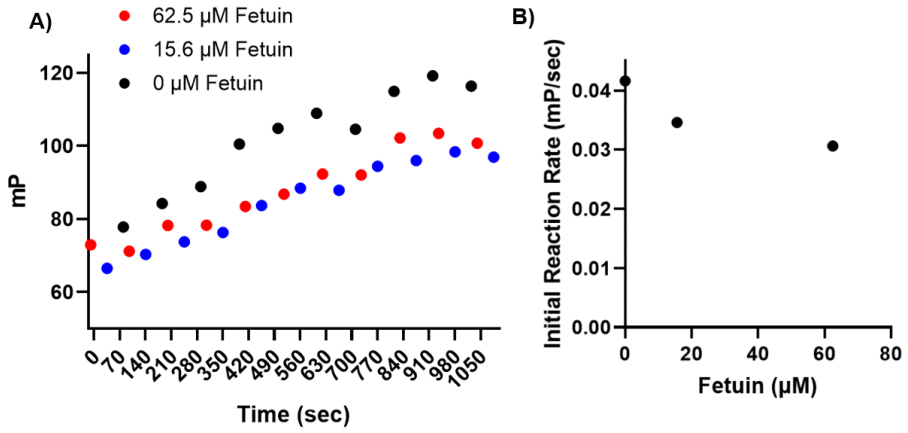

Figure 3.15: ST8Sia2 Activity in FP Assay Does Not Require Fetuin Acceptor. (A) Raw ST8Sia2 reaction data at various concentrations of accepting glycoprotein fetuin. Reactions were carried out In MES buffer (20 mM MES, 150 mM NaCl, 0.01% Triton X-100, pH 6) at 37 °C. Reaction mixtures contained 500 nM ST8Sia2, 250nM 9'-FITC CMP-Neu5Ac and various concentrations of fetuin. **(B)** Slopes of the linear reaction rate at various concentrations of fetuin (n=1).

As autopolysialylation activity of ST8Sia2 Fc-construct was detectable in the FP assay, the *in vitro* inhibition of autopolysialylation was explored. To assess this, reaction mixtures in pH 6 MES buffer were prepared containing 500 nM ST8Sia2, 250 nM 9'-FITC Neu5Ac and variable amounts of CTP. The linear slopes were plotted against the concentration of CTP to generate an IC_{50} curve **(Figure 3.16)**. The IC_{50} value calculated for CTP inhibition of ST8Sia2 was 1.0 μM, representing a novel IC_{50} using an FP-based inhibition assay for ST8Sia2. It is important to note that although the experiments were performed on the same day, the uninhibited rates vary two-fold when compared to the preliminary experiment presented in Figure 3.17. The inhibition of ST8Sia2 by CMP-3F_{ax}-Neu5Ac in pH 6.5 MES buffer was attempted with a new batch of purified enzyme, but no detectable rates were observed. As such, the calculation of an IC_{50} value was not collected.

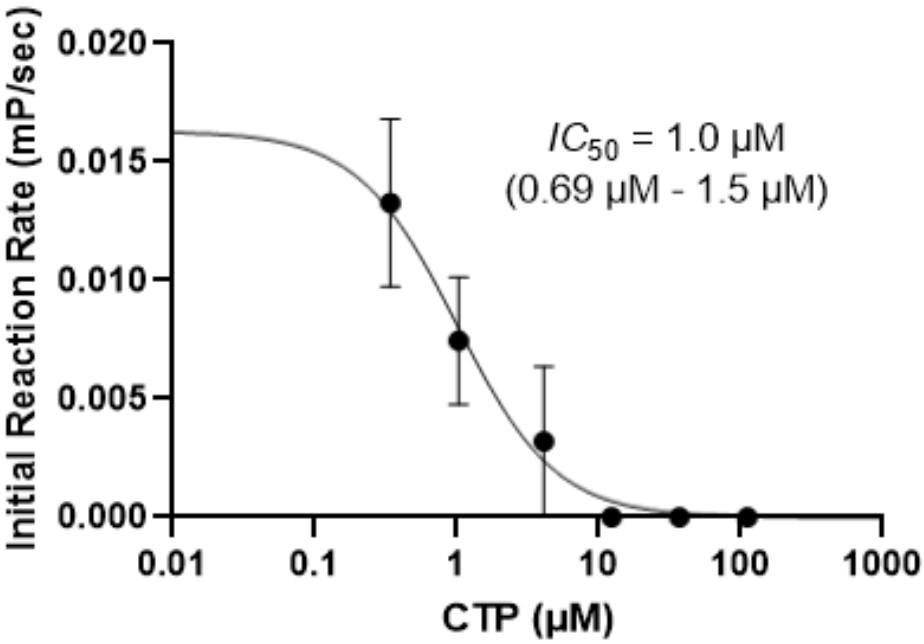

Figure 3.16: FP Assay Captures CTP Inhibition of ST8Sia2 Autopolysialylation. Reaction was carried out in pH 6 MES buffer at room temperature. Reaction mixture contained 500 nM ST8Sia2, 250 nM 9'-FITC-Neu5Ac and various concentrations of CTP. Error bars represent standard deviation (n=3). Bracket values represent 95% confidence intervals calculated from non-linear regression in PRISM, setting bottom constraint to 0 and top constraint to the uninhibited reaction rate.

3.3: Discussion

3.3.1: Assessment of Inhibitor Potency with the CMP-Glo Assay

The CMP-Glo assay did not possess the characteristics of an ideal inhibition assay capable of measuring differential inhibitor potency against sialyltransferases. While the quantitative measurements of the assay allow for direct measurements of reaction kinetics, it became evident that background signal and assay interference were fundamental problems. For any CMP-Glo experiment, a background well must always be included that contains any reaction components that generate nonspecific signal. In these assays, CMP-Neu5Ac and CMP-3F_{ax}-Neu5Ac caused a dose dependant to increase in the signal generated by the assay. The cause of this background signal may be due to the non-enzymatic hydrolysis of CMP-Sia generating free CMP during the reaction incubation, as CMP-Sia has been demonstrated to be less stable at elevated temperatures and acidic pH (3-5)[108]. Considering this, we altered the pH of the reaction buffer to 8 and observed a reduction in background signal. Despite this, background signal persisted, suggesting that the proprietary CMP-Glo kit components may be able to generate signal directly from CMP-Sia. Furthermore, work in the Macauley lab has found that CMP-3F_{ax}-Neu5Ac is stable in slightly acidic conditions, which may be due to the stabilizing effect of the fluorine on C3. This observation suggests that the background observed from CMP-3F_{ax}-Neu5Ac was not due to acid hydrolysis. Nonetheless, the background signal was still quite large at pH 8, representing roughly a quarter of the total signal, and background subtractions were required for every tested condition.

More importantly, the interference caused by various kit components drastically reduces the value of the CMP-Glo assay in the assessment of sialyltransferase inhibitors. The false detection of inhibition in biochemical assays due to assay interference is not a new problem. For example, pan-assay interference compounds (PAIN's) have been identified and reviewed thoroughly, known to cause issues across various biochemical assays[109]. The observation that

CDP inhibited the kit components at concentrations greater than 50 μM was interesting, as CDP is structurally similar to the CMP substrate used by the CMP-Glo kit to generate signal and was therefore expected to generate background signal. The mechanisms by which this non-specific inhibition occurs are not well understood. It is possible that these components inhibit the CMP-Glo luciferase enzyme used to generate the luminescent signal. Alternatively, they may slow the conversion of CMP to ATP, leading to a reduction of the ATP needed by the luciferase enzyme to generate signal. These findings are valuable, as other laboratories have recently began using this assay for determination of IC_{50} and K_i values for novel sialyltransferase inhibitors, which could be compromised if these underlying artifacts are not controlled for[110,111].

Despite these shortcomings, an IC_{50} value for CDP towards ST6Gal1 was experimentally calculated to be 180 μM. Using the four-fold dilution strategy, the highest CDP concentration that could be tested without assay interference was 200 μM. This is problematic, as ideal inhibition curves should test concentrations that far exceed the IC_{50} to fully plot the points at high concentrations. A previously calculated K_i value of 10 μM for CDP towards ST6Gal1 was found using an HPLC separation and UV visualization strategy[54]. The observed inhibition potency was weaker in the CMP-Glo assay, which may be attributed to performing the reaction in pH 8 conditions. The CMP-Glo kit generates quantitative data and is a useful tool to assess substrate specificities and enzymatic parameters such as K_M and V_{max}. However, the drawbacks of the assay make it a poor candidate for inhibition applications, and the fluorescence polarization assay was subsequently investigated as a continuous method for assessing inhibition.

3.3.2: Establishing and Optimizing a Fluorescence Polarization Based Assay

In previous literature, fluorescein was conjugated to the 9’ position of CMP-Neu5Ac, demonstrating its use in enzymatic fluorescence polarization assays[66]. Two potential limitations arise with the use of 9’-FITC CMP-Neu5Ac as a tracer in the FP assay. First, the fluorescence of fluorescein is pH dependant, exhibiting limited fluorescence below pH 6[112]. Second, recent

literature has demonstrated that ST6Gal1 prefers bulky substituents on the C5 of CMP-Neu5Ac when compared to C9, due to projection into the solvent when conjugated to C5[24]. This motivated the synthesis of a tracer with a pH insensitive fluorophore conjugated to C5 of CMP-Neu5Ac, which was performed by Dhanraj Kumawat in the Macauley lab. However, this new tracer (5'-BODIPY CMP-Neu5Ac) performed poorly compared to the 9'-FITC tracer. While a change in mP was observed over time, the maximal signal (mP) in reactions using the 5'-BODIPY tracer was ~60 mP compared to ~150 mP for the 9'-FITC tracer. The poor performance of the 5'-BODIPY tracer in this enzymatic FP assay may be due to a phenomenon known as the 'propellor effect'. Here, a long linker between donor sugar and fluorophore leads to increased rates of fluorophore rotation compared to the bound probe, causing decreased mP signal[113].

When assessing reaction linearity with respect to reaction components, important considerations were uncovered. When asialofetuin was titrated in enzymatic reaction mixtures, larger concentrations were observed to consistently increase in the baseline mP value. This may be attributed to the increased viscosity of the solution when higher glycoprotein concentrations are present. As the FP assay indirectly measures activity by measuring relative rates of molecular rotation, factors that affect the viscosity of the fluid are also expected to cause deviations in molecular rotation. This artefact prevents the use of large concentrations of glycoprotein acceptor, which may otherwise be desired to increase reaction rates or generate Michaelis-Menten plots. A consequence of this artefact was exhibited for ST3Gal1, as asialofetuin concentrations above 250 µM could not be tested, making asialofetuin's K_M for ST3Gal1 impossible to plot with the tested conditions. However, ST6Gal1 catalyzed reactions were successfully plotted with non-linear regression against various acceptor concentrations, generating a Michaelis-Menten curve and a K_M value of 8.3 µM towards asialofetuin. This value was consistent with a calculated literature value of 6.4 µM, however this value is expressed as a concentration of terminal galactose residues, which may obfuscate the comparison[114].

3.3.3: Initial Assessment of Differential Inhibition Using FP Assay

The initial reaction conditions chosen for inhibition assessments in the FP assay used a pH 8 Tris buffer. This buffer was chosen due to its use in the CMP-Glo assay to reduce the background signal associated with weak acidic conditions. This was not required for the FP assay as background is not generated from free CMP, but was chosen so that results between the assays could be compared. On the surface, no obvious issues existed using these conditions, as IC_{50} values for CMP, CDP, CTP, CMP-3F_{ax}-Neu5Ac and CMP-7F-Neu5Ac were all collected towards ST6Gal1 and ST3Gal1. Focusing on the nucleotide inhibitors, ST3Gal1 exhibited selective inhibition by CTP when compared to CMP as evidenced by a 10-fold lower IC_{50} value. ST6Gal1 was inhibited by CDP and CTP with IC_{50} values of 190 and 160 μM respectively. However, CMP exhibited weaker inhibitory potency than CDP or CTP, a finding that is consistent with previous literature on human ST6Gal1[114].

The IC_{50} for CMP-3F_{ax}-Neu5Ac towards ST6Gal1 was calculated to be 660 μM in pH 8 Tris buffer. It is important to note that IC_{50} values of similar magnitude were calculated reproducibly, even when assessed using the 5'-BODIPY tracer. However, this value is 70-fold larger than values calculated using a similar fluorescence polarization assay in the literature, which found an IC_{50} value of 9.5 μM[73]. This was an alarming observation as cell-based lectin binding assays and *in vivo* tumor growth studies have demonstrated high potency of peracetylated 3F_{ax}-Neu5Ac, effective at concentrations far below 660 μM[79]. One initial explanation for this observation is that observed reduction of sialylated glycans in these studies may be due to global feedback inhibition of GNE, which would not require potent competitive inhibition of sialyltransferases. Interestingly, ST6Gal1 and ST3Gal1 were inhibited by CMP-7F-Neu5Ac with greater potency than CMP-3F_{ax}-Neu5Ac, as evidenced by three-fold reduction in calculated IC_{50} values. However, previous studies have indicated that 7-fluoro sialic acid is tolerated as a substrate by bacterial sialyltransferases, as well as human ST6Gal1[115]. If CMP-7F-Neu5Ac is

significantly incorporated by human sialyltransferases in the FP inhibition assay, it would compete for the enzyme active site and slow the transfer of tracer sugar, reducing the observed mP signal. This mechanism would be more accurately described as substrate competition, rather than competitive inhibition. Secondary assays will be required to determine if the rate of transfer of CMP-7F-Neu5Ac confounds the IC_{50} values calculated in the FP assay.

3.3.4: Factors that Affect Observed Inhibition Potency in the FP Assay

To reproduce the low micromolar IC_{50} value demonstrated in the literature for CMP-3F_{ax}-Neu5Ac towards ST6Gal1, both reaction pH and glycoprotein acceptor were varied to produce four IC_{50} curves. In their work, the researchers used reaction mixtures buffered to pH 6.5 containing asialofetuin acceptor concentrations of 0.1 mg/mL (~2.7 μM). It is important to note that ST6Gal1 demonstrates maximal activity near pH 6, and the *trans*-Golgi has been characterized at ~pH 6, with tight regulatory controls[116]. Given this, higher rates of reaction were expected at pH 6.5, but the downstream effect on the IC_{50} value has not been characterized in the literature. For these experiments, the pH 8 condition was prepared using 20 mM HEPES buffer instead of 20 mM Tris. This choice was motivated by recent published work demonstrating that Tris derivatives can act as a substrate for bacterial sialyltransferases[102]. This has not been demonstrated with human sialyltransferases to date, but if the tracer sugar is conjugated to Tris by ST6Gal1 in the FP assay, the change in rotational rate will be small, failing to generate an mP signal. This would lead to slower observed reaction rates, acting a potential confound in the assay. In this work, pH 8 Tris buffer reduced reaction rates for an ST6Gal1 catalyzed reaction when compared to pH 8 HEPES buffer by ~30%. This can be explained by either inhibition of ST6Gal1 by Tris, or by Tris acting as an acceptor. This is the first demonstration of Tris-dependant reduction of reaction rates for human ST6Gal1, and further characterization of this effect should be investigated by detecting sialylated Tris structures. This may be of particular importance to

commercial sialyltransferase applications, as Tris buffer is commonly used in commercial kits as a reaction or storage buffer.

A strong effect of pH on calculated IC_{50} values was determined for CMP-3F$_{ax}$-Neu5Ac inhibition towards ST6Gal1. When saturating acceptor concentrations were present in reaction mixtures (55.6 μM, six-fold greater than K_M), the IC_{50} value calculated at pH 8 were three-fold higher than pH 6.5. When lower acceptor concentrations were present in reaction mixtures (2.7 μM, ~$\frac{1}{2}$ K_M), the IC_{50} value calculated at pH 8 were again three-fold higher than pH 6.5. At both acceptor concentrations tested, a reduction of pH from 8 to 6.5 led to a three-fold reduction in calculated IC_{50} values. Intriguingly, the condition that closely resembled the established literature conditions contained 2.7 μM acceptor glycoprotein at pH 6.5, resulting in an IC_{50} value of 110 μM, 10-fold higher than the literature value. However, when acceptor concentration was increased to 55.6 μM, a comparable IC_{50} value of 15 μM was calculated. When considering the acceptor concentration (asialofetuin) at each pH, a strong influence on the calculated IC_{50} values was observed. At pH 8, increasing the acceptor concentration from 2.7 μM to 55.6 μM led to a six-fold increase of IC_{50}, while in pH 6.5 conditions, increasing the acceptor concentration led to a seven-fold increase in IC_{50}. These deviations have not yet been characterized in the literature, but this work clearly demonstrates their importance when assessing sialyltransferase inhibitors. When reactions were carried out at pH 6.5, the IC_{50} values of CMP-3F$_{ax}$-Neu5Ac towards ST6Gal1 were similar to the K_M of the native CMP-Neu5Ac donor of ST6Gal1[103–105]. Furthermore, the calculated values corroborate the collaborative work carried out by the Klassen lab, which measured a K_d of 50 μM for CMP-3F$_{ax}$-Neu5Ac using a mass spectroscopy-based assay.

The relationship between these pH and the resulting IC_{50} values may be understood in relation to the effects on the reaction rate. When comparing pH, increased reaction rates at pH 6.5 led to reduced IC_{50} values. When comparing acceptor concentrations, increased reaction rates with achieved by increasing acceptor concentrations led to reduced IC_{50} values as well.

Another perspective to elucidate these interactions considers that IC_{50} values are known to vary with substrate concentration, while K_i values are alternative constants that do not vary with substrate concentration. To understand the relationship between these two parameters, the Cheng-Prusoff equation can be applied.

$$K_i = IC_{50} / [1 + ([S]/K_M)]$$

Effect of pH: The Cheng-Prusoff equation defines the relationship between IC_{50} and K_i values across various concentrations of competing substrate[117]. Notably, when the substrate concentration is very small relative to its affinity constant K_M, such that the [S] upon K_M term approaches 0, calculated IC_{50} values are theoretically equal to K_i. In this work, the tracer molecules 9'-FITC CMP-Neu5Ac and 5'-FITC CMP-Neu5Ac compete with competitive inhibitors for access to the enzyme active site, and are present in the reaction mixture at a concentration of 250 nM. According to the Cheng-Prusoff equation, the only way for IC_{50} values to deviate significantly from the theoretical K_i in these experiments is if the K_M for the 9'-FITC tracer is significantly below 1 µM. This has not yet been demonstrated for 9'-FITC CMP-Neu5Ac in the literature, but such a finding would be unexpected as the K_M value for the native donor sugar CMP-Sia is reported between 50-120 µM[103–105]. Assuming that the tracer exhibits a similar affinity similar to that of CMP-Sia, the different IC_{50} values calculated represent different underlying K_i values. This interpretation is consistent with the observed pH sensitivity of the calculated IC_{50} values. If the affinity of the 9'-FITC tracer is pH dependant towards ST6Gal1, then the dissociation constant K_i will be altered.

Effect of Glycoprotein Acceptor Concentration: Applying the Cheng-Prusoff equation does not explain the observation that different asialofetuin acceptor concentrations alter the IC_{50} values in the FP assay. Sialyltransferases undergo a conformational change upon binding the donor-sugar, a prerequisite for binding of the glycan acceptor. This behaviour is referred to as a sequential-

ordered mechanism, and has been characterized for bacterial and mammalian sialyltransferases[118]. An implication of this mechanism is that the formation of the enzyme substrate complex is only affected by the concentration and affinity of the donor-sugar. Therefore, while the concentration of the glycoprotein acceptor may influence the overall reaction rate by modulating k_{cat}, it should not influence the K_i value of the donor sugar. This implies that when changing the acceptor concentration in the FP assay, the differential IC_{50} values observed do not represent different underlying K_i values. Understanding the mechanism by which glycoprotein acceptors influence IC_{50} values in the FP assay will be imperative to rule out a potential confounding artefact in the assay.

Effect of Tracer: Initially, 5'-BODIPY CMP-Neu5Ac was investigated as a tracer due to evidence that ST6Gal1 can tolerate bulky 5' modifications[24]. However, this tracer performed poorly for reasons that remain poorly understood. Three factors may explain this, the length of the linker (propellor effect), the identity of the fluorophore, and the position on the donor-sugar. To assess the important of position on the donor-sugar, 5'-FITC CMP-Neu5Ac was assessed as a tracer at both pH 8 and 6.5 using high acceptor concentrations to be compared to 9'-FITC. These conditions were chosen as they provided the optimized rate and provided values that agreed best with literature. When comparing the calculated IC_{50} values for CMP-3F_{ax}-Neu5Ac in pH 8 buffer, both tracers generated similar IC_{50} values. However, when assessed using pH 6.5 buffer, the IC_{50} generated using the 5'-FITC tracer was two-fold higher than was found with the 9'-FITC tracer.

The work introduces the importance of reaction pH, buffer composition, acceptor glycoprotein concentration, and identity of the fluorescent tracer to the interpretation of IC_{50} values generated in a previously described FP-based assay. The calculation of reliable IC_{50}/K_i values will represent a key step in pre-clinical assessments of selective sialyltransferase inhibitors. The FP-based assay offers robust measurements at reasonable cost, but to be used for this purpose it must generate valid IC_{50} values that are parsimonious with secondary, quantitative assays.

Therefore, experimental conditions must be fully characterized, ensuring that all calculated IC_{50} values can accurately related to K_i by the Cheng-Prusoff equation without interference of assay artefacts.

3.3.5: Assessing Inhibition of Polysialylation for Polysialyltransferase ST8Sia2

As the ST8Sia2 Fc-construct was successfully cloned in Chapter 2, its activity was investigated in the FP-based assay. Initially, a cross titration of ST8Sia2 and glycoprotein acceptor fetuin was assessed in pH 8 Tris buffer, with no activity detected in all conditions tested. However, when pH 6 MES buffer was used, and reaction mixtures were incubated at 37°C, activity was detected at various concentrations of fetuin. Intriguingly, the highest reaction rates were observed when no fetuin was present in the reaction mixture. This observation may be explained by the process of autopolysialylation, where a polysialyltransferase uses its own glycans as acceptors[50]. In Chapter 2, the ST8Sia2 Fc-construct ran at a larger size than expected in the SDS-PAGE, consistent with the presence of PolySia on the purified construct. Assuming that ST8Sia2 exhibits a substrate preference towards its own PolySia glycans, increasing concentrations of fetuin (which do not possess PolySia) may compete for these sites, reducing the overall reaction rate. Alternatively, the IgG_1 Fc fused to the ST8Sia2 Fc-construct possesses a single *N*-glycan site which has been observed to be partially sialylated in studies focusing on Fcγ receptor binding[119]. If sialylated, this glycan could potentially act as a substrate for ST8Sia2. This can be addressed in future experiments by treating ST8Sia2 Fc-construct with TEV protease to remove the Fc prior to assessment of function.

To assess if the signal generated from autopolysialylation could be inhibited in the FP assay to calculate *in vitro* IC_{50} values, CTP was introduced to reaction mixtures containing 500 nM ST8Sia2 and 250 nM 9'-FITC tracer. Notably, as ST8Sia2 was both the enzyme and the acceptor in this reaction, its concentration could not be reduced without massive loss of signal. A novel IC_{50} of 1.0 μM was calculated in this experiment, which is lower than any IC_{50} calculated for

ST6Gal1 and ST3Gal1, suggesting that CTP is a potent inhibitor of ST8Sia2. One potential explanation for this observation is that ST8Sia2 possesses a positively charged, poly-basic region called the poly-sialyltransferase domain[42,43]. This domain is understood to stabilize the binding of PolySia, a polymer of Neu5Ac residues each carrying a negatively charged carboxylate. At pH 6, CTP carries 4 negative charges, which may form ionic interactions with the poly-basic poly-sialyltransferase domain. There are two notable limitations to discuss. First, the enzyme concentration used was greater than that of the tracer. A key assumption when assessing Michaelis-Menten kinetics is that the concentration of enzyme is far lower than the substrate. Second, when a separate batch of ST8Sia2 was assessed using identical conditions to measure the IC_{50} of CMP-3F_{ax}-Neu5Ac, no enzyme activity was detected. This may be due to loss of ST8Sia2 activity during purification of the new batch. Notably, ST8Sia2 had been frozen for 2 months prior to this assessment. While ST6Gal1 did not lose activity over this storage period, it is possible that ST8Sia2 did. To solve this, experiments measuring ST8Sia2 activity may require freshly purified enzyme. More work needs to be done to ensure that the signal generated in the FP-based assay is reproducibly capturing autopolysialylation activity of ST8Sia2.

These results are exciting, as few tools exist to study the reactions of polysialyltransferases. Polysialyltransferases are unique in that they generate multiple products in their catalysis, characterized by different numbers of Neu5Ac residues. This makes the quantification of reaction rates challenging with established separation-based strategies. In this work, the FP-based inhibition assay has preliminarily demonstrated the ability to detect autopolysialylation activity of ST8Sia2, and allow for calculation of IC_{50} values.

3.4: Conclusions

This chapter demonstrates successful assessment of inhibition against sialyltransferase Fc-constructs cloned in Chapter 2. The CMP-Glo assay was investigated for inhibition of sialyltransferases, and demonstrated problematic assay interference. In its place, an FP-based assay established in previous literature was developed and optimized. Using this assay, IC_{50} values for nucleotide and CMP-Neu5Ac analog inhibitors were calculated for ST6Gal1 and ST3Gal1. When investigated further, various reaction conditions including pH and glycoprotein acceptor concentration led to large deviation in the calculated IC_{50} values. These differences were characterized, but require further investigation to elucidate the implications on the IC_{50} values generated in the FP assay. Lastly, CTP inhibition of ST8Sia2 autopolysialylation activity was demonstrated *in vitro.*

3.5: Materials and Methods

Sialyltransferase Reaction with Inhibition for CMP-Glo Assay.

To perform the CMP-Glo Assay for a time-course inhibition assessment of CDP, sialyltransferase reaction mixtures were prepared as follows. To each plate well, 12.5 µL of 2X sialyltransferase buffer (40 mM Tris, 150 mM NaCl, pH = 8) was added. Then, 2.5 µL of 10X acceptor solution and 2.5 µL of 10X donor sugar solution were added to respective wells. Then 2.5 µl of 10X CDP solutions were added to respective plate wells. Prior to the addition of enzyme to start the reaction, the reaction mixtures were incubated at 37°C for 10 minutes to prevent temperature changes during the reaction. Reactions were initiated by addition of 5 µL 5X sialyltransferase solution. During incubation, 20 µL of CMP-Glo Enzyme was added to 500 µL of CMP-Glo detection buffer and thoroughly mixed. To wells of a white opaque 96-well plate, 25 µL of CMP-Glo detection reagent + CMP-Glo enzyme was added as required. At various time points, 25 µL of reaction mixture was added to each plate well as required. Addition of reaction mixture to CMP-Glo

detection buffer quenches the reaction, allowing for a time-course to be assessed for the stopped assay. After the final time point, the opaque plate was stored in a dark environment for 1 hour as per manufacturer's instruction and read on a ID5 SpectraMax plate reader with 1000 ms integration time for total luminescence. Background subtraction was carried out in wells containing identical reaction conditions with the addition of water instead of enzyme. Signal generated in background controls was subtracted from total luminescence for final assessment and quantification.

Table 3.3: Sialyltransferase Reactions for CMP-Glo Assay

Reagent	**Detail**	**Manufacturer**
Opaque White 96-well Plate	781965	Cole-Parmer
CMP-Glo Detection Buffer	VA1131	Promega
CMP-Glo Glo-Enzyme	VA1131	Promega
Tris Base	BP152-5	Fischer Chemical
MES	BP300-100	Fischer Biotech
Triton X-100	9002-91-1	Sigma Chemical
Sodium Chloride	S9625	Sigma-Aldrich
Asialofetuin	A4781	Sigma-Aldrich
CMP-Neu5Ac	3063-71-6	Nacalai USA
Cytidine Diphosphate	C9755	Sigma-Aldrich

Sialyltransferase Reaction with Inhibition in Fluorescence Polarization Assay.

To perform the Fluorescence Polarization assay for semi-quantitative inhibition, 40 µL reaction mixtures were prepared as follows. 20µL of 2X sialyltransferase buffer (40mM Tris/HEPES/MES, 300 mM NaCl, 0.02% Triton X-100) was added to wells of a black 396-well plate. To each well, 5 µL of 8X acceptor solution and 5 µL of 8X donor sugar (tracer) solution were added. Then 5 µL of 8X inhibitor solutions were added to the respective wells, with care taken to ensure minimal cross-contamination. For assessments without inhibitor, 5 µL water is added in place of the inhibitor solution. If reactions were to be carried out at 37 °C, the 396 well plate would be incubated at 37 °C for at least 10 minutes to allow for equilibration of the plate, prior to addition of enzyme.

If reactions were to be carried out at room temperature, reactions were initiated with 5 µL of 8X sialyltransferase solution and immediately loaded into a SpectraMax ID5 instrument for FP measurements. Care must be taken to add the enzyme quickly and accurately, as the first measurement only occurs once all wells are loaded. To minimize this effect when assessing inhibition at various concentrations of inhibitor, enzyme was loaded to wells containing the highest amount of inhibitor first, and the lowest amount of inhibitor last. The SpectraMax ID5 protocol used an integration time of 200 ms and a read height of 0.83 mm. The samples were excited at 485 nm and emission was detected at 535 nm. All parallel and perpendicular RLU values were blank subtracted from a well containing only 20 µL 2X sialyltransferase buffer and 20 µL to ensure erroneous measurements due to background signal did not confound calculated mP values.

Once data was collected, linearity was assessed manually, and slopes for the linear regions were generated for each individual reaction well in Excel. Slopes were plotted to a four-parameter non-linear regression on PRISM, with error bars representing standard deviation of slope measurements. To fit the regression, the average slopes of the uninhibited reactions were used as the top constraint. The bottom constraint was set to 0.

Table 3.4: Sialyltransferase Reaction Components for FP Assay

Reagent	**Detail**	**Manufacturer**
Greiner Black 396-well Plate	781209	Greiner Bio-One
Tris Base	BP152-5	Sigma-Aldrich
Sodium Chloride	S9625	Sigma-Aldrich
MES	BP300-100	Fischer Biotech
HEPES	H3375	Sigma-Aldrich
Triton X-100	9002-91-1	Sigma Chemical
Asialofetuin	A4781	Sigma-Aldrich
Fetuin	F3385	Sigma-Aldrich
9'-FITC CMP-Neu5Ac	Synthesized by Dhanraj Kumawat in the Macauley Lab	
5-FITC CMP-Neu5Ac	Synthesized by Dhanraj Kumawat in the Macauley Lab	
5'-BODIPY CMP-Neu5Ac	Synthesized by Dhanraj Kumawat in the Macauley Lab	

Table 3.5: Sialyltransferase Inhibitors used in FP Assay

Reagent	Detail	Manufacturer
Cytidine Monophosphate	C1006	Sigma-Aldrich
Cytidine Diphosphate	CD9755	Sigma-Aldrich
Cytidine Triphosphate		Carbosynth
CMP-3F$_{ax}$-Neu5Ac	Synthesized by Dhanraj Kumawat in the Macauley Lab	
CMP-7F-Neu5Ac	Synthesized by Dhanraj Kumawat in the Macauley Lab	

Chapter 4

Conclusions and Future Directions

4.1: Conclusion

The ability to modulate the presentation of cell surface sialic acid will allow for investigation of sialic acid dependant receptor binding interactions, which may offer therapeutic potential in pathologies characterized by dysregulated sialic acid expression. Inhibition of sialyltransferases is a promising target for sialic acid modulation, but new tools are needed to study the great complexity introduced when studying inhibition towards 20 different human sialyltransferases, which use various accepting substrates. Prodrug inhibitors that mimic sialic acid have demonstrated strong potential in living systems as evidenced by reductions of cell surface sialic acid, but the mechanism of action is not fully understood. To study the direct and potentially selective inhibition of sialyltransferases with enzymatic assays, researchers require recombinant human sialyltransferases. Moreover, enzymatic assays are required to accurately measure inhibition. These assays must tolerate many inhibitors and accepting substrates, so that all 20 human sialyltransferases can be investigated.

In Chapter 2, a recombinant cloning design was developed, using a stable CHO Flp-in mammalian expression system. For successful protein expression, an IgG_1 Fc fusion strategy was used, generating 'Fc-constructs' which also contained a 6x His and Strep II tag for two step purification. An ELISA strategy was employed to directly measure expression yields from media, but failed to selectively detect sialyltransferase Fc-constructs. These recombinant enzymes were then assessed for activity using the CMP-Glo assay, demonstrating that the constructs exhibited substrate preferences (LacNAc vs. lactose) and kinetic parameters (K_M and V_{max}) that matched previous literature.

In Chapter 3, inhibition assays were developed and optimized to measure inhibition of sialyltransferase Fc-constructs. The CMP-Glo assay was used to determine an IC_{50} for CDP towards human ST6Gal1 but exhibited assay interference from various compounds and was not used for further investigation of inhibitor potency. Then, a fluorescence polarization-based assay was developed. Once established, the assay generated IC_{50} values for various inhibitors including CMP-3F$_{ax}$-Neu5Ac and CMP-7F-Neu5Ac toward human ST6Gal1 and ST3Gal1, which initially deviated significantly from established literature values. Upon further investigation, reaction conditions that influenced IC_{50} values were identified, including pH and acceptor glycoprotein concentration. Using specific conditions led to the calculation of IC_{50} values that agreed more closely with established literature values. Finally, the polysialyltransferase ST8Sia2 was found to possess auto-polysialyltransferase activity in the FP-based assay and inhibition potency of CTP was determined.

4.2: Future Directions

The recombinant sialyltransferases and inhibition assays presented in this Thesis possess great potential for the study of differential sialyltransferase inhibition. Herein, four human sialyltransferases constructs have been generated, leaving 16 sialyltransferases to be expressed using the strategy. To improve the expression yields of sialyltransferases, different fusion strategies, exogenous signal sequences, or expression systems should be considered. Storage conditions for the purified Fc-constructs require characterization, including the glycerol content and buffer composition. Furthermore, it will be important to determine if enzyme activity is lost over time in storage to ensure enzymatic assays are not confounded by loss of function over time. As an example, ST8Sia2 may have lost its activity over time, indicating that better storage conditions are required.

The recombinant sialyltransferases generated in this Thesis have uses beyond inhibition assays. Applications such as chemoenzymatic synthesis of sialosides should be investigated, as

an alternative to otherwise complicated and time-consuming synthetic strategies. This application may also be considered for the glycosylation of expressed proteins, such as antibodies, which require sialylation for their effector functions. Furthermore, various enzymatic assays can be employed to investigate substrate and donor sugar preferences across the 20 human sialyltransferases. Differential preferences between sialyltransferases can be investigated using a bump and hole approach for the development of selective sialyltransferase inhibitors, which have not been described to date. Lastly, the application of recombinant sialyltransferases to cells may allow for direct modification of the cell surface, also known as cell surface glycan remodelling, to investigate the impact of altered cell surface sialic acid expression.

The FP-based inhibition assay introduced in Chapter 3 has great potential for the assessment of differential sialyltransferase inhibitor potency. However, the impact of using a non-native donor sugar conjugated to a fluorophore needs to, ideally, be more completely characterized. For this, other enzymatic assays such as the CMP-Glo assay can be used to determine the catalytic efficiency of the non-native donor sugars when compared native CMP-Neu5Ac. Comparing the 9'FITC and 5'FITC donor sugars used in this work, it is expected that the 5'FITC sugar will be tolerated preferentially, but this may be dependant on the sialyltransferase assessed. Identifying an ideal donor-sugar for use in the FP-based assay will include characterizing three features: position of conjugation, fluorophore identity, and length of linker between fluorophore and donor sugar.

Using the optimized FP-based inhibition assay with Fc-construct sialyltransferases, inhibition potency of CMP-3F_{ax}-Neu5Ac can be assessed against all human sialyltransferases which use glycoprotein acceptors. For sialyltransferases that use glycoprotein or disaccharide acceptors, biological conjugation strategies may be employed to conjugate these smaller acceptors into larger presentations which can generate robust mP signal. In Chapter 3, CMP-7F-Neu5Ac was found to inhibit sialyltransferases with similar potency to CMP-3F_{ax}-Neu5Ac. For cell-

based applications of Neu5Ac analog inhibitors, the active inhibitor must be generated from a peracetylated prodrug. Therefore, work needs to be done to establish if CMP-7F-Neu5Ac can be generated in cells. Furthermore, if CMP-7F-Neu5Ac is transferred by sialyltransferases, the FP-based assay signal would appear inhibited as the donor-sugar tracer would compete for the active site. The relative rate of transfer between CMP-7F-Neu5Ac and the donor-sugar tracers used must be characterized using a quantitative enzymatic assay to determine if the inhibition seen in the FP-based assay represents direct inhibition or substrate competition.

With these considerations, all the tools required to measure differential inhibition of sialyltransferases have been put in place. Once developed further, these tools will be able to detect the differential inhibition of novel derivatives of CMP-3F_{ax}-Neu5Ac across the entire GT29 family of human sialyltransferases. Ideally, derivatives of Neu5Ac analog inhibitors will be synthesized that selectively inhibit an individual sialyltransferase. The FP-based assay represents a robust real time assay with low cost and high throughput, allowing for assessment of many inhibitors. These derivatives may also be designed to prevent global feedback inhibition of GNE, allowing them to be used in cells as a selective inhibitor of sialyltransferases. Once developed, selective sialyltransferase inhibitors can then be used for research purposes to selectively alter cell surface sialic acid or investigated for therapeutic application. Such applications could include prevention of viral influenza infection, modulation of dysregulated immune responses, and cancer therapies.

References

1. Varki, A. *et al.* Essentials of Glycobiology. *Cold Spring Harbor (NY* **039**, 2015–2017 (2009).

2. Trottein, F. *et al.* Glycosyltransferase and sulfotransferase gene expression profiles in human monocytes, dendritic cells and macrophages. *Glycoconj J* **26**, 1259–1274 (2009).

3. Angata, T. & Varki, A. Chemical diversity in the sialic acids and related α-keto acids: An evolutionary perspective. *Chem Rev* **102**, 439–469 (2002).

4. Tsuchida, A. *et al.* Synthesis of Disialyl Lewis a (Lea) Structure in Colon Cancer Cell Lines by a Sialyltransferase, ST6GalNAc VI, Responsible for the Synthesis of α-Series Gangliosides. *Journal of Biological Chemistry* **278**, 22787–22794 (2003).

5. Guo, X., Elkashef, S. M., Loadman, P. M., Patterson, L. H. & Falconer, R. A. Recent advances in the analysis of polysialic acid from complex biological systems. *Carbohydr Polym* **224**, (2019).

6. Yu, R. K., Tsai, Y. T. & Ariga, T. Functional roles of gangliosides in Neurodevelopment: An overview of recent advances. *Neurochem Res* **37**, 1230–1244 (2012).

7. Barthel, S. R., Gavino, J. D., Descheny, L. & Dimitroff, C. J. Targeting selectins and selectin ligands in inflammation and cancer. *http://dx.doi.org/10.1517/14728222.11.11.1473* **11**, 1473–1491 (2007).

8. Cappenberg, A., Kardell, M. & Zarbock, A. Selectin-Mediated Signaling—Shedding Light on the Regulation of Integrin Activity in Neutrophils. *Cells* **11**, (2022).

9. Duan, S. & Paulson, J. C. Siglecs as Immune Cell Checkpoints in Disease. A*nnurev Immunol* **38**, 365–395 (2020).

10. Kuhn, B. *et al.* The structure of human α-2,6-sialyltransferase reveals the binding mode of complex glycans. *Acta Crystallographica Section D* **69**, 1826–1838 (2013).

11. Grewal, R. K. *et al.* Structural Insights in Mammalian Sialyltransferases and Fucosyltransferases: We Have Come a Long Way, but It Is Still a Long Way Down. *Molecules 2021, Vol. 26, Page 5203* **26**, 5203 (2021).

12. Harduin-Lepers, A. Comprehensive Analysis of sialyltransferases in Vertebrate Genomes. *Glycobiology Insights* **2,** (2010).

13. Lopez P. H. H. *et al.* Mice lacking sialyltransferase ST3Gal-II develop late-onset obesity and insulin resistance. *Glycobiology* **27**, 129–139 (2017).

14. Ikeda, M. *et al.* Identification of novel candidate genes for treatment response to risperidone and susceptibility for schizophrenia: integrated analysis among pharmacogenomics, mouse expression, and genetic case-control association approaches. *Biol Psychiatry* **67**, 263–269 (2010).

15. Harrus, D., Harduin-Lepers, A. & Glumoff, T. Unliganded and CMP-Neu5Ac bound structures of human α-2,6-sialyltransferase ST6Gal I at high resolution. *J Struct Biol* **212**, 107628 (2020).

16. Wang, P. H. *et al.* Altered mRNA expressions of sialyltransferases in ovarian cancers. *Gynecol Oncol* **99**, 631–639 (2005).

17. Garnham, R., Scott, E., Livermore, K. E. & Munkley, J. ST6GAL1: A key player in cancer. *Oncology Letters* vol. 18 983–989 Preprint at https://doi.org/10.3892/ol.2019.10458 (2019).

18. Park, J. J. & Lee, M. Increasing the α 2, 6 sialylation of glycoproteins may contribute to metastatic spread and therapeutic resistance in colorectal cancer. *Gut and Liver* vol. 7 629–641 Preprint at https://doi.org/10.5009/gnl.2013.7.6.629 (2013).

19. Antony, P. *et al.* Epigenetic inactivation of ST6GAL1 in human bladder cancer. *BMC Cancer* **14**, (2014).

20. Chiodelli, P. *et al.* Contribution of vascular endothelial growth factor receptor-2 sialylation to the process of angiogenesis. *Oncogene* **36**, 6531–6541 (2017).

21. Oriol, R., le Pendu, J. & Mollicone, R. Genetics of ABO, H, Lewis, X and Related Antigens. *Vox Sang* **51**, 161–171 (1986).

22. Wlasichuk, K. B. *et al.* Determination of the Specificities of Rat Liver Gal(βl-4)GlcNAc a2,6-Sialyltransferase and Gal(β1-3/4)GlcNAc a2,3-Sialyltransferase Using Synthetic Modified Acceptors. *The Journal of Biological Chemistry* **268,** (1993).

23. Ortiz-Soto, M. E. & Seibel, J. Expression of Functional Human Sialyltransferases ST3Gal1 and ST6Gal1 in Escherichia coli. *PLoS One* **11**, (2016).

24. Noel, M. *et al.* Probing the CMP-Sialic Acid Donor Specificity of Two Human β-d-Galactoside Sialyltransferases (ST3Gal I and ST6Gal I) Selectively Acting on O- and N-Glycosylproteins. *Chembiochem* **18**, 1251 (2017).

25. Capicciotti, C. J. *et al.* Cell-Surface Glyco-Engineering by Exogenous Enzymatic Transfer Using a Bifunctional CMP-Neu5Ac Derivative. *J Am Chem Soc* **139**, 13342–13348 (2017).

26. van der Poel, S. *et al.* Hyperacidification of trans-Golgi network and endo/lysosomes in melanocytes by glucosylceramide-dependent V-ATPase activity. *Traffic* **12**, 1634–1647 (2011).

27. Rao, F. *et al.* Structural insight into mammalian sialyltransferases. *Nature Structural & Molecular Biology* **16**, 1186–1188 (2009).

28. Pietrobono, S. *et al.* ST3GAL1 is a target of the SOX2-GLI1 transcriptional complex and promotes melanoma metastasis through AXL. *Nat Commun* **11**, (2020).

29. Wu, X. *et al.* Sialyltransferase ST3GAL1 promotes cell migration, invasion, and TGF-β1-induced EMT and confers paclitaxel resistance in ovarian cancer. *Cell Death Dis* **9**, (2018).

30. Lee, Y. Kurosawa, N. Hamamoto, T. Nakaoka T. & Tsuji, S. Molecular cloning and expression of Galβ1,3GalNAcα2,3-sialyltransferase from mouse brain. *Eur J Biochem* **216**, 377–385 (1993).

31. Lin, W. *et al.* Sialylation of CD55 by ST3GAL1 facilitates immune evasion in cancer. *Cancer Immunol Res* **9**, 113–122 (2021).

32. Zhang, N., Lin, S., Cui, W. & Newman, P. J. Overlapping and unique substrate specificities of ST3GAL1 and 2 during hematopoietic and megakaryocytic differentiation. *Blood Adv* **6**, 3945–3955 (2022).

33. Kono, M. *et al.* Mouse β-galactoside α2,3-sialyltransferases: Comparison of in vitro substrate specificities and tissue specific expression. *Glycobiology* **7**, 469–479 (1997).

34. Kitagawa, H. P. J. C. Cloning of a novel alpha 2,3-sialyltransferase that sialylates glycoprotein and glycolipid carbohydrate groups. *J Biol Chem* **269**, 1394–1401 (1994).

35. Rohfritsch, P. F. *et al.* Probing the substrate specificity of four different sialyltransferases using synthetic β-d-Galp-(1 → 4)-β-d-GlcpNAc-(1 → 2)-α-d-Manp-(1 → O) (CH2)7CH3 analogues: General activating effect of replacing N-acetylglucosamine by N-propionylglucosamine. *Biochimica et Biophysica Acta (BBA) - General Subjects* **1760**, 685–692 (2006).

36. Mondal, N. *et al.* ST3Gal-4 is the primary sialyltransferase regulating the synthesis of E-, P-, and L-selectin ligands on human myeloid leukocytes. *Blood* **125**, 687 (2015).

37. Carvalho, A. S. *et al.* Differential expression of α-2,3-sialyltransferases and α-1,3/4-fucosyltransferases regulates the levels of sialyl Lewis a and sialyl Lewis x in gastrointestinal carcinoma cells. *Int J Biochem Cell Biol* **42**, 80–89 (2010).

38. Hugonnet, M., Singh, P., Haas, Q. & von Gunten, S. The Distinct Roles of Sialyltransferases in Cancer Biology and Onco-Immunology. *Front Immunol* **12**, 5495 (2021).

39. Yang, W. H., Nussbaum, C., Grewal, P. K., Marth, J. D. & Sperandio, M. Coordinated roles of ST3Gal-VI and ST3Gal-IV sialyltransferases in the synthesis of selectin ligands. *Blood* **120**, 1015–1026 (2012).

40. Villanueva-Cabello, T. M., Gutiérrez-Valenzuela, L. D., Salinas-Marín, R., López-Guerrero, D. v. & Martínez-Duncker, I. Polysialic Acid in the Immune System. *Front Immunol* **12**, 5987 (2022).

41. Sato, C. & Kitajima, K. Polysialylation and disease. *Mol Aspects Med* **79**, (2021).

42. Nakata, D., Zhang, L. & Troy, F. A. Molecular basis for polysialylation: A novel polybasic polysialyltransferase domain (PSTD) of 32 amino acids unique to the α2,8-polysialyltransferases is essential for polysialylation. *Glycoconj J* **23**, 423–436 (2006).

43. Angata, K. & Fukuda, M. Polysialyltransferases: Major players in polysialic acid synthesis on the neural cell adhesion molecule. *Biochimie* vol. 85 195–206 Preprint at https://doi.org/10.1016/S0300-9084(03)00051-8 (2003).

44. Mühlenhoff, M., Rollenhagen, M., Werneburg, S., Gerardy-Schahn, R. & Hildebrandt, H. Polysialic acid: Versatile modification of NCAM, SynCAM 1 and neuropilin-2. *Neurochem Res* **38**, 1134–1143 (2013).

45. Seidenfaden, R., Gerardy-Schahn, R. & Hildebrandt, H. Control of NCAM polysialylation by the differential expression of polysialyltransferases ST8SiaII and ST8SiaIV. *Eur J Cell Biol* **79**, 680–688 (2000).

46. Kojima, N., Yoshida, Y., Kurosawa, N., Lee, Y.-C. & Tsuji, S. Enzymatic activity of a developmentally regulated member of the sialyltransferase family (STX)" evidence for 2,8-sialyltransferase activity toward N-linked oligosaccharides. *FEBS Letters* **360**, (1995).

47. Scheidegger, E. P., Sternberg, L. R., Roth, J. & Lowe, J. B. A Human STX cDNA Confers Polysialic Acid Expression in Mammalian Cells. *Journal of Biological Chemistry* **270**, 22685–22688 (1995).

48. Kojima, N., Yoshida, Y. & Tsuji, S. A developmentally regulated member of the sialyltransferase family (ST8Sia II, STX) is a polysialic acid synthase. *FEBS Letters* **373**, 122 (1995).

49. Ehrit, J. *et al.* Exploring and Exploiting Acceptor Preferences of the Human Polysialyltransferases as a Basis for an Inhibitor Screen. *ChemBioChem* **18**, 1332–1337 (2017).

50. Close, B. E. *et al.* The polysialyltransferase ST8Sia II/STX: posttranslational processing and role of autopolysialylation in the polysialylation of neural cell adhesion molecule. *Glycobiology* **11**, 997–1008 (2001).

51. Kurosawa, N., Kojimas, N., Inoue, M., Hamamoto, T. & Tsujip, S. Cloning and Expression of GalP1,3GalNA~-specific GalNAc a2,6-Sialyltransferase. *The Journal of Biological Chemistry* **269**, 19048–19053 (1994).

52. Takashima, S., Tsuji, S. & Tsujimoto, M. Comparison of the Enzymatic Properties of Mouse β-Galactoside α2,6-Sialyltransferases, ST6Gal I and II. *The Journal of Biochemistry* **134**, 287–296 (2003).

53. Kono, M. *et al.* Mouse β-galactoside α2,3-sialyltransferases: Comparison of in vitro substrate specificities and tissue specific expression. *Glycobiology* **7**, 469–479 (1997).

54. Schaub, C., Müller, B. & Schmidt, R. R. New sialyltransferase inhibitors based on CMP-quinic acid: development of a new sialyltransferase assay. *Glycoconj J* **15**, 345–354 (1998).

55. Skropeta, D., Schwörer, R., Schwörer, S., Haag, T. & Schmidt, R. R. Asymmetric synthesis and affinity of potent sialyltransferase inhibitors based on transition-state analogues. *Glycoconj J* **21**, 205–219 (2004).

56. Zegzouti, H., Engel, L., Hennek, J., Alves, J. & Vidugiris, G. Detection of Glycosyltransferase Activities with Homogeneous Bioluminescent Detection Assays. (2014).

57. Kellman, B. P. *et al.* Elucidating Human Milk Oligosaccharide biosynthetic genes through network-based multi-omics integration. *Nature Communications 2022 13:1* **13**, 1–15 (2022).

58. Skropeta, D. *et al.* Sialyltransferase Inhibitors as Potential Anti-Cancer Agents. *Australian Journal of Chemistry* **74**, (2021).

59. Yang, M., Brazier, M., Edwards, R. & Davis, B. G. High-throughput mass-spectrometry monitoring for multisubstrate enzymes: Determining the kinetic parameters and catalytic activities of glycosyltransferases. *ChemBioChem* **6**, 346–357 (2005).

60. Nagahori, N. & Nishimura, S. I. Direct and Efficient Monitoring of Glycosyltransferase Reactions on Gold Colloidal Nanoparticles by Using Mass Spectrometry. *Chemistry – A European Journal* **12**, 6478–6485 (2006).

61. Kitov, P. *et al.* A quantitative, high-throughput method identifies protein–glycan interactions via mass spectrometry. *Commun Biol* **2**, (2019).

62. Li, Z. *et al.* CUPRA-ZYME: An Assay for Measuring Carbohydrate-Active Enzyme Activities, Pathways, and Substrate Specificities. *Anal Chem* **92**, 3228–3236 (2020).

63. Hall, M. D. *et al.* Fluorescence polarization assays in high-throughput screening and drug discovery: a review. *Methods Appl Fluoresc* **4**, 022001 (2016).

64. Berezin, M. Y. & Achilefu, S. Fluorescence lifetime measurements and biological imaging. *Chem Rev* **110**, 2641–2684 (2010).

65. Parker, G. J., Law, T. L., Lenoch, F. J. & Bolger, R. E. Development of High Throughput Screening Assays Using Fluorescence Polarization: Nuclear Receptor-Ligand–Binding and Kinase/Phosphatase Assays. *SLAS Discovery* **5**, 77–88 (2000).

66. Rillahan, C. D., Brown, S. J., Register, A. C., Rosen, H. & Paulson, J. C. High-throughput screening for inhibitors of sialyl- and fucosyltransferases. *Angewandte Chemie - International Edition* **50**, 12534–12537 (2011).

67. Wang, L., Liu, Y., Wu, L. & Sun, X. L. Sialyltransferase inhibition and recent advances. *Biochimica et Biophysica Acta (BBA) - Proteins and Proteomics* **1864**, 143–153 (2016).

68. Jung, K. H., Schwörer, R. & Schmidt, R. R. Sialyltransferase Inhibitors. *Trends in Glycoscience and Glycotechnology* **15**, 275–289 (2003).

69. Guo, X. *et al.* An efficient assay for identification and quantitative evaluation of potential polysialyltransferase inhibitors. *Analyst* **145**, 4512–4521 (2020).

70. Guo, J., Li, W., Xue, W. & Ye, X. S. Transition State-Based Sialyltransferase Inhibitors: Mimicking Oxocarbenium Ion by Simple Amide. *J Med Chem* **60**, 2135–2141 (2017).

71. Burkart, M. D. *et al.* Chemo-enzymatic synthesis of fluorinated sugar nucleotide: useful mechanistic Probes for glycosyltransferases. *Bioorg Med Chem* **8**, 1937–1946 (2000).

72. Chokhawala, H. A., Cao, H., Yu, H. & Chen, X. Enzymatic synthesis of fluorinated mechanistic probes for sialidases and sialyltransferases. *J Am Chem Soc* **129**, 10630–10631 (2007).

73. Rillahan, C. D. *et al.* Global Metabolic Inhibitors of Sialyl- and Fucosyltransferases. *Nat Chem Biol* **8**, 661 (2012).

74. Krause, S. *et al.* Localization of UDP-GlcNAc 2-epimerase/ManAc kinase (GNE) in the Golgi complex and the nucleus of mammalian cells. *Exp Cell Res* **304**, 365–379 (2005).

75. van Scherpenzeel, M. *et al.* Dynamic tracing of sugar metabolism reveals the mechanisms of action of synthetic sugar analogs. *Glycobiology* **32**, 239–250 (2022).

76. Burkart, M. D. *et al.* Chemo-enzymatic synthesis of fluorinated sugar nucleotide: useful mechanistic Probes for glycosyltransferases. *Bioorg Med Chem* **8**, 1937–1946 (2000).

77. Ni, L. *et al.* Crystal structures of Pasteurella multocida sialyltransferase complexes with acceptor and donor analogues reveal substrate binding sites and catalytic mechanism. *Biochemistry* **46**, 6288–6298 (2007).

78. Chiu, C. P. C. *et al.* Structural analysis of the sialyltransferase CstII from Campylobacter jejuni in complex with a substrate analog. *Nature Structural & Molecular Biology 2004 11:2* **11**, 163–170 (2004).

79. Büll, C. *et al*. Targeting Aberrant Sialylation in Cancer Cells Using a Fluorinated Sialic Acid Analog Impairs Adhesion, Migration, and In Vivo Tumor Growth. *Mol Cancer Ther* **12**, (2013).

80. Macauley, M. S. *et al.* Systemic blockade of sialylation in mice with a global inhibitor of sialyltransferases. *J Biol Chem* **289**, 35149–35158 (2014).

81. Kerjaschki, D., Sharkey, D. J. & Farquhar, M. G. Identification and characterization of podocalyxin - The major sialoprotein of the renal glomerular epithelial cell. *Journal of Cell Biology* **98**, 1591–1596 (1984).

82. Shuichi Tsuji. Molecular Cloning and Functional Analysis of Sialyltransferases. *The Journal of Biochemistry* **120**, 1–13 (1996).

83. Kimple, M. E., Brill, A. L. & Pasker, R. L. Overview of Affinity Tags for Protein Purification. *Current protocols in protein science* **73**, (2013).

84. Gräslund, T., Nilsson, J., Lindberg, A. M., Uhlén, M. & Nygren, P. Å. Production of a Thermostable DNA Polymerase by Site-Specific Cleavage of a Heat-Eluted Affinity Fusion Protein. *Protein Expr Purif* **9**, 125–132 (1997).

85. Zhou, H., Liu, Z., Sun, Z., Huang, Y. & Yu, W. Generation of stable cell lines by site-specific integration of transgenes into engineered Chinese hamster ovary strains using an FLP-FRT system. *J Biotechnol* **147**, 122–129 (2010).

86. Sasakis, K. *et al.* Expression Cloning of a G,-specific a=2,8=Sialyltransferase (GD3 Synthase). *Journal of Biological Chemistry* **269**, (1994).

87. Breen, K. C. The role of protein glycosylation in the control of cellular N-sialyltransferase activity. *FEBS Lett* **517**, 215–218 (2002).

88. Chen, C. & Colley, K. J. Minimal structural and glycosylation requirements for ST6Gal I activity and trafficking. *Glycobiology* **10**, 531–583 (2000).

89. Weinstein, J., Lee, E. U., McEntree, K., Lai, P. H., & Paulson J. C. Primary structure of beta-galactoside alpha 2,6-sialyltransferase. Conversion of membrane-bound enzyme to soluble forms by cleavage of the NH2-terminal signal anchor. *J Biol Chem.* **262**, 17735–17743 (1987).

90. Seto, N. O. L., Palcic, M. M., Hindsgaul, O., Bundle, D. R. & Narang, S. A. Expression of a Recombinant Human Glycosyltransferase from a Synthetic Gene and its Utilization for Synthesis of the Human Blood Group B Trisaccharide. *Eur J Biochem* **234**, 323–328 (1995).

91. Paulson, J. C. & Colleys, K. J. Glycosyltransferases Structure, Localization, and Control of Cell Type-Specific Glycosylation. *The Journal of Biochemistry* **264**, 17615–17618 (1989).

92. Rao, F. v. *et al.* Structural insight into mammalian sialyltransferases. *Nat Struct Mol Biol* **16**, 1186–1188 (2009).

93. Shi, X. & Jarvis, D. L. Protein N-Glycosylation in the Baculovirus-Insect Cell System. *Curr Drug Targets* **8**, 1116 (2007).

94. Moremen, K. W. *et al.* Human glycosylation enzymes for enzymatic, structural and functional studies. *Nat Chem Biol* **14**, 156 (2018).

95. Moremen, K. W. *et al.* Expression system for structural and functional studies of human glycosylation enzymes. *Nat Chem Biol* **14**, 156–162 (2018).

96. Zhang, L., Leng, Q. & Mixson, A. J. Alteration in the IL-2 signal peptide affects secretion of proteins in vitro and in vivo. *Journal of Gene Medicine* **7**, 354–365 (2005).

97. Pagan, J. D., Kitaoka, M. & Anthony, R. M. Engineered Sialylation of Pathogenic Antibodies In Vivo Attenuates Autoimmune Disease. *Cell* **172**, 564 (2018).

98. Rodrigues, E. *et al.* A versatile soluble siglec scaffold for sensitive and quantitative detection of glycan ligands. *Nature Communications 2020 11:1* **11**, 1–13 (2020).

99. Wu, Z. L., Ethen, C. M., Prather, B., Machacek, M. & Jiang, W. Universal phosphatase-coupled glycosyltransferase assay. *Glycobiology* **21**, 727–733 (2011).

100. Close, B. E. & Colley, K. J. In vivo autopolysialylation and localization of the polysialyltransferases PST and STX. *Journal of Biological Chemistry* **273**, 34586–34593 (1998).

101. Bhide, G. P., Zapater, J. L. & Colley, K. J. Autopolysialylation of polysialyltransferases is required for polysialylation and polysialic acid chain elongation on select glycoprotein substrates. *Journal of Biological Chemistry* **293**, 701–716 (2018).

102. Konietzny, P. B. *et al.* Enzymatic Sialylation of Synthetic Multivalent Scaffolds: From 3′-Sialyllactose Glycomacromolecules to Novel Neoglycosides. *Macromol Biosci* **22**, (2022).

103. Korekane, H. *et al.* Involvement of ST6Gal I in the biosynthesis of a unique human colon cancer biomarker candidate, alpha2,6-sialylated blood group type 2H (ST2H) antigen. *J Biochem* **148**, 359–370 (2010).

104. Malissard, M., Zeng, S. & Berger, E. G. Expression of functional soluble forms of human beta-1, 4-galactosyltransferase I, alpha-2,6-sialyltransferase, and alpha-1, 3-fucosyltransferase VI in the methylotrophic yeast Pichia pastoris. *Biochem Biophys Res Commun* **267**, 169–173 (2000).

105. Chinoy, Z. S. *et al.* Selective Engineering of Linkage-Specific α2,6-N-Linked Sialoproteins Using Sydnone-Modified Sialic Acid Bioorthogonal Reporters. *Angewandte Chemie - International Edition* **58**, 4281–4285 (2019).

106. Meng, L. *et al.* Enzymatic basis for N-glycan sialylation: Structure of rat α2,6-sialyltransferase (ST6GAL1) reveals conserved and unique features for glycan sialylation. *Journal of Biological Chemistry* **288**, 34680–34698 (2013).

107. Heise, T. *et al.* Potent Metabolic Sialylation Inhibitors Based on C-5-Modified Fluorinated Sialic Acids. *J Med Chem* **62**, 1014–1021 (2019).

108. Ruano, M. J., Cabezas, J. A. & Hueso, P. Degradation of cytidine 5′-monophospho-N-acetylneuraminic acid under different conditions. *Comp Biochem Physiol B Biochem Mol Biol* **123**, 301–306 (1999).

109. Jasial, S., Hu, Y. & Bajorath, J. How Frequently Are Pan-Assay Interference Compounds Active? Large-Scale Analysis of Screening Data Reveals Diverse Activity Profiles, Low Global Hit Frequency, and Many Consistently Inactive Compounds. *J Med Chem* **60**, 3879–3886 (2017).

110. Montgomery, A. P. *et al.* Design, synthesis and evaluation of carbamate-linked uridyl-based inhibitors of human ST6Gal I. *Bioorg Med Chem* **28**, 115561 (2020).

111. Dobie, C., Montgomery, A. P., Szabo, R., Yu, H. & Skropeta, D. Synthesis and biological evaluation of selective phosphonate-bearing 1,2,3-triazole-linked sialyltransferase inhibitors. *RSC Med Chem* **12**, 1680–1689 (2021).

112. Martin, M. M. & Lindqvist, L. The pH dependence of fluorescein fluorescence. *J Lumin* **10**, 381–390 (1975).

113. Sörme, P., Kahl-Knutsson, B., Huflejt, M., Nilsson, U. J. & Leffler, H. Fluorescence polarization as an analytical tool to evaluate galectin–ligand interactions. *Anal Biochem* **334**, 36–47 (2004).

114. Scudder, P. R. & Chantler, E. N. Glycosyltransferases of the human cervical epithelium. II. Characterization of a CMP-N-acetylneuraminate: galactosyl-glycoprotein sialyltransferase. *Biochim Biophys Acta* **660**, 136–141 (1981).

115. Geissner, A. *et al.* 7-Fluorosialyl glycosides are hydrolysis resistant but readily assembled by sialyltransferases providing easy access to more metabolically stable glycoproteins. *ACS Cent Sci* **7**, 345–354 (2021).

116. Rivinoja, A., Pujol, F. M., Hassinen, A. & Kellokumpu, S. Golgi pH, its regulation and roles in human disease. *Ann Med* **44**, 542–554 (2012).

117. Burlingham, B. T. & Widlanski, T. S. An Intuitive Look at the Relationship of Ki and IC50: A More General Use for the Dixon Plot. *J Chem Educ* **80**, 214–218 (2003).

118. Qasba, P. K., Ramakrishnan, B. & Boeggeman, E. Substrate-induced conformational changes in glycosyltransferases. *Trends Biochem Sci* **30**, 53–62 (2005).

119. Subedi, G. P. & Barb, A. W. The immunoglobulin G1 N-glycan composition affects binding to each low affinity Fc γ receptor. *MAbs* **8**, 1512–1524 (2016).